Performance Investigation of Glazing Systems in Combination with Internal Solar Shading

Theme:	Master project
Student name:	Jakob Hedegaard and Tore Dahl Iversen
Date:	10/06-2015
Period:	4^{th} semester M.Sc.

STUDENT REPORT
AALBORG UNIVERSITY

Title:	Performance Investigation of Glazing Systems in Combination with Internal Solar Shading
Semester:	4th M.Sc.
Semester theme:	Master project
Project period:	02/02-15 - 10/06-15
ECTS:	30
Supervisors:	Rasmus Lund Jensen and Olena Kalyanova Larsen
Student names:	Jakob Hedegaard and Tore Dahl Iversen

Jakob Hedegaard

Tore Dahl Iversen

Copies:	6
Pages, total:	108
Appendices:	10
Supplements:	CD

Synopsis:

In Denmark consulting engineers are getting more and more inclined towards using internal dynamic solar shading devices instead of external static shadings. The main two reasons are that external shading is both highly sensitive to the inclement weather and it often conflicts with the architectural design of the building façade.
Though when simulating a combined window and internal shading system in the widely used building simulations program, BSim, the solar heat gain of a building is overestimated. The reason for the overestimation is that the shading coefficient is considered constant, whereas in reality it changes depending on the incidence angle of the sun. Therefore this project will focus on estimating a correction factor for the shading coefficient, which can help increase the accuracy of the simulated results in BSim.
Since it is not known how a change in window and shading type affects the size of overestimation in BSim, it is chosen to look at two different window types in combination with different types of shading. Thereby it will be possible to investigate if a one general correction factor for all types of window and shading types is sufficient, or weather a unique factor should be made for each combination.

By signing this document, each member of the group confirms that all participated in the project work and thereby all members are collectively liable for the content of the report. Furthermore, all group members confirm that the report does not include plagiarism.

Executive summary

The later years there has been a big change in the way buildings are designed. Generally the building envelope is more insulated, and simultaneously the glazing area in buildings is increased. This makes it more challenging to avoid overheating in the buildings. In this connection solar shading is an useful tool to prevent the solar radiation from entering the building in periods, where there are risk of overheating. For this purpose the external solar shading has often been the preffered type of solar shading, as it has the highest efficiency. However the external solar shading is vulnerable to weather conditions, which in coastal areas like Denmark are relatively windy. This means that the maintenance cost for external solar shadings in coastal areas. Further external solar shading affects the aesthetic appearance of the building to a great extent. All of the above highlights why it is interesting to examine the performance of different internal solar shading in combination with different windows.

An experiment is carried out at the test facilities called *the Cube*, which is a small building containing a test room with a southern orientated window. At the Cube the performance of a highly reflecting and a highly absorbing internal solar shading is examined. Both solar shadings are tested on a double glazed and a triple glazed window. By measuring the solar radiation on the southern facade and doing a energy balance for the test room, it is possible to determine the total g-value for the window and solar shading.

BSim is a Danish simulation program, which is used by Danish engineers to evaluate the indoor environment and energy consumption of buildings. When a solar shading is created in BSim, only a constant value for the shading coefficient is given. In reality the shading coefficient is depended on the angle of incidence. This indicates that BSim is not calculating the solar radiation through a window and solar shading correctly. By comparing the results from the experiment with the same window and shading systems built up in BSim, it is concluded that BSim is overestimating the solar radiation through a window.

This overestimation will cause a greater demand for cooling. In order to take this overestimation into account, correction factors are made for the four combinations of window and shading system. The correction factors should be multiplied with shading factors. Using the correction factors, the overestimation of solar radiation through a window is evened out over a year. The analysis shows that the correction factor for a highly absorbing solar shading does not change very much when the window is changed. However the correction factor for a highly reflecting solar shading is far more depended on the window properties.

Dansk Resumé

De senere år har der været en markant udvikling i måden at designe bygninger på. Forskellen består i høj grad i, at mængden af isoleringen i klimaskærmen er steget, samtidig med vinduesarealet i bygninger også er steget. Dette resulterer i større udfordringer for at undgå overophedning inde i bygningerne. Solafskærmning et brugbart værktøj til at forhindre solstrålingen i at komme ind i bygningen i perioder, hvor der er risiko for overophedning. Ofte har udvendig solafskærmning været at forestrække, da det er den type solafskærmning, som har den bedste effektivitet. Dog skal det siges, at udvendig solafskærmning er følsom overfor vejrforholdene. I områder omgivet af hav, som Danmark, vil den store mængde vind sætte begrænsninger for udformningen af den udvendige solafskærmning, samtidig med vedligeholdesesomkostningerne for solafskærmningen vil være relativ store. Herudover påvirker udvendig solafskærmning den æstestiske udformning af bygningen mere, end andre typer solafskærmning vil gøre det. Alt dette understreger, hvorfor det er interessant at undersøge virkningen af forskellige indvendige solafskærmninger kombineret med forskellige vinduestyper.

Et eksperiment er udført på testlokaliteten, *Terningen*. Terningen er en lille bygning, der bl.a. indeholder et testrum med et stort sydvendt vindue. Både en meget reflekterende og en meget absorberende afskærmningen er testet på et 2-lags og 3-lags vindue. Ved at måle solindstrålingen på den sydvendte facade samt at lave en energibalance for testrummet, er det muligt at bestemme en samlet g-værdi for hver kombination af vindue og solafskærmning.

BSim er et dansk simuleringsprogram, der ofte er benyttet af danske ingeniører til at evaluere en bygnings indeklima og energiforbrug. Når en solafskærmning skal opbygges i BSim, angives der blot en konstant værdi for solafskærmningsfaktoren. I virkeligheden er solafskærmningsfaktoren afhængig af indfaldsvinklen, hvilket indikerer, at BSim ikke beregner solindfaldet gennem et vindue og solafskærmning helt korrekt. Ved at bygge vinduerne og solafskærmninger op i BSim og sammenligne solindfaldet gennem disse med det beregnede solindfald fra eksperimentet, bliver det konkluderet, at BSim laver en mindre overestimering af solindfaldet gennem et vindue med solafskærmning.

Denne overestimering af solindfald vil i perioder resultere i et højere kølebehov. For at tage forhold til denne overestimering er korrektionsfaktorer for de 4 kombinationer af vindue og solafkærmning lavet. Disse korrektionsfaktorer skal multipliceres med solafskærmningsfaktoren. Ved at benytte disse korrektionsfaktorer vil der ikke være nogen overestimeringen af solindfald set over et år. Denne analyse viser, at korrektionsfaktoren for en højabsorberende solafskærmning ikke ændres meget, når vinduet ændres. For en højreflekterende solafskærmingen vil vindueegenskaberne have stor indflydelse på korrektionsfaktoren, hvorfor denne ændres markant, når vinduet ændres.

Preface

This master thesis is devised of students at 4th semester of the master education *Indoor Environmental and Energy Engineering* at Aalborg University. The project is completed in the summer of 2015 and it focuses on the subject *Energy performance of glazing systems in combination with internal solar shading.*

The project will contain references, all of which are collected in a bibliography at the end of the report. All the sources in the report are given by the Harvard method and divided in books, articles, homepages and theses. Referring to books is done at the following way; author, title, ISBN-number, edition, publisher, year. For articles; author, title, edition, date, year. For homepages; author, title, URL-address, year, date of use. Tables and figures without source reference are self-made. If a source reference is located before the full stop it refers to the concerned sentence, otherwise it is referring to the previous section, if it is located after the full stop.

Regarding the preparation of the project the group want to express our gratitude to the supervisor of the project.

- Olena Kalyanova Larsen
- Rasmus Lund Jensen

Contents

1 Introduction

In modern time the focus on minimizing the energy consumption and emission of greenhouse gasses has grown drastically. Since the building sector accounts for approximately 40 % of the total energy consumption and 36 % of the total CO_2-emission in the EU, there is a clear ambition to decrease this energy consumption as well as the emission of greenhouse gasses. The EU has stated that they will reduce both the energy consumption and greenhouse gas emission with 20 % in 2020 compared 2005. [European Commission, 2006]
In Denmark the requirements to reduction of energy consumption of buildings are even more strict and ambitious. According to the Danish Building Regulation, the energy consumption of buildings from 2008 should be reduced with 25 % in 2010, with 50 % in 2015 and with 75 % in 2020. [Energistyrelsen, 2015] In order to be able to meet these requirements in the future, it is necessary the make use of sustainable and energy efficient technologies along with using an appropriate control strategies for these.

During the later years there has been a tendency towards insulating buildings more in order to decrease the transmission losses from the building envelope. This has a beneficial effect in periods where the building has a heating demand, but in periods with cooling demand this will make it even more challenging to avoid overheating. Another tendency in the building sector, which increases the probability of overheating, is that the window area of office façades are significantly increased.

Windows have various functions in a house, aside from protecting against the outdoor climate, windows create a visual contact with the surroundings and allow daylight to enter the building. Furthermore, windows have a large impact on the energy consumption of a house, as they are often the least insulated part of the building envelope. Typically the U-value of a window is 4 - 10 times larger than the other elements in the building envelope. [Thomasz M. Mróz, 2003] However this is not the only way windows affect the energy consumption of buildings. These large open areas allow solar radiation to enter the building, which will cause a heat gain. How this affects the energy consumption depends on the situation. In periods where there is a heating demand in the building, the solar heat gain will reduce this heat demand. Conversely in warmer periods of the year the solar heat gain will result in overheating of rooms or an increased cooling demand, if a cooling system in installed in the given room.
In order to control when and in which extent the solar radiation enters the building, dynamic solar shading has become an essential tool in modern building designs. Even though static solar shading has been applied in buildings since ancient time, dynamic solar shading and the control of this has taken over due to the shifting heating and cooling demand in modern buildings.

A simple and easy controllable solution for dynamic solar shading is internal shading. This gives the users the ability to manually control when the shading is active. Therefore Danish consulting engineers are inclined towards using the implementations of internal solar shading in office buildings. Another incentive for choosing an internal shading solution is that it rarely harms the architectural design of a building. Whereas static external shading solutions often conflicts with the architectural expression of a building. So since engineers has to find solutions, which satisfies the architectural ideas, internal solar shading becomes highly interesting.

The interplay between different glazing and internal shading systems is however not that well defined. Therefore this project will focus of the interplay between different types of windows compared with different types of internal shading. This will be investigated through a number of measurements, which should help clarify this interplay.

Another issue for Danish consulting engineers is the way the Danish indoors environment and energy simulation tool BSim interprets the shading coefficient of internal solar shading. This coefficient is considered constant and independent of the incidence angle of the solar radiation on a window. Though in real life the shading coefficient is indeed dependent on the angle of incidence. Therefore another focus in this project will be on how to correct this simple way of interpreting the shading coefficient in BSim.

1.1 Thesis Statement

In this project the work will be based on the following thesis statement.

Is it possible to optimize the shading coefficient by a correction factor and to what extend does this factor depend on the type of glazing and shading.

1.2 Scope

To evaluate the thesis statement the total g-value of a combined glazing and shading system has been evaluated through several experiments. These experiments shall result in a incidence angle dependent total g-value of a double and a triple glazed window combined with a highly absorbing and highly reflecting internal blind respectively. Each of these will be compared to the total g-value of corresponding glazing and shading systems simulated in BSim. This comparison will form the basis of an accuracy evaluation of the shading coefficient used in BSim. The variation in windows and shadings are chosen to see whether the different combinations give different sized of errors in BSim as a result of the simple way of interpreting the shading coefficient.

Part I

Theory

2 Window and Shading Properties

For this project some important window and shading property factors will be frequently used. These factor will be presented at explained in this chapter.
The chapter will also bring focus on the three most common types of solar shading, external, integrated and internal shading. The three types has individual advantages and disadvantaged, which will be shed light on in the following along with their interplay with windows.

2.1 Shading Coefficient

The shading coefficient is a factor commonly used in building simulations programs to explain the efficiency of a given solar shading device. Basically this coefficient described the amount of solar heat passing through a combined window and shading system in proportion to the amount of solar heat passing through only the window. This is given be equation 2.1.

$$SC = \frac{g_t}{g_w} \tag{2.1}$$

Where:

SC	The shading coefficient of a solar shading device [-]
g_w	The g-value of the window [-]
g_t	The total g-value of a combined window and solar shading system [-]

Both the g-value for a window and the total g-value for at combined window and shading system will be described in the following sections of this chapter. When these are explained an example of the shading coefficient will be presented for different types of windows and solar shading types.

2.2 Window g-value

The solar energy transmittance of a window, or also called the g-value, described the solar energy passing through a window. The solar energy can be divided into three main parts, which are presented in figure 2.1 on the next page.

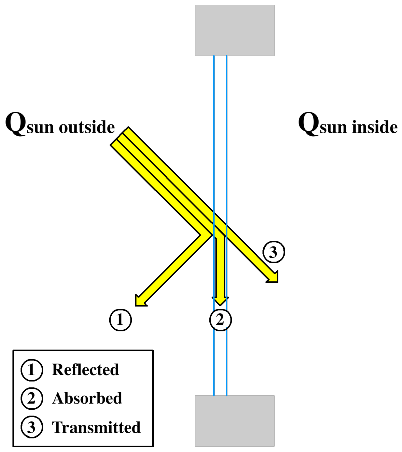

Figure 2.1: A graphical representation of a window with the solar radiation outside the window, $Q_{\text{sun outside}}$, and the solar heat gain inside the room, $Q_{\text{sun inside}}$.

In accordance with the figure, a part of the solar radiation is reflected when hitting the window. Another part in absorbed in the glazing system and the last part is transmitted straight through the window.
From 2.1 the g-value of a window can be explained from equation 2.2.

$$g_w = \frac{Q_{sun\ inside}}{Q_{sun\ outside}} \tag{2.2}$$

Where:

g_w	The g-value of the window [-]
$Q_{sun\ outside}$	The solar radiation reaching the outside of the window [W]
$Q_{sun\ inside}$	The solar heat gain inside the room [W]

So the g-value of a window is the correlation between the amount of solar radiation reaching the outside of the window and the amount coming through the window and inside the room. Though it would seem that $Q_{\text{sun inside}}$ only consists of the transmitted solar radiation, it is not that simple.
Besides the three primary energy streams shown in figure 2.1, a number of secondary energy streams also occurs in a situation like this. In the glazing and the cavities repeated reflections occur, causing new absorption and transmission situations.
The energy absorbed in the glazing system has to be released somewhere. This energy is partly released back into the outdoor surroundings, but another part is lead into the room through a combination of conduction, convection and long wave radiation. [H.E. Hansen, 2006]

2.3 Total g-value

To be able to evaluate the shading coefficient, the total g-value, g_t, still needs to be clarified. This value depends on the type of solar radiation. As mentioned in the beginning of this chapter the three most common types, internal, integrated and external, will be explained.

Hence the total g-value of a window combined with each of these three types of shading will also be explained in the following.

2.3.1 Internal

Internal solar shading is the most common type of shading available. It is places in the inside of the window with a manual control for the user. Usually a blinds or venetian blinds are used in houses and office buildings. These are shown in figure 2.2.

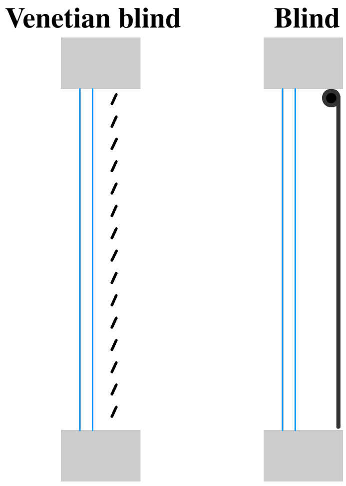

Figure 2.2: Three different designs of internal solar shading.

Interplay With Window

For a regular blind figure 2.3 shows how the incident solar radiation acts when reaching the window and the solar shading device.

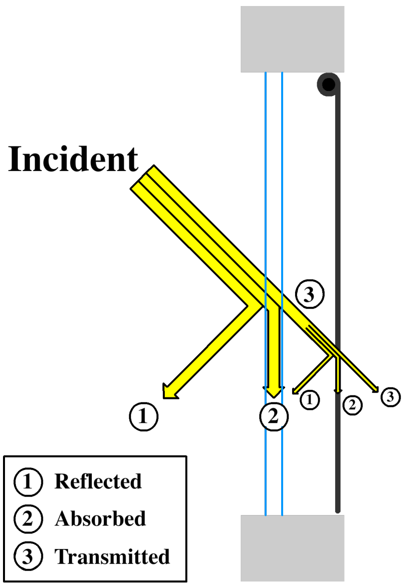

Figure 2.3: The reflectance, absorbance and transmittance of the incident solar radiation when reaching the window and solar shading respectively.

As seen in figure 2.3, a part of the incident solar radiation is reflected by the window, another part is absorbed by the window and the rest is transmitted through the window. The transmitted solar radiation reaches the internal solar shading device. Once again a part of this transmitted solar radiation is reflected by the shading device, while another part is absorbed and the last part is transmitted through shading.

According to DS/EN 13363-1, the total solar energy transmittance for a combination of glazing and internal solar protection device is given by equation 2.3.[Dansk Standard, 2007]

$$g_t = g_w \cdot \left(1 - g_w \cdot \rho_{e,B} - \alpha_{e,B} \cdot \frac{G}{G_2}\right) \tag{2.3}$$

Where:

g_w	The g-value of the window [-]
g_t	The total g-value of a combined window and solar shading system [-]
$\rho_{e,B}$	The reflectance of the solar protection device [-]
$\alpha_{e,B}$	The absorbance of the solar protection device [-]
G_2	Thermal conductance coefficient $[\mathrm{W/(m^2 \cdot K)}]$
G	Given by $\mathrm{G} = \left(\frac{1}{\mathrm{U_g}} + \frac{1}{\mathrm{G_2}}\right)^{-1}$, (where $\mathrm{U_g}$ is the u-value of the window) $[\mathrm{W/(m^2 \cdot K)}]$

In the following two sections some of the advantages and disadvantages with internal solar shading will be presented. This is done to be able to way the pros and cons for each solution type up against each other.

Advantages

- On of the great advantages about internal solar shading is that it is protected from the inclement weather. This results in no or little maintenance costs along with a long life span of the solar protection device.
- The selling price of internal solar shading is typically relatively cheap. This along with the low maintenance costs makes the internal solar shading solution the most economic solution of the three.
- Internal solar shading can be installed in existing buildings without having to change the building design or the construction of the window.
- Internal solar shading can be manually controlled by the users. So during a day with changing sun conditions the users can control the amount sun coming into the room. [Karsten Duer, Jacob Brick Laustsen and Svend Svendsen, 2009]

Disadvantages

- One of the largest disadvantages with internal solar shading is that is has to deal with solar radiation, which has already entered the room. Therefore the solar heat absorbed in the shading device mainly stays inside the room. Furthermore the reflected solar energy has to pass back through the window before exiting the room again. Therefore some of the energy reflected on the shading stays in the room as well.

– The use of internal solar shading often leads to a relatively big loss in daylight. At least when choosing a shading device which has no openings such as the blind illustrated in figure 2.2 on page 7. The daylight loss happens because the blind has to cover the whole window to keep out as much heat from the solar radiation as possible. If a venetian blinds is used the louvres can be set to keep out direct solar radiation but let diffuse radiation come into the room, which is also illustrated in figure 2.2 on page 7. This leads to enhanced daylight conditions.

2.3.2 Integrated

Integrated solar shading is placed between the exterior and the middle pane of a triple glazed window. It is typically designed as a venetian blind with a manual control from inside the building. This is shown in figure 2.4

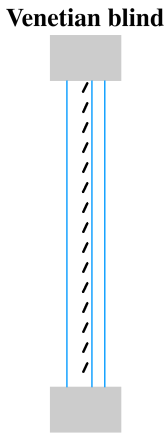

Figure 2.4: A solution for integrated solar shading in a triple glazed window.

Interplay With Window

Figure 2.5 on the next page shows how the incident solar radiation is reflected, absorbed and transmitted through the first layer of glazing before reaching the integrated solar protection.

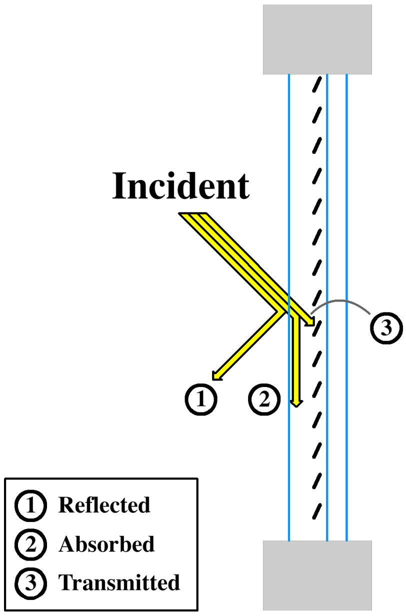

Figure 2.5: The reflectance, absorbance and transmittance of the incident solar radiation when reaching the window just before the solar protection device.

When the solar energy transmitted through the window reached the integrates venetian blind, some of the solar energy is reflected and some is absorbed in the venetian blind. The rest is reflected between the louvres of the venetian blind before being transmitted through. This is shown in figure 2.6.

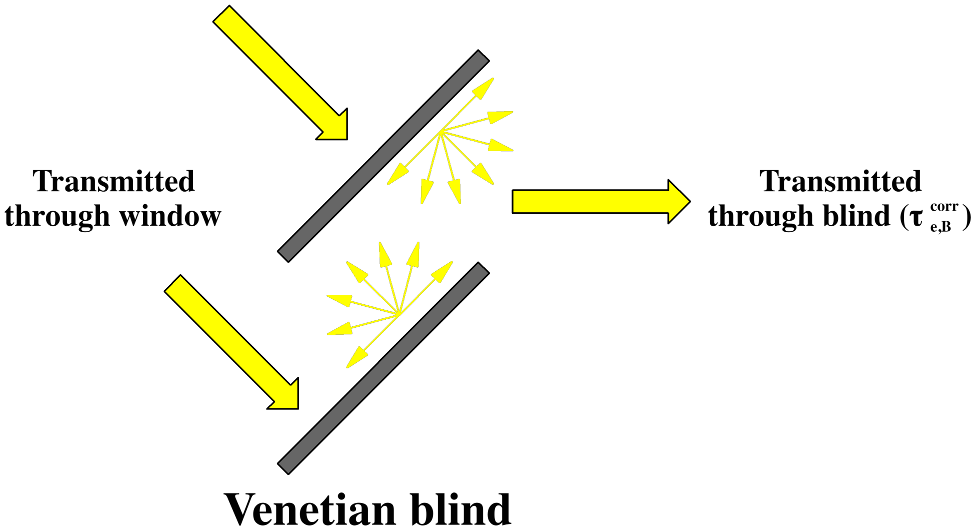

Figure 2.6: How the solar radiation is transmitted through a venetian blind.

Because the solar energy is reflected between the louvres numerous times, the transmitted energy is considered as the outcome of the numerous reflections inside the room. Since this is not the regular way to consider transmittance through a shading system, DS/EN 13363-1 gives a corrected transmission values through for the venetian blind. It also give a corrected reflection and absobance. All three corrected values are given in equation 2.4 on the next page. [Dansk Standard, 2007]

$$\begin{aligned}\tau_{e,B}^{corr} &= 0.65 \cdot \tau_{e,B} + 0.15 \cdot \rho_{e,B} \\ \rho_{e,B}^{corr} &= \rho_{e,B} \cdot (0.75 + 0.70 \cdot \rho_{e,B}) \\ \alpha_{e,B}^{corr} &= 1 - \tau_{e,B}^{corr} - \rho_{e,B}^{corr}\end{aligned} \tag{2.4}$$

Where:

$\rho_{e,B}$	The reflectance of the solar protection device [-]
$\alpha_{e,B}$	The absorbance of the solar protection device [-]
$\tau_{e,B}$	The transmittance through the solar protection device [-]
$\tau_{e,B}^{corr}$	The corrected transmittance through the solar protection device [-]
$\rho_{e,B}^{corr}$	The corrected reflectance by the solar protection device [-]
$\alpha_{e,B}^{corr}$	The corrected absorbance by the solar protection device [-]

The total solar energy transmittance for a combination of glazing and integrated solar protection is given by equation 2.6 on page 13.[Dansk Standard, 2007]

$$g_t = g_w \cdot \tau_{e,B}^{corr} + g_w \cdot (\alpha_{e,B}^{corr} + (1 - g_w) \cdot \rho_{e,B}^{corr})\frac{G}{G_3} \tag{2.5}$$

Where:

g_w	The g-value of the window [-]
g_t	The total g-value of a combined window and solar shading system [-]
$\tau_{e,B}^{corr}$	The corrected transmittance through the solar protection device [-]
$\rho_{e,B}^{corr}$	The corrected reflectance by the solar protection device [-]
$\alpha_{e,B}^{corr}$	The corrected absorbance by the solar protection device [-]
G_3	Thermal conductance coefficient $[\mathrm{W/(m^2 \cdot K)}]$
G	Given by $\mathrm{G} = \left(\frac{1}{\mathrm{U_g}} + \frac{1}{\mathrm{G_3}}\right)^{-1}$, (where $\mathrm{U_g}$ is the u-value of the window) $[\mathrm{W/(m^2 \cdot K)}]$

In the following two sections some of the advantages and disadvantages with integrated solar shading will be presented.

Advantages

- Just as internal solar shading, integrated solar shading is protected from the inclement weather. So maintenance costs are kept at a minimum.
- During cold periods of the year the integrated solar shading device may decrease the heat loss to the outside by working as an extra layer in the window. [Karsten Duer, Jacob Brick Laustsen and Svend Svendsen, 2009]
- An integrated solar shading device typically provides a better thermal shading effect than an internal shading device. Because the integrated shading is not placed in the

room, the solar radiation absorbed in the integrated shading it not released in the room. This heat is on the other hand released into the gap between the external and the middle layer of glazing, which is shown in figure 2.5 on page 10.

Disadvantages

- Integrated solar shading can not be added to an existing window construction. This solution can only be used when changing the windows of a building or in new buildings.
- If an integrated shading device breaks a replacement can be expensive. In a case like this the whole window has to be replaces since the glazing layers cannot be replaced one by one.

2.3.3 External

External solar shading is placed on the outside of the window. It comes in different types of which some are shown in figure 2.7.

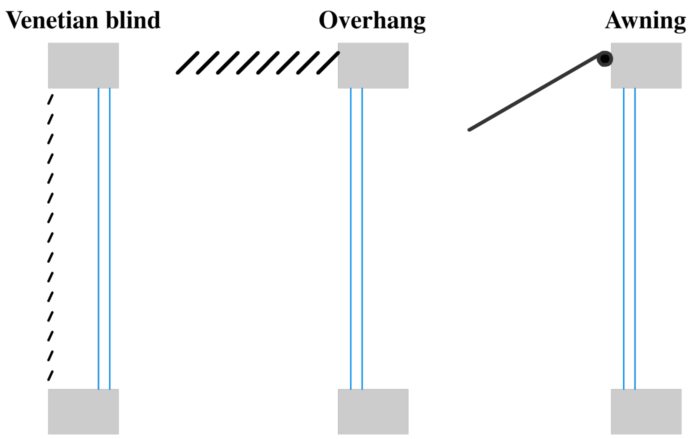

Figure 2.7: Three different designs of external solar shading.

Interplay With Window

Figure 2.8 on the next page shows how the incident solar radiation is behaving when reaching the external solar protection device followed by the window.

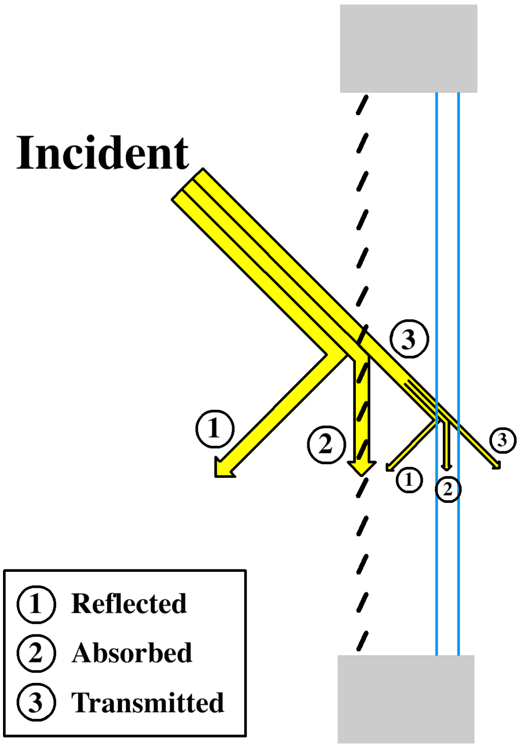

Figure 2.8: The reflectance, absorbance and transmittance of the incident solar radiation when reaching the solar shading and the window respectively.

As illustrated in figure 2.8, the incident solar radiation is partly reflected and absorbed by the solar protection device and the rest is transmitted through. The transmitted part reaches the window, where it is partly reflected and absorbed by the window. The rest is transmitted all the way through the window into the room.

According to DS/EN 13363-1, the total solar energy transmission for a combination of an external solar protection device and a window is given by equation 2.6. [Dansk Standard, 2007]

$$g_t = g_w \cdot \tau_{e,B} + \alpha_{e,B} \cdot \frac{G}{G_2} + \tau_{e,B} \cdot (1 - g_w) \cdot \frac{G}{G_1} \tag{2.6}$$

Where:

g_w	The g-value of the window [-]
g_t	The total g-value of a combined window and solar shading system [-]
$\alpha_{e,B}$	The absorbance of the solar protection device [-]
$\tau_{e,B}$	The transmittance through the solar protection device [-]
G_2	Thermal conductance coefficient $[\mathrm{W/(m^2 \cdot K)}]$
G_1	Thermal conductance coefficient $[\mathrm{W/(m^2 \cdot K)}]$
G	Given by $\mathrm{G} = \left(\frac{1}{\mathrm{U_g}} + \frac{1}{\mathrm{G_1}} + \frac{1}{\mathrm{G_2}}\right)^{-1}$, (where $\mathrm{U_g}$ is the U-value of the window) $[\mathrm{W/(m^2 \cdot K)}]$

In the following two sections some of the advantages and disadvantages with external solar shading will be presented.

Advantages

- Because the external solar shading is located outside the window, the solar energy is stopped before entering the room. This is illustrated on figure 2.8 on the preceding page.
- Unlike integrated shading, external shading can be added to existing buildings without having to change the window.
- As opposed to the internal and integrated solar shading devices, an external solar shading does not have to be vertical. When implementing non vertical shading solutions a larger amount of daylight may enter the room, and if it is a good design, this should not lead to an excess in solar heat gain inside the room.

Disadvantages

- One of the great disadvantages about external solar shading is the fact that it is exposed to the inclement weather. This leads to high maintenance costs and a much lower life span than the internal and integrated.
- External solar shading solutions often conflict with the architects design ideas. Therefore it can be difficult to integrate on a building.

2.4 Analysis of SC

The goal of this section is to be able to evaluate the size of the shading coefficient for the two different window types compared with different types of solar shading.

In this project two different types of windows will be used for the experiments. The design and properties of these windows will be described more into detail in chapter 6 on page 31, *Glazing and Shading Systems*. Though in this section the g-value of the two windows will be used for a comparison of the shading coefficient for different window types.
The two windows used in this project are:

- Double glazed with $g_w = 0.36$
- Triple glazed window with $g_w = 0.54$

To examine the influence on the shading coefficient if using a highly reflecting solar shading or a highly absorbing, a range of fictive shading types has been used. The energy performance factors for these shading types are presented in table 2.1 on the facing page.

No.	τ_v	ρ_v	α_v
1	10 %	10 %	80 %
2	10 %	20 %	70 %
3	10 %	30 %	60 %
4	10 %	40 %	50 %
5	10 %	50 %	40 %
6	10 %	60 %	30 %
7	10 %	70 %	20 %
8	10 %	80 %	10 %

Table 2.1: Energy performance factors for the different fictive shading types, where τ_v is the transmittance, ρ_v is the reflectance, and α_v is the absorbance of the shading.

As the table shows, it is chosen to evaluate 8 different shading types, which ranges from high to low absorbance and thereby low to high reflectance.

A calculation of the shading coefficient has been conducted, using the described window types. The calculation has been made for an internal, integrated and external shading device, which all has the energy performance factors presented in table 2.1. The expression for calculating the shading coefficient can be seen in equation 2.1 on page 5. In figure 2.9 the results of the calculations are graphically presented.

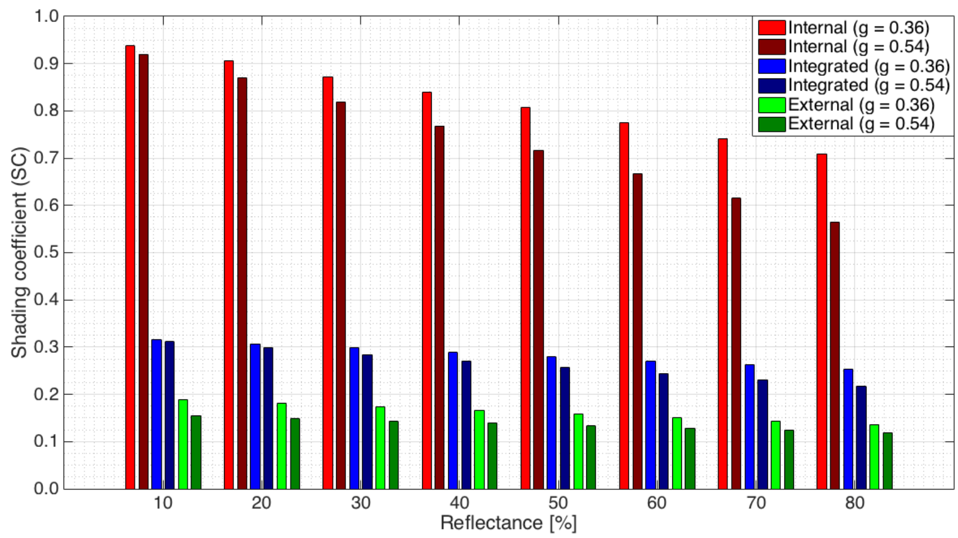

Figure 2.9: The shading coefficient of two different window types for internal, integrated and external solar shading respectively.

– As mentioned in the disadvantages for internal solar shading in the current chapter, one of the largest weaknesses with internal solar shading is that the solar energy is already inside the room when it is being shaded. At this point it is only a certain portion of the heat gain that can be removed by the shading. Therefore figure 2.9 shows that the shading coefficient for the internal shading is remarkably larger than the shading coefficient for both integrated and external shading for both window types. When using integrated shading, the solar energy is not yet inside the room, though some of the energy is already absorbed in the window. That is why the shading coefficient is larger for the integrated compared to the external, where the solar energy has not reached any part of the window before reaching the shading itself.

– When looking isolated at the two red bars in figure 2.9 on the previous page, the two window types can be compared for internal solar shading. These bars show that when a large part of the solar energy is reflected, a higher g-value leads to a lower and better shading coefficient. This makes sense since the solar energy reflected on the internal shading has to pass back through the glazing system. In this case a larger window g-value will transmit a larger part of the reflected energy back through the window.

– When looking isolated at the two blue bars in figure 2.9 on the preceding page, the two window types can be compared for integrated solar shading. This shows more or less the same tendency as the internal shading. Though the difference between the two window is not as significant when the reflectance is at a high level. The reason for this is that the reflected solar energy does not have to pass back through the whole window but only the outer layer of glazing.

– Finally when looking isolated at the two green bars in figure 2.9 on the previous page, the two window types can be compared for external solar shading. These bars show a tendency much like the one for the integrated solar shading.

The calculations made for this analysis of the shading coefficient can be found on the appendix CD as number 1.

3 Solar Geometry

In this chapter a definition of the solar radiations angle of incidence on a window will be presented. Furthermore the window properties dependence of the incidence angle will be cover later in the chapter.

3.1 Incidence Angle

It is beneficial to know how the position of the sun is changing, as this will influence what happens when the solar radiation reaches the window. The position of the sun is described by two angles; solar azimuth angle and solar altitude angle. The principal of the two angles is illustrated in figure 3.1.

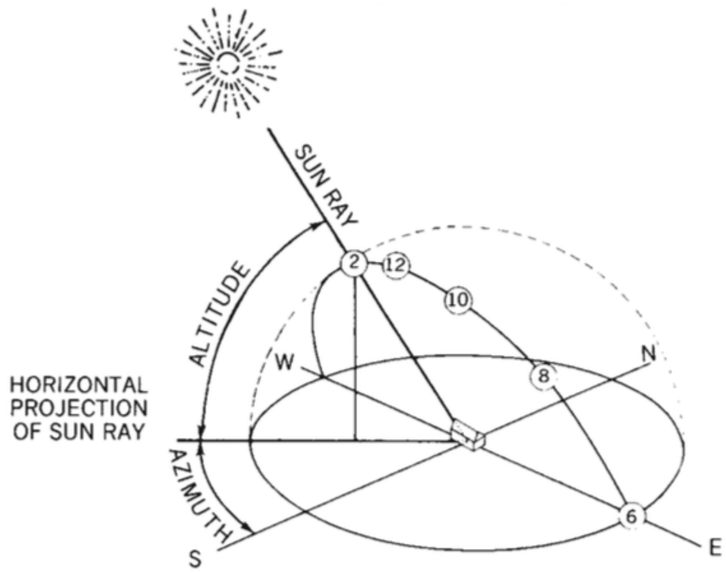

Figure 3.1: The figure shows how the azimuth and altitude angle are defined. [Per Kvols Heiselberg, 2008]

As figure 3.1 illustrates, the solar azimuth angle is the angle between south and the projection of the solar radiation in the horizontal plane. This angle is calculated positive towards west and negative towards east. The solar altitude angle is defined as the angle between the horizontal plane at the Earth and the vertical plane of the sun. These angles will vary over the day as well as over the year as the sun follows its path on the sky.

If the azimuth and altitude angle for a specific point are known for a year, it is possible to create a sun chart diagram, which visually is showing the position of the sun expressed with the solar azimuth and altitude angle. In figure 3.2 on the following page a sun chart diagram is made for Aalborg, which is the location for the test facilities for this project.

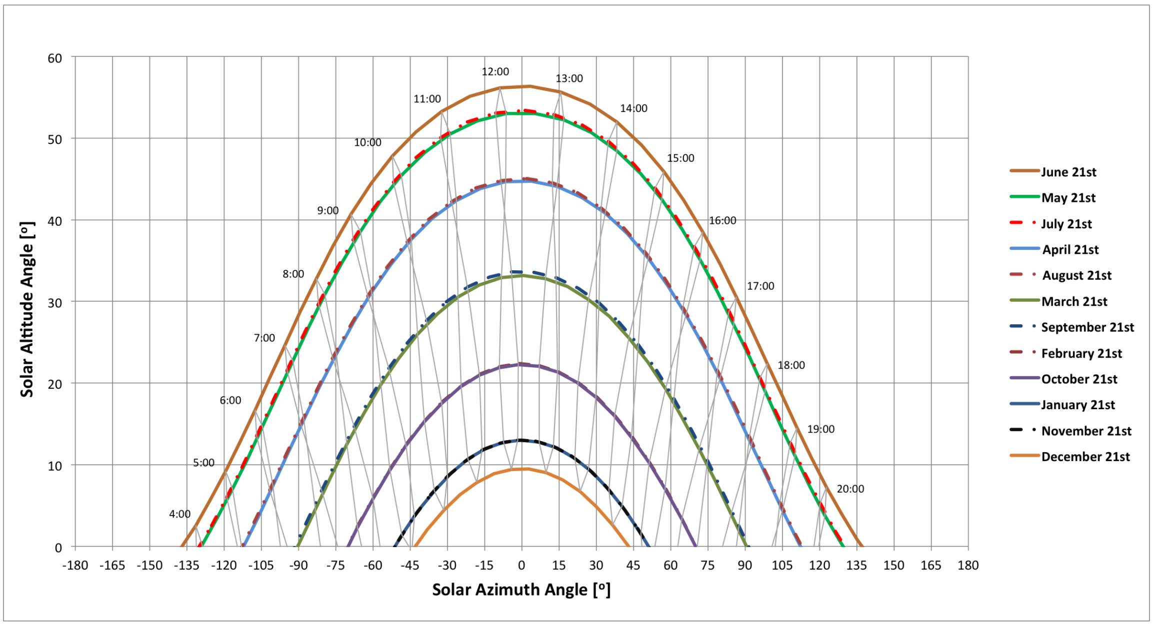

Figure 3.2: The sun chart diagram shows the position of the sun expressed with the solar azimuth and altitude angle.[Charlotte B. Henriksen, Mathias Villumsen, 2012]

The sun chart diagram in figure 3.2 is made for the 21st of every month in the year. This is done because the longest day of the year usually is 21st of June, while the 21st of December is considered the shortest day of the year. Also equinoxes will occur around the 21st of March and the 21st of September. It can be seen from the figure that the sun stands the highest on the sky the 21st of June compared to the other days included in the graph. It is also noticed that the sun stands the lowest of all the chosen days on the 21st of December. Further it should be noted that the altitude angle does not exceed 60° at any time.

How the shifting position of the sun will influence a surface depends, aside from the position of the sun, on the slope and orientation of the surface. In order to take these two factors into account the term, angle of incidence, is introduced.
Where the azimuth and altitude angle described the position of the sun in relation to a point, the angle of incidence describes the position of the sun in relation to a given surface. The angle of incidence is given as the angle between the solar radiation and the normal line of the surface. The closer the incidence angle for solar radiation on a window is to 0°, the more solar radiation will transmit through the window.

In figure 3.3 on the next page an illustration of the incidence angle on a window is presented.

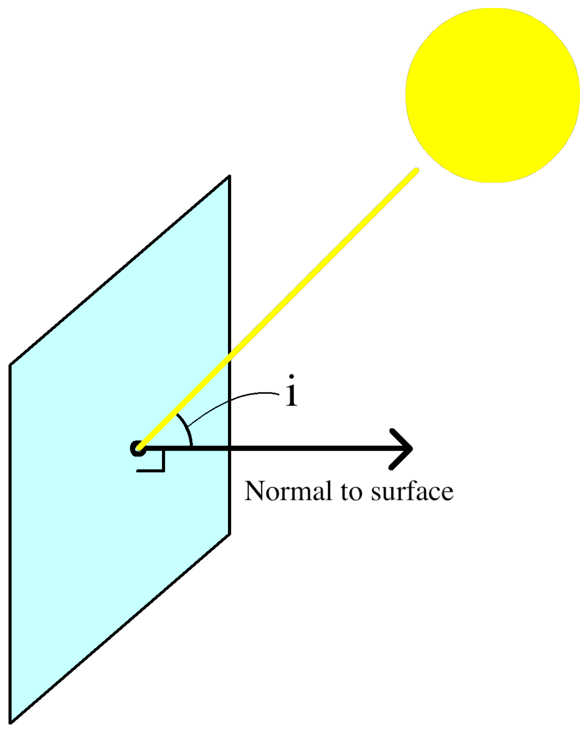

Figure 3.3: An illustration of the suns incidence angle on a window.

During the experiments of this project the widows in the test facilities has been placed in a vertical position at all times. This takes slope of the window out of the expression for the angle of incidence.
The angle of incidence on a vertical surface can be calculated from the altitude and azimuth angle. This is shown in equation 3.1 [H.E. Hansen, 2006].

$$\cos(i) = \cos(\gamma_{sun} - \gamma_{surface}) \cdot \cos(h_{sun}) \tag{3.1}$$

Where:

i	Angle of incidence [°]
γ_{sun}	Azimuth angle of the sun [°]
$\gamma_{surface}$	Azimuth angle of the surface [°]
h_{sun}	Altitude angle of the sun [°]

3.2 Angle Depended Properties

Normally when the g-value is given for a window, it is given as a single value for the normal radiation on the window. That is for solar radiation with an incidence angle following the normal angle of the window. However the g-value is depended on the angle of incidence. So for all other incident angles than i = 0° the g-values will be wrong. Figure 3.4 on the next page shows how the transmittance and reflectance of a homogeneous glass plane changes in relation to a varied angle of incidence.

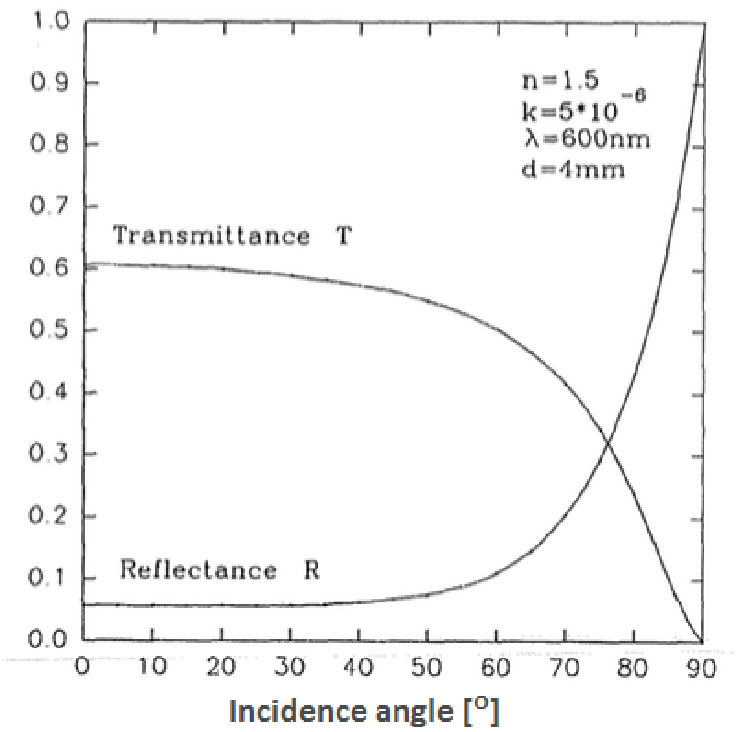

Figure 3.4: The graph shows the angle of incidence in relation to transmittance and reflection of a homogeneous glass pane for the given d, λ, n and k.[Furler, 1991]

As it can be seen from figure 3.4 the reflectance will increase drastically when the angle of incidence exceeds 60°. Correspondingly the transmittance decreases significnatly when the angle of incidence is above 60°. It should be noticed that it will not be exactly like this for every glazing system. The exact shape of the curves will depend on the properties of the window. The break of the curves would probably happen at another angle of incidence than 60° if the curves were made for a different window. However the tendencies of the graph can be considered valid for most glazing systems.

It was concluded from the above that the higher angle of incidence the more solar radiation will be reflected and the less will be transmitted through the glazing. In figure 3.5 on the next page the correlation between the g-value of three different windows and the angle of incidence is presented.

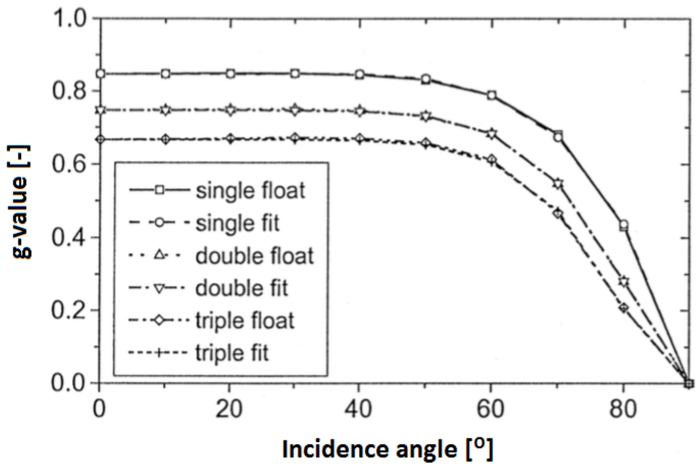

Figure 3.5: The graph shows the g-value of three different windows in relation to the angle of incidence.[J. Karlsson, 2000]

As it can be seen from figure 3.5, the correlation between g-value and angle of incidence looks similar to the correlation from figure 3.4 between transmittance and angle of incidence. Though it would be assumed that the curve for the g-value would be somewhat higher that the transmittance. The reason being that the window g-value is a combination of the transmitted energy along with a some other secondary energy contributions compared to the amount of solar radiation on the outer surface if the window. This is explained more into detail in section 2.2 on page 5, *Window g-value.*

According to figure 3.5, when the angle of incidence exceeds 60°, more solar radiation will be reflected and thereby less transmitted, which of course will result in a lower g-value.

How the properties for a solar shading device is changing in relation to the angle of incidence is more uncertain. However it is assumed to follow approximately the same tendency as for the window. This will be investigated later in this project.

All the correlations between the angle of incidence and transmittance, reflectance and g-value respectively has been made for direct solar radiation. The reason for this is that direct solar radiation has a unique incidence angle on the window a all times.
However this is not the case for diffuse sky radiation. Diffuse sky radiation is the solar radiation scattered by air molecules, aerosol particles and clouds which reaches the given surface of interest.[H.E. Hansen, 2006] Since this type of solar radiation is coming from the whole sky, it does not have a specific incidence angle. Therefore the window g-value for diffuse solar radiation is typically given by g_{60}. This means the g-value for an incidence angle of 60°.[H.E. Hansen, 2006]

4 | Aim

In the initial face of the project, the project group talked to Steffen E. Maagaard, competency manager (Danish: kompetencechef) at the Danish consulting engineering company, MOE. He explained that in coastal areas where the wind is stronger, engineers are typically cautious about using external solar shading. The reason being the external shadings vulnerability to the inclement weather and namely rough wind conditions. Because a relatively large area of Denmark consists of cost, Danish engineers are very eager to find a solar shading solutions, which performs as well as external shading but is protected from the weather.
This is where internal and integrated solar shading becomes interesting. As mentioned earlier in this chapter both of these solutions have certain disadvantages. To implement an integrated shading solution the whole window has to be changed. Whereas internal solar shading has the disadvantage of lower efficiency, which results in a larger heat gain to the room.
It is though interesting to study the performance of internal solar shading, since it is a cheap and user friendly solution with no maintenance costs. The focus of this project will be on internal solar shading only. So external and integrated shading solutions are disregarded throughout the rest of the project.

- According to Steffen E. Maagaard, one of the problems for consulting engineers when designing a glazing system combined with internal solar shading is the limited way of describing the total g-value of the system. In accordance with DS/EN 13363-1 equation 2.3 on page 8 states that the total g-value is independent on the suns incidence angle. As mentioned the g-value is calculated with the assumption that the sun is perpendicular to the glazing and shading system. Though when the sun is perpendicular to the glazing and shading system the reflection of the solar radiation is at the minimum level. This leads to an overestimation of the g-value since the sun is rarely or never perpendicular to the window. Hence the calculated g-value according to DS/EN 13363-1 assumes that the solar heat gain entering the room is higher than it is in reality.

- During the talk with Steffen E. Maagaard he explained that when changing between a double and a triple glazed window the influence on the total g-value of the combined glazing and shading system is not well defined either.
  Since a part total g-value depends on numerous reflections between the different glazing layers and the shading device, it is fair to assume that the number of glazing layers has an impact on the g-value. This impact will be analysed through experiments using a double and a triple glazed window respectively.

- It would be assumed that the size of the numerous reflection contributions, mentioned in the previous item, would be dependent on the reflectance level of the shading device. Therefore different types of shading should be tested in combination with the two window types. Both windows will be tested with a highly absorbing and a highly reflecting blind.

- Furthermore the majority of Danish consulting engineers within the field of indoor environment and energy use the Danish building simulation tool BSim. In BSim the g-value of a window is dependent of the incidence angle on the relevant window. However the g-value of a solar shading device in BSim is calculated from the assumption that the sun is perpendicular to the shading. Consequently the g-value of a glazing system combined with internal solar shading is overestimated in BSim.
  - On the basis of this issue, a study will be made in this project. During this study the project group will try to determine the significance of the overestimation of the total g-value using both hand calculations and BSim.
    The study of the g-value accuracy in BSim will be divided into periodic studies. This means that it will be investigated in which periods of the year that this overestimation is most significant and has the largest influence on the energy consumption of buildings.

Part II

Experiment

5 Description of "the Cube"

For the experimental work of this project a test facility called the Cube is used. This is located south-east of Aalborg City near by the main campus of Aalborg University as illustrated on figure 5.1.

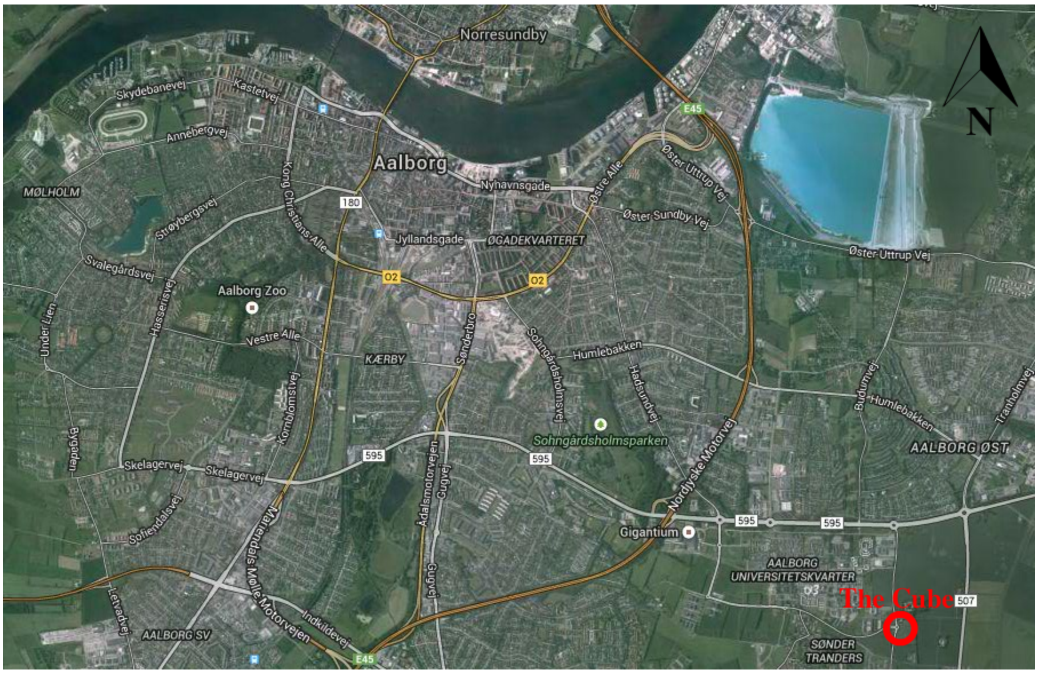

Figure 5.1: The picture shows that the Cube is located south-east of Aalborg city. [Eniro Danmark A/S, 2015]

5.1 Geometry

The Cube consist of a number of rooms, which will be describes further into detail in this chapter. A picture of the Cube is presented in figure 5.2.

Figure 5.2: A picture of the test facility "the Cube".

The window is placed in the test zone of the facility and it is facing directly south. In figure 5.3 the ground plan of the Cube can be seen.

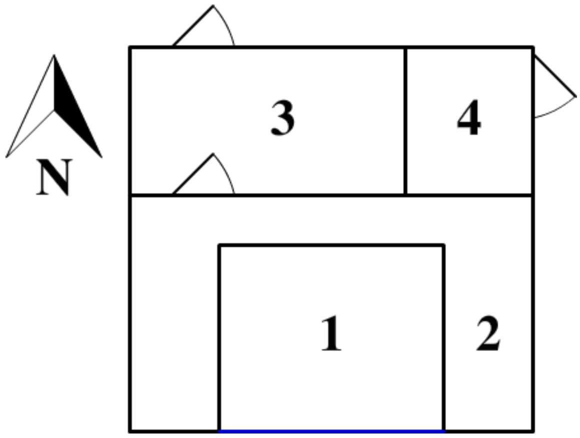

Figure 5.3: Top view of the Cube. Zone 1: Test zone. Zone 2: Guarding zone. Zone 3: Instrument room. Zone 4: Engine room.

As the figure shows the test zone is surrounded by the guarded zone. The guarded zone surrounds the test zone in all directions except for the southern façade, which is facing outside. The temperature of the guarded zone can be controlled and measured, which produces a higher accuracy.

The floor area and the volume of the test zone is presented in table 5.1.

Zone	Floor area [m^2]	Room volume [m^3]
1 (test zone)	9.94	27.32

Table 5.1: The floor area and volume of the Cube.

5.2 Systems

In order to control the temperature and air change rate in the test zone, it is essential to have systems that can provide the appropriate amount of heating, cooling and ventilation. These systems at the Cube is explained in the following.

The test zone is heated up by two electrical radiators, which is controlled by a set point in the test zone. The two radiators are placed below the window, and they can at its maximum perform heating at an effect of approximately 1700 W. There is no heating system in the guarded zone, although an electrical radiator can easily be added if needed. In figure 5.4 on the next page a section cut of the Cube is illustrated, where the cooling and ventilation system among other things can be seen.

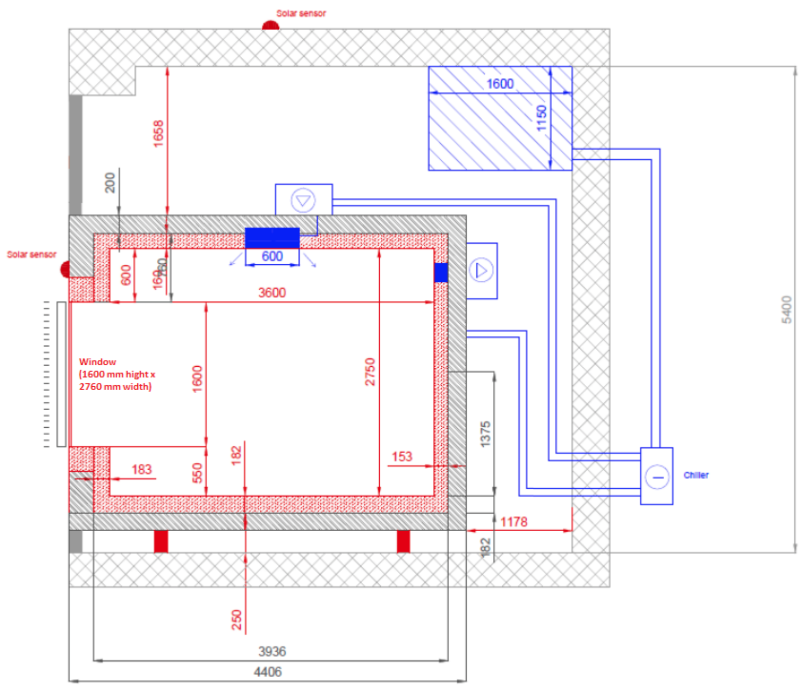

Figure 5.4: The Cube seen from the side. The illustration includes the cooling and ventilation systems together with all the measures of the geometry.[Dreau, 2014]

As the figure shows,there are two ventilation systems in the Cube; one for the test zone and one for the guarding zone.The ventilation system for the test zone is supplied with air from the guarding zone, just as the exhausted air from the test zone goes back to the guarding zone. During measurements this ventilation system will ventilate the test zone with a airflow of $2.5\,\mathrm{l/s \cdot m^2}$, which correspond to an air change rate of $3.27\,\mathrm{h^{-1}}$. There is a bigger ventilation system in the guarding zone and this is supplied with outdoor air.
As it also can be seen from figure 5.4 a chiller is connected to three different cooling systems. The chiller is supplied with distilled water, which is cooled down and distributed to the different cooling systems. The ventilation system in the guarding zone has a cooling coil that receives cool down water from the chiller. Further there is placed a chilled beam FF in front of the inlet in the test zone. This chilled beam cools down the inlet air for the test zone and is also connected to the chiller. The cooling capacity of the chilled beam is approximately 550 W. The last cooling system connected to the chiller is the radiant wall. The radiant wall is equipped with tubes inside of itself. Cooled down water from the chiller is circulating in these tubes, which decreases the surface temperature of the wall and thereby increases the radiant cooling in the test zone. The radiant wall has a cooling capacity of approximately 250 W.

Section A.1 on page 87, *Measuring Devices and Uncertainties*, in appendix is explaining which measuring devices are used for the experiment, and what the uncertainties of these are.

6 Glazing and Shading Systems

In the following chapter the chosen window and shading types will be presented along with their properties. This will be followed up be a calculation of the total g-value of the different window and shading types in combination.

6.1 Glazing Systems

For the experiments two different windows have been used. The first window is a Pilkington window with two layers of glazing divided by a cavity of 90 % of argon and 10 % of air. The design of the double glazed window is shown in figure 6.1 on the left.
The second window is a Sanit-Gobain window with three layers of glazing. This results in to cavities, which are both filled with 90 % of argon and 10 % of air. The design of the triple glazed window is shown in figure 6.1 on the right.

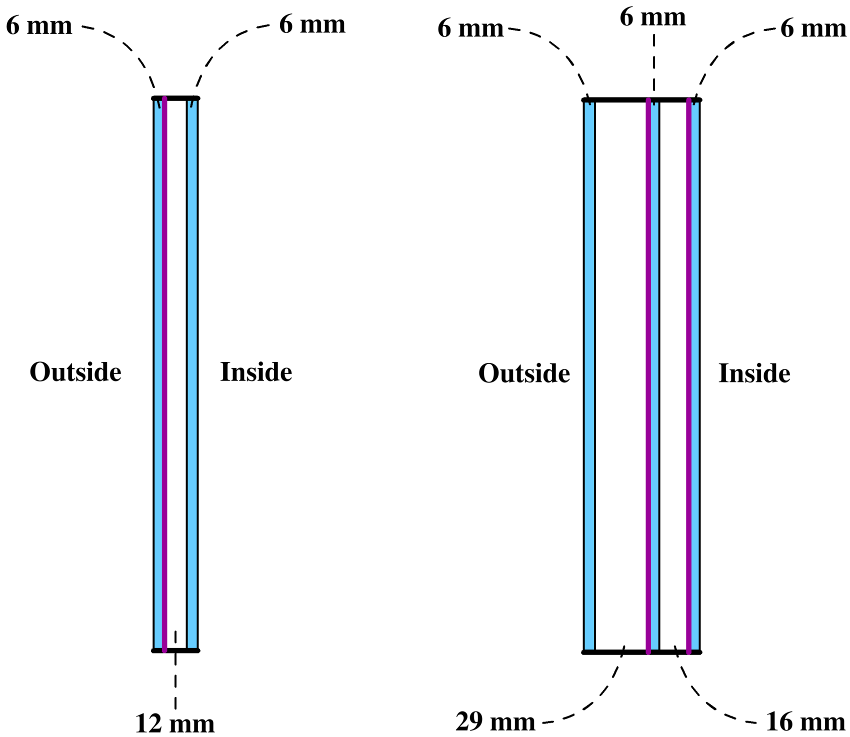

Figure 6.1: The design of the double glazed Pilkington window is presented to the left, and the triple glazed Saing-Gobain window in shown on the right. The purple collar indicates coating on the glazing. The thickness of each layer is shown on the figure.

The energy performance factors for both windows are shown in table 6.1 on the following page along with the U-value and g-value of each window.

Window	No. of glazing	g-value [-]	U-value $\left[\frac{\mathrm{W}}{\mathrm{m^2K}}\right]$	τ_v	ρ_v	α_v
Pilkington	2	0.36	1.20	32 %	35 %	33 %
Saint-Gobain	3	0.54	0.56	44 %	31 %	25 %

Table 6.1: Energy performance factors for the two windows, where τ_v is the transmittance, ρ_v is the reflectance, and α_v is the absorbance of the window. Also the g-value and the u-value is presented.

6.2 Shading Systems

There has also been used two different types of solar shading. Both of them are internal blinds from the French manufacturing company Mermet. When choosing the two different types of blinds the main idea was to have a dark and highly absorbing blind and a bright and highly reflecting blind. This resulted in a dark blind called Charcoal Grey and a bright blind called White Pearl. Both can be seen in figure 6.2.

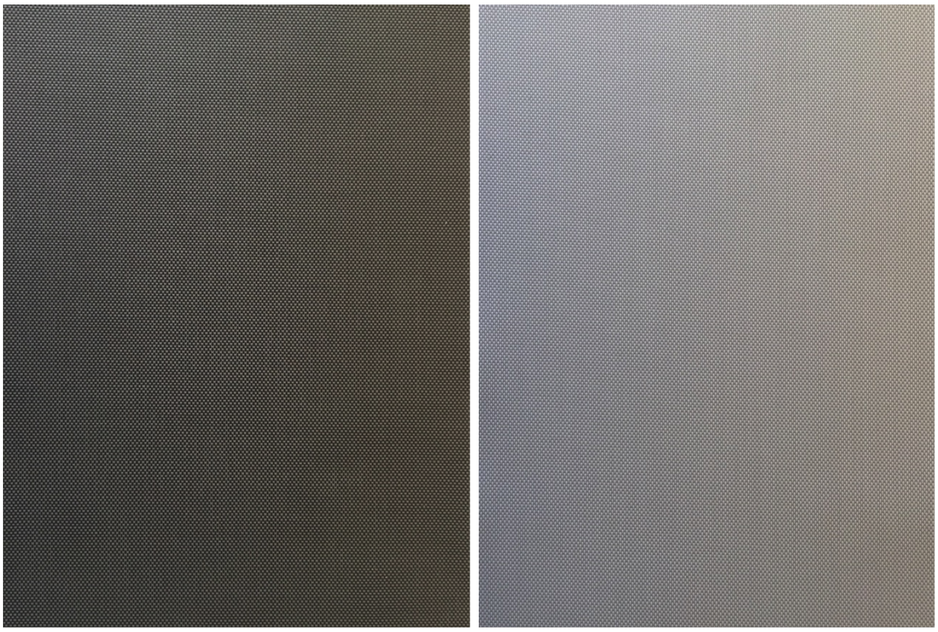

Figure 6.2: The dark blind, Charcoal Grey, is in the left picture, while the bright blind, White Pearl, is in the right picture.

The energy performance factors for the two blind are presented in table 6.2.

Blind	τ_v	ρ_v	α_v
Charcoal Grey	9 %	11 %	80 %
White Pearl	17 %	52 %	31 %

Table 6.2: Energy performance factors for the two blinds, where τ_v is the transmittance, ρ_v is the reflectance, and α_v is the absorbance of the blind.

6.3 Combined Glazing and Shading

As described in chapter 2 on page 5, the total g-value of a combined glazing and shading system can be calculated from equation 2.3 on page 8 obtained in DS/EN 13363-1. Since the necessary window and shading properties are known, and presented in the two previous sections, the theoretical total g-value of the different combined glazing and shading systems can be obtained. A calculation example using the double glazed window in combination with the Charcoal Grey shading is presented in equation 6.1.

$$\begin{aligned} g_t &= g \cdot \left(1 - g \cdot \rho_{e,B} - \alpha_{e,B} \cdot \frac{G}{G_2}\right) \\ \Rightarrow g_t &= 0.36 \cdot \left(1 - 0.36 \cdot 0.11 - 0.8 \cdot \frac{1.15\,\mathrm{W/m^2 \cdot K}}{30\,\mathrm{W/m^2 \cdot K}}\right) = 0.33 \end{aligned} \tag{6.1}$$

When the total g-value for each window and shading combination is known, the shading coefficient can be calculated from equation 2.1 on page 5 from chapter 2 on page 5. A calculation example using the same shading and window type as before is presented in equation 6.2.

$$\begin{aligned} SC &= \frac{g_t}{g_w} \\ \Rightarrow SC &= \frac{0.33}{0.36} = 0.93 \end{aligned} \tag{6.2}$$

The shading coefficients are used in BSim later on in the project.

The total g-value and the shading coefficient for all four combinations are presented in table 6.3.

Window	Double glazed		Triple glazed	
Shading	White Pearl	Charcoal Grey	White Pearl	Charcoal Grey
Total g-value	0.29	0.33	0.39	0.50
Shading Coefficient	0.80	0.93	0.71	0.93

Table 6.3: The total g-value of the four different combinations of windows and shadings.

Since the triple glazed window has a g-value of 0.54 and the double glazed window only has a g-value of 0.36, the total g-value for the combinations with the triple glazed window are higher. In the table it is also visible that the total g-value is lower for the combinations with the White Pearl blind compared to those with the Charcoal Grey blind. The reason for this is that the White Pear has a higher reflectance by which is keeps out a larger part of the solar radiation.

The correlation between highly reflecting or highly absorbing shading types compared to windows with a high of low g-value is presented in chapter 2 on page 5.

The data sheets for the different windows and solar shadings used in the experiment can be found in section A.2 on page 91, *Data Sheets of Glazing and Shading Systems*, in appendix.

7 Measurements

As mentioned earlier in the project, different solar shading devices in combination with different window types have been compared for this project. They have been compared on their ability to decrease the solar heat gain on sunny days. For this purpose four experiments have been conducted in the Cube. In this chapter a presentation of the different measurements will be described along with the energy balance of the Cube.

7.1 Execution

The main goal of the measurements is to be able to evaluate the heat gain from the sun inside the experimental zone of the Cube. When this heat gain is known, the total g-value of the glazing system and blind combined can be calculated. This is done by measuring all other heat gains and losses in the experimental zone of the Cube, and the heat gain from the sun can be calculated from the energy balance of the zone. This will be described more into detail i the in section 7.2 on the following page.

To be able to calculate the most accurate energy balance in the experimental zone, the temperature is kept constant during all measurements. Because thermal comfort is not a criteria taken into account in this project, the temperature can be kept at a level outside the comfort zone. When keeping the temperature constant, the thermal mass of the room is taken out of the equation, which leads to a lower uncertainty.
After several initial measurements the project group has learned that a suitable constant temperature for the zone is 29 °C. This temperature can be maintained both during warm sunny days as well as during cold nights.

For all measurements the controllable cooling from the radiant cooling wall and the chilled beam is kept constant. Thereby only the heating from the radiators fluctuate during the measurements according the amount of the heat gain from the sun. The sizes of the different parameters in the energy balance will be presented in section 7.2 on the next page.

To be able the evaluate the interaction between the two window types and the two types of blinds, four different measurements have been conducted. In table 7.1 it is shown which blind and window type is used for each of the four measurements.

Measurement No.	Window	Blind	Measuring period
1	Double glazed Pilkington	White Pearl	April 8 - April 11
2	Double glazed Pilkington	Charcoal Grey	April 3 - April 6
3	Triple glazed Sanit-Gobain	White Pearl	April 29 - May 4
4	Triple glazed Sanit-Gobain	Charcoal Grey	May 4 - May 11

Table 7.1: The window and blind type used for each of the four conducted measurements.

7.2 Energy Balance

The energy balance of the Cube is expressed by equation 7.1.

$$
\begin{aligned}
Q_{Air} = {} & \overbrace{Q_{Sun}}^{\text{Uncontrolled heating}} + \overbrace{Q_{Radiator}}^{\text{Controlled heating}} + \overbrace{Q_{Infiltration} + Q_{Transmission}}^{\text{Uncontrolled cooling}} \\
& + \underbrace{Q_{Chilled\ beam} + Q_{Radiant\ wall} + Q_{Ventilation}}_{\text{Controlled cooling}}
\end{aligned}
\tag{7.1}
$$

Where:

Q_{Air}	The change in internal energy in the room [W]
Q_{Sun}	The solar heat gain in the room [W]
$Q_{Radiator}$	The heating power from the radiators in the room [W]
$Q_{Chilled\ beam}$	The cooling power from the chilled beam in the room [W]
$Q_{Radiant\ wall}$	The cooling power from the radiant wall in the room [W]
$Q_{Ventilation}$	The cooling power from the ventilation system in the room [W]
$Q_{Infiltration}$	The heat loss through infiltration in the room [W]
$Q_{Transmission}$	The heat loss through transmission and line loss in the room [W]

The change in internal energy in the room is calculated for a time step of 1 second and is given by equation 7.2.

$$Q_{Air} = V_{Room} \cdot \rho_{Air} \cdot C_{P,Air} \cdot \frac{\delta T}{\delta t} \tag{7.2}$$

Where:

Q_{Air}	The change in internal energy in the room [W]
V_{Room}	The volume of the room [m^3]
ρ_{Air}	The density of air $\left[\frac{\mathrm{kg}}{\mathrm{m}^3}\right]$
$C_{P,Air}$	The specific heat capacity of air $\left[\frac{\mathrm{J}}{\mathrm{kg \cdot K}}\right]$
δT	The temperature difference in the room each second [°C]
δt	The time step [s]

Ideally the change in internal energy, Q_{air} should be 0 W during the whole period of the measurements, because the temperature of the room is set to be constant. There has though been minor fluctuations during the measurements. On figure 7.1 on the next page Q_{air} is graphically presented during a period of approximately three and a half days.

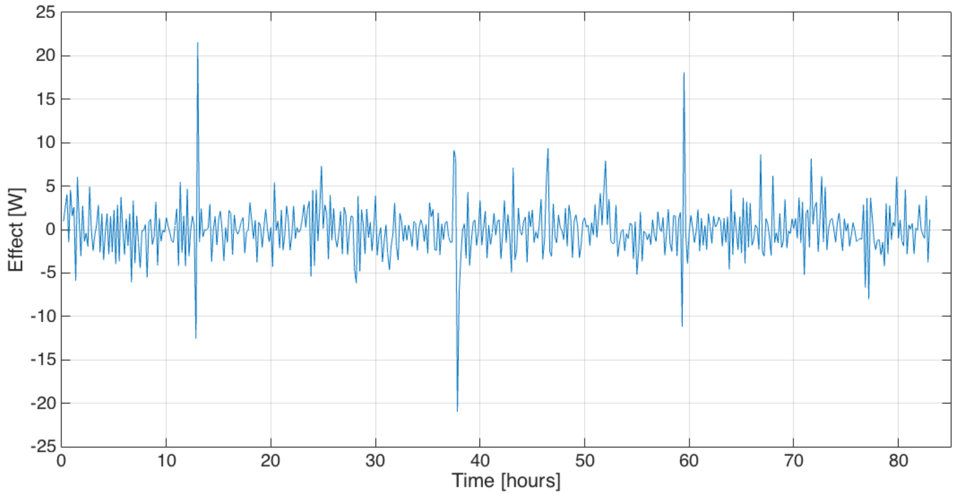

Figure 7.1: Graphical presentation of the change in internal energy, Q_{air}. The data is averaged over every 10 min to get a smoother and presentable graph.

With the exception of a few values, Q_{air} fluctuates between 5 W and −5 W. Later on in this chapter it will be clear that this can be considered relatively close to zero compared to the rest of the parameters from the expression in equation 7.1 on the facing page.

Controlled Cooling

The chilled beam is located in the ceiling of the experimental zone of the Cube. This is connected to a chiller, which lets cold water through the beam.

The west oriented wall in the experimental zone of the Cube is a radiant cooling wall, which contributed to the cooling of the room as well. This is also connected to a chiller, which lets cold water through the radiant wall.

The cooling power of these two cooling systems is calculated by equation 7.3.

$$Q_{Cooling} = q_c \cdot \rho_{Water} \cdot C_{P,Water} \cdot \Delta T \tag{7.3}$$

Where:

$Q_{Cooling}$	Controlled cooling from the chilled beam and radiant cooling wall [W]
q_c	The water flow from the chiller through the cooling system $\left[\frac{\mathrm{m}^3}{\mathrm{s}}\right]$
ρ_{Water}	The density of water $\left[\frac{\mathrm{kg}}{\mathrm{m}^3}\right]$
$C_{P,Water}$	The specific heat capacity of water $\left[\frac{\mathrm{J}}{\mathrm{kg\cdot K}}\right]$
ΔT	The difference between the inlet and return temperature [°C]

The cooling added to the room by the ventilation system is given by equation 7.4.

$$Q_{Ventilation} = q_v \cdot \rho_{Air} \cdot C_{P,air} \cdot (T_{Inlet} - T_{Room}) \tag{7.4}$$

Where:

$Q_{Ventilation}$	The cooling power from the ventilation system in the room [W]
q_v	The air flow into the room $\left[\frac{m^3}{s}\right]$
ρ_{Air}	The density of air $\left[\frac{kg}{m^3}\right]$
$C_{P,air}$	The specific heat capacity of air $\left[\frac{J}{kg \cdot K}\right]$
T_Inlet	The inlet temperature from the ventilation system [°C]
T_Room	The temperature of the test zone in the Cube [°C]

As mentioned earlier the ventilation system for the experimental zone is supplied with air from the guarding zone. The temperature in the guarding zone has a set point of 21 °C, in order to get a relatively large cooling load from the ventilation system. With a temperature set point in the experimental zone of 28 °C, ΔT for the ventilation system is approximately 7 °C.

The cooling power from the chilled beam, the radiant wall and the ventilation system is graphically presented in figure 7.2. The plot is for a period of approximately 3 and a half days.

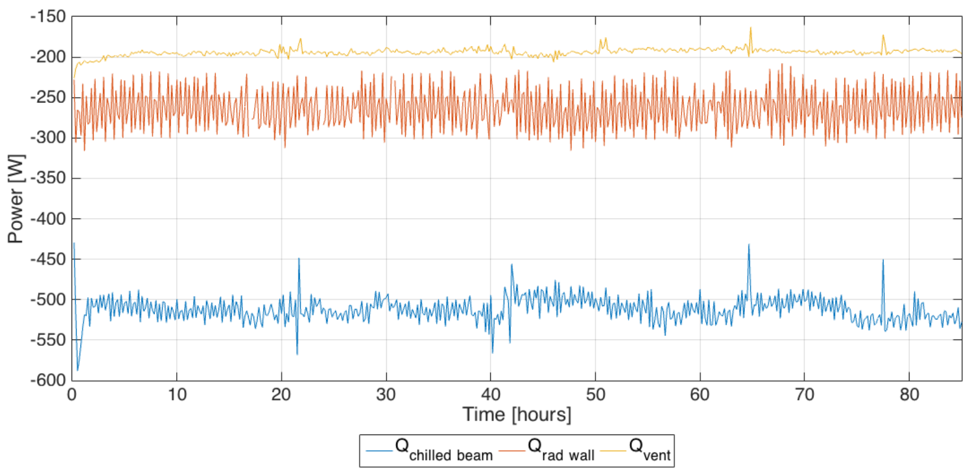

Figure 7.2: The power of the three controlled cooling systems in the experimental zone of the Cube. The data is averaged over every 10 min to get smoother and presentable graphs.

The temperature in the guarded zone is controlled by a large ventilation system, which makes the this temperature quite steady. As before mentioned the ventilation inlet air for the experimental zone is taken from the guarded zone. Hence the ventilation inlet temperature is quite steady as well. The temperature is also kept constant. Therefore Q_{Vent} in figure 7.2 stays at a relatively steady level.
The cooling power from $Q_{Rad\ wall}$ is more fluctuating though. The water flow is about 0.123 l/s ± 0.002 l/s. So this does not fluctuate much. The inlet and return water of the radiant cooling wall has a temperature difference of around 0.6 °C ± 0.15 °C. So the temperature difference has a percentage deviation of ± 25 %, which leads to the fluctuating results in the power of the radiant wall.

The cooling power of the chilled beam is less fluctuating than the radiant cooling wall. The chilled beam is supplied with water from the same chiller as the radiant wall, though the flow is lower and the temperature difference is higher than for the radiant wall. The deviations of the flow and temperature difference are not known for the chilled beam since the power is calculated in advance and given directly in Watts. Though instant values of the flow and temperature difference can be read in the Cube. This shows that the flow is approximately 0.218 l/s, and the temperature difference is around 2.3 °C. Because the chilled beam is connected to the same chiller, it is fair to assume that the deviations are the same. Thereby the percentage deviation of the temperature difference is only around ± 7 %. Therefore the power of the chilled beam is more steady than the power of the radiant wall, which can be seen in figure 7.2 on the preceding page.

Uncontrolled Cooling

In the Cube only the south wall is facing outside. The rest of the walls are all facing the guarding zone. The infiltration flow is only known to the outside. This means that the infiltration from the guarded zone is not taken into consideration. This is obviously an error. Though the pressure difference between the two zone is controlled and kept a zero, which minimizes the flow. So despite the temperature difference of around 7 °C between the two zones, the infiltration loss towards the guarded zone is kept at a minimum. The infiltration towards the outside is given by equation 7.5.

$$Q_{Infiltration} = q_i \cdot \rho_{Air} \cdot C_{P,air} \cdot (T_{Outdoor} - T_{Room}) \tag{7.5}$$

Where:

$Q_{Infiltration}$	The heat loss through infiltration in the room [W]
ρ_{Air}	The density of air $\left[\frac{\text{kg}}{\text{m}^3}\right]$
$C_{P,air}$	The specific heat capacity of air $\left[\frac{\text{J}}{\text{kg}\cdot\text{K}}\right]$
q_i	The infiltration air flow from outside into the room $\left[\frac{\text{m}^3}{\text{s}}\right]$
$T_outdoor$	The outdoor temperature [°C]

The transmission loss for the experimental zone of the Cube is divided into several parts. For each construction layer of the Cube the transmission loss is calculated from equation 7.6, which is given in DS 418.

$$Q_{Transmission} = \sum (A \cdot U \cdot \Delta T) \tag{7.6}$$

Where:

$Q_{Transmission}$	The heat loss through transmission and line loss in the room [W]
A	The area of each construction element [m^2]
U	The u-value of each construction element $\left[\frac{\mathrm{W}}{\mathrm{m}^2\cdot\mathrm{K}}\right]$
ΔT	The temperature difference between inside and the other side of each layer $\left[\frac{\mathrm{W}}{\mathrm{m}^2\cdot\mathrm{K}}\right]$

The heat loss from the two uncontrolled cooling parameters, infiltration and transmission, are graphically presented in figure 7.3. The plot is for a period of approximately three and a half days.

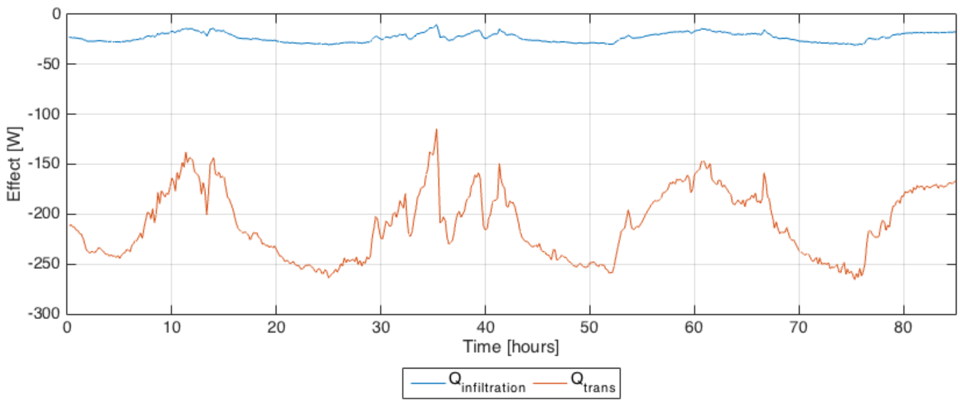

Figure 7.3: The heat loss from the two uncontrolled cooling parameters, infiltration and transmission. The data is averaged over every 10 min to get smoother and presentable graphs.

Because the infiltration loss and a part of the transmission loss is dependent of the outside temperature, the losses are increased during night time when the temperature outside decreases. This is visible in figure 7.3 for both parameters.

Heating Parameters

The Cube is automatically heated by two radiators. These are connected to a power meter, which directly gives the power of the two radiators. The radiators are controlled from a set point of 28 °C in the experimental zone.

Since all other parameters in equation 7.1 on page 36 are known, the solar heat gain can be calculated by solving for $\mathrm{Q_{Sun}}$ in the equation. The correlation between the two heating parameters, $\mathrm{Q_{Radiator}}$ and $\mathrm{Q_{Sun}}$, is presented in figure 7.4 on the next page. The plot is for a period of approximately three and a half days.

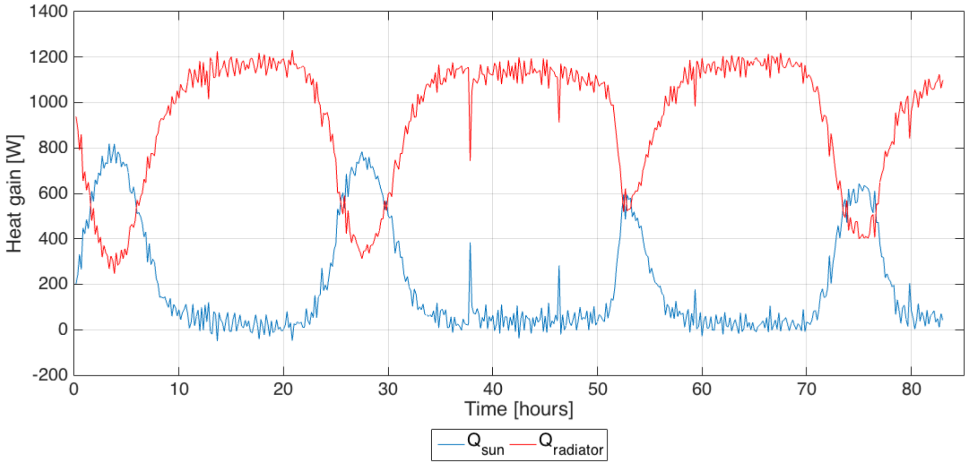

Figure 7.4: The heat gain from the two heating parameters, the radiators and the sun. The data is averaged over every 10 min to get smoother and presentable graphs.

The figure shows that during night time, where the sun is not present, the heating power is relatively steady around 1200 W. When the solar radiation increases during the day, the power of the radiators drops correspondingly.

The calculations of the energy balance is attached on the appendix CD as number 2.

Part III

Data Treatment

8 Solar Heat Transmittance

For the four different measurements, presented in table 7.1 on page 35, the goal is to be able to evaluate the total g-value of the combined glazing and shading systems during daily periods. In this chapter the experiment with the double glazed window combined with the highly reflecting White Pearl solar shading will be used as an example on how to calculated and evaluate the g-value. The calculation method is the same for each of the four situations, which is why the detailed g-value calculation of the three remaining experiments will not presented. After the presentation of the calculation method, the g-value for each measurement will be analysed and compared to each other.

All data for the graphs in this chapter are hourly average values.
Several of the graphs in this chapter are plotted with a 24 hour day on the x-axis. They should be read in a way that 1 on the x-axis correspond to the average of the data from 00:00 to 01:00. This means that the x-axis goes from hour 1 to hour 24.

8.1 Combination 1: Double glazing/White Pearl

As mentioned the double glazed window combined with the White Pearl solar shading will be used as a thorough example of how to calculate and evaluate the total g-value. This is done in the following section.
The experimental g-value can be determined by comparing the total solar radiation just outside the window with the solar heat gain inside the room. The solar heat gain inside the room is calculated from the energy balance with equation 7.1 on page 36. The solar radiation outside the window is measured with a pyranometer. In figure 8.1 these two parameters are graphically presented for a four day period between the 8th and the 11th of April.

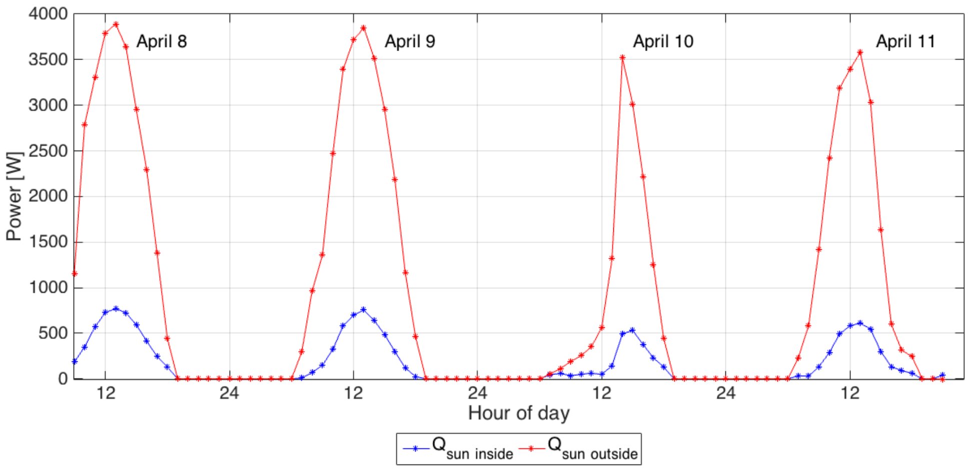

Figure 8.1: The solar radiation outside the window compared to the solar heat gain inside the room calculated from the energy balance.

As expected the combined glazing and shading system keeps out a relatively large part of the solar radiation reaching the window. Figure 8.1 on the previous page shows that the two graphs follow approximately the same tendency. During night time where the sun is down the solar power inside and outside the room is zero. When the sun rises both curves start rising and they both peak around noon. It is not visible on this graph that the time of peak is located around noon, but this will be clear in several graphs later on in the report. In chapter 2 on page 5, *Window and Shading Properties*, the theoretical expression for calculating both the window g-value and the total g-value was given.
The experimental total g-value for the window and shading can be calculated from equation 8.1.

$$g_{t\ (exp)} = \frac{Q_{Sun\ inside}}{Q_{Sun\ outside}} \tag{8.1}$$

Where:

$g_{t\ (exp)}$	The experimentally determined total solar heat transmittance [-]
$Q_{Sun\ inside}$	The solar heat gain inside the room [W]
$Q_{Sun\ outside}$	The solar radiation just outside the window [W]

The total g-value iscalculated for each hour during the four day period. The calculated g-values are presented in figure 8.2.

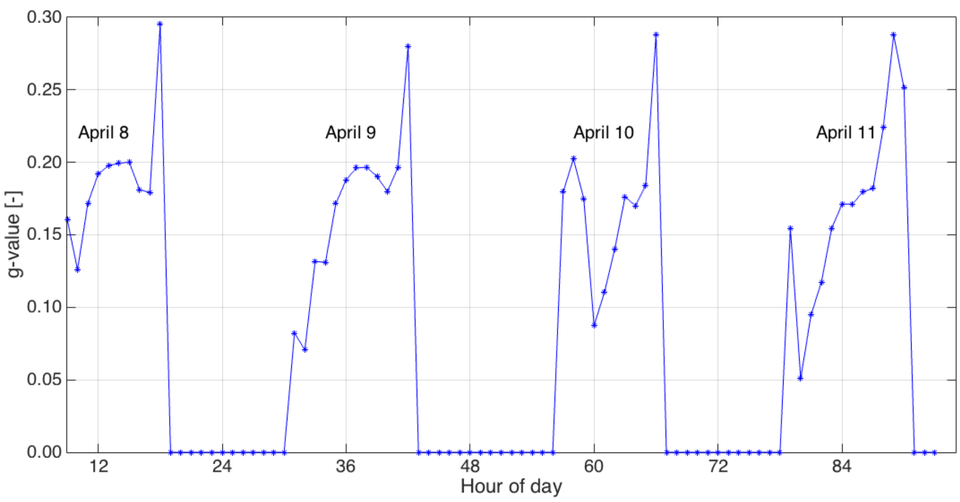

Figure 8.2: The experimentally conducted total g-value of the combined double glazed window and the White Pearl blind.

The suns incidence angle on the window changes during the days as presented in chapter 3 on page 17. Therefore it is interesting to find days that give the clearest representation of the g-value for the longest period of time, since this would give the most comprehensive picture of the g-values dependence of the angle of incidence.
The 8th and the 9th of April were both mainly sunny days with few clouds on the sky. These two days also give the clearest representation of the g-value during the day. The

10th and the 11th of April, were a bit more cloudy than the others. On cloudy days the percentage of diffuse solar radiation will normally rise. To see if this is the case the amount of diffuse and direct solar radiation is plotted for the four day period in figure 8.3.

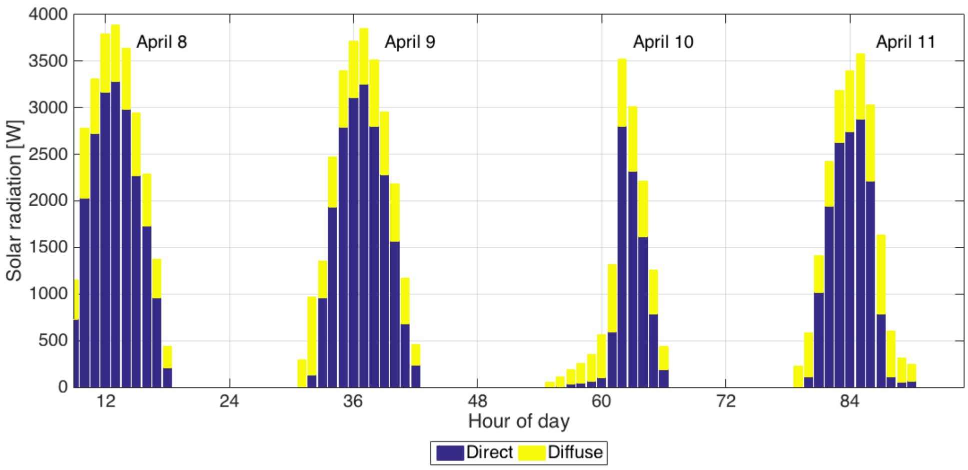

Figure 8.3: The experimentally conducted total solar heat transmittance of the combined double glazed window and the White Pearl blind.

As expected the figure shows that the amount of direct solar radiation is at a higher level during the first two days. On the contrary the diffuse solar radiation is more dominant for the last two days. So it would seem that the clearest picture of the incidence angle dependent g-value is obtained on clear and sunny days. This is in good correspondence with the theory about diffuse solar radiation explained in chapter 3 on page 17, *Solar Geometry*, which states that the g-value for diffuse solar radiation is independent of the angle of incidence.
Therefore it is chosen to take a closer look at the sunny day of April 9.

In figure 8.4 the solar heat gain inside the room is plotted along with the solar radiation outside the window. This is done for the 24 hour period of April 9.

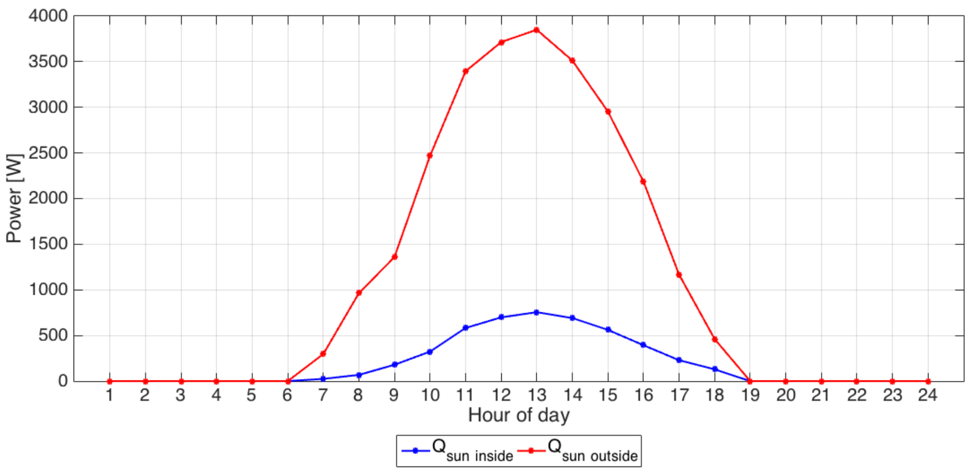

Figure 8.4: The solar power inside and outside the room for the 9th of April using the double glazed window and the White Pearl blind.

The figure shows that solar radiation both inside room and outside the window peaks at 13 on the x-axis. As earlier explained 13 corresponds to the average value from 12:00 to 13:00. So it makes sense that the peak of the solar radiation is around midday.
The graph also shows that the solar heat gain inside the room has a steeper positive slope in the morning than the negative slope in the afternoon. On the contrary the solar radiation outside the window looks more symmetrical about midday. This has quite a drastic effect on the g-value during the day. In figure 8.5 the g-value is graphically presented for the 9th of April.

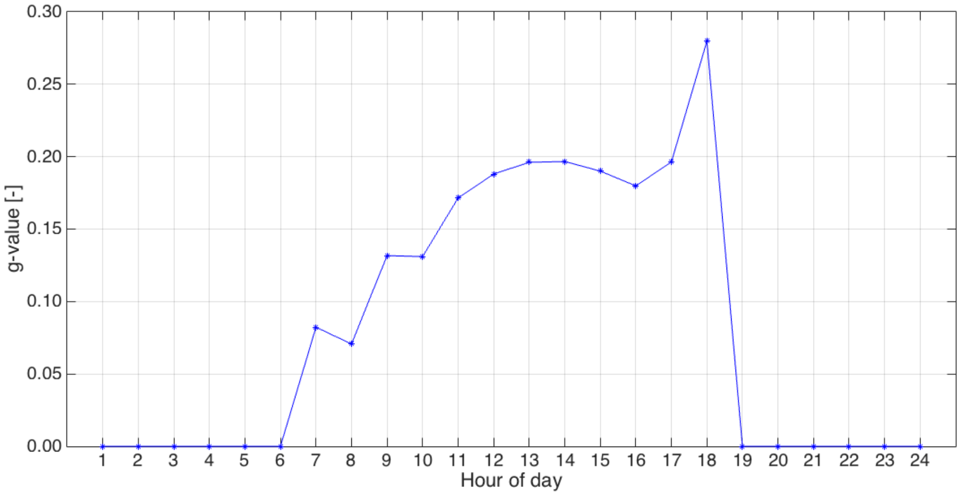

Figure 8.5: The total g-value for the double glazed window combined with the White Pearl solar shading for April 9.

The figure shows that the softer slope of the solar heat gain during the afternoon results in an increased g-value. To see how this corresponds with the theory of the g-values dependence of the incidence angles, presented in chapter 3 on page 17, *Solar Geometry*, the incidence angle is plotted along with the g-value in figure 8.6.

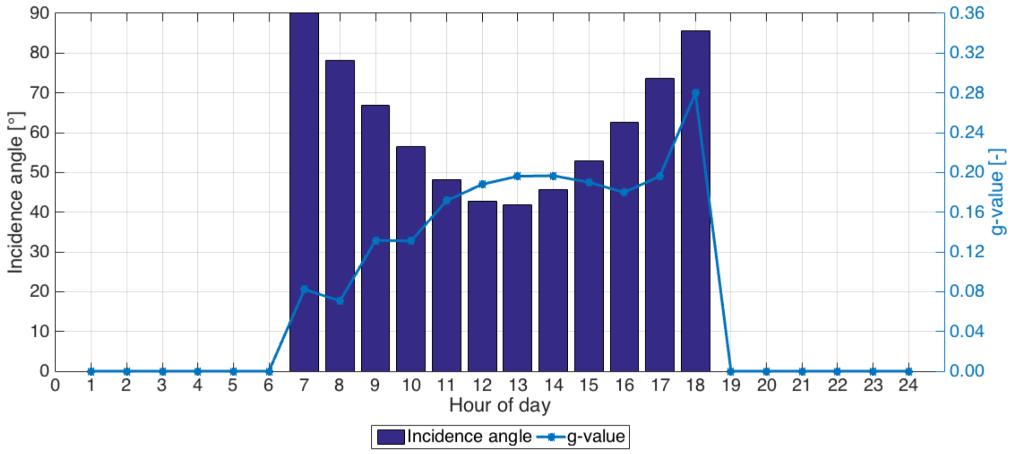

Figure 8.6: The incidence angle and the total g-value for the double glazed window combined with the White Pearl solar shading for the April 9.

According to the theory from chapter 3 on page 17, *Solar Geometry*, the g-value should increase when the incidence angle decreases. This fits relatively well during the morning period in figure 8.6. Though in the afternoon the g-value does not decrease with the increase of the incidence angle.
If referring back to figure 8.2, it is seen that this lack of correlation during the afternoon is not unique for the 9th of April. Indeed this is the case for all four days during the measuring period. The tendency for all four days shows that the g-value stays at a relatively high level during the beginning of the afternoon and at the end of the day it accelerates and peaks at a value around 0.30. This could be an indication of error in the measurements during the afternoon.
It has been decided to focus on the morning part of the g-value graphs when moving on in the project. This means the part stretching from 0 to 13 on the 24 hour graphs.

Though the morning part of the g-value graph for the 9th of April, seen in figure 8.6 on the preceding page, is more smooth and according to theory, it has a couple of minor oscillations. To see what might cause these oscillations, the amount of diffuse and direct solar radiation is plotted on the same graph as the g-value in figure 8.7

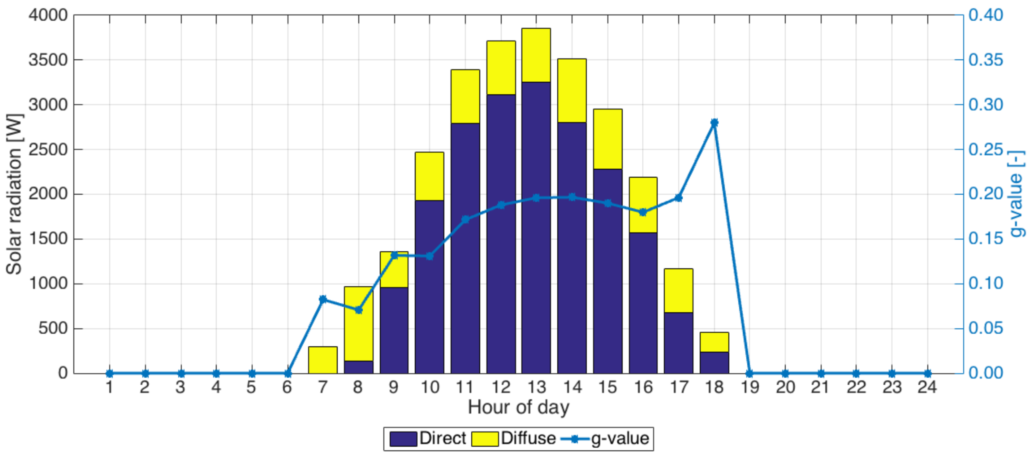

Figure 8.7: The total g-value for the double glazed window combined with the White Pearl solar shading compared to the amount of direct and diffuse solar radiation for the 9th of April.

It becomes clear from this figure, that the direct solar radiation at 7 on the x-axis is close to or equal to zero. In figure 8.6 on the preceding page it was visible that the incidence angle at this point is close to 90°. If a large amount of direct solar radiation reached the window at a high incidence angle like this one, it would result in a small total g-value. Though the diffuse solar radiation can be considered independent of the incidence angle, since the radiation is evenly distributed from the whole sky. Therefore an increased amount of diffuse solar radiation at a high angle of incidence may be the reason for the increase in g-value.
Also in point 9 on the x-axis an unexpected rise in the g-value occurs. This is harder to explain since the amount of direct solar radiation in this point is still at a relatively high level. In the beginning of this chapter figure 8.1 on page 43 11th of April has a relatively

sunny morning period but a more cloudy afternoon. Therefore the it is decided to take a closer look at the g-value and the amount of diffuse and direct solar radiation for April 11. This is presented in figure 8.8.

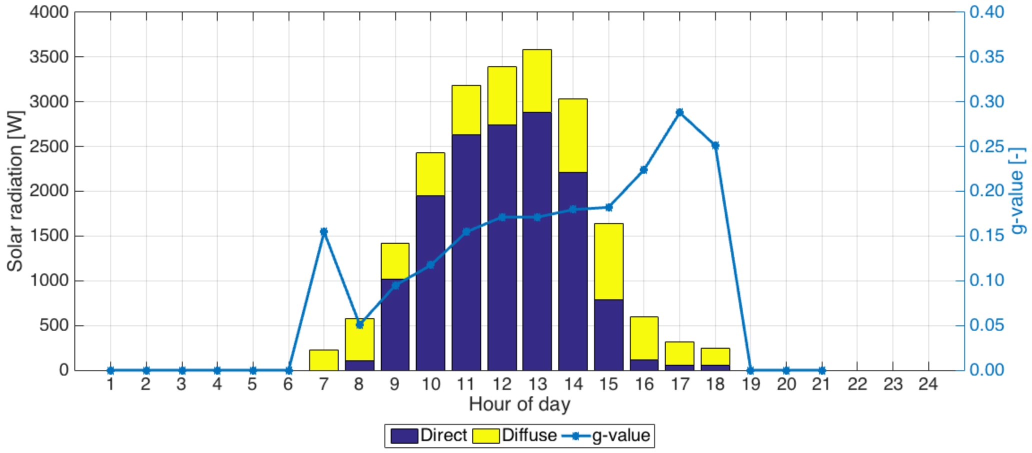

Figure 8.8: The total g-value for the double glazed window combined with the White Pearl solar shading compared to the amount of direct and diffuse solar radiation for the 11th of April.

As expected the afternoon contains a relatively low amount of direct solar radiation due to the cloudy weather. Though the morning period is more dominated by direct solar radiation. The general amount of total solar radiation is a bit lower during the whole day compared to April 9 but it is still at a reasonable level for measuring the g-value. An interesting thing about figure 8.8 is the thing that happens in point 9 on the x-axis, or rather the thing that does not happen. Because as figure 8.7 on the previous page showed that a sudden increase in g-value occurred at point 9 on April 9, figure 8.8 shows that the g-value follows the expected curve through point 9. If the amount of direct and diffuse solar radiation at point 9 for April 9 and 11 are compared it is seen that these are much alike. Therefore it seems fair to consider the increase in g-value in point 9 on April 9 as a result of measurement error.

To be able to compare the g-value of the two days in a comprehensive way, they are both plotted in figure 8.9 on the next page. As mentioned the focus is only on the morning period, so the plot is made up until 13 pm.

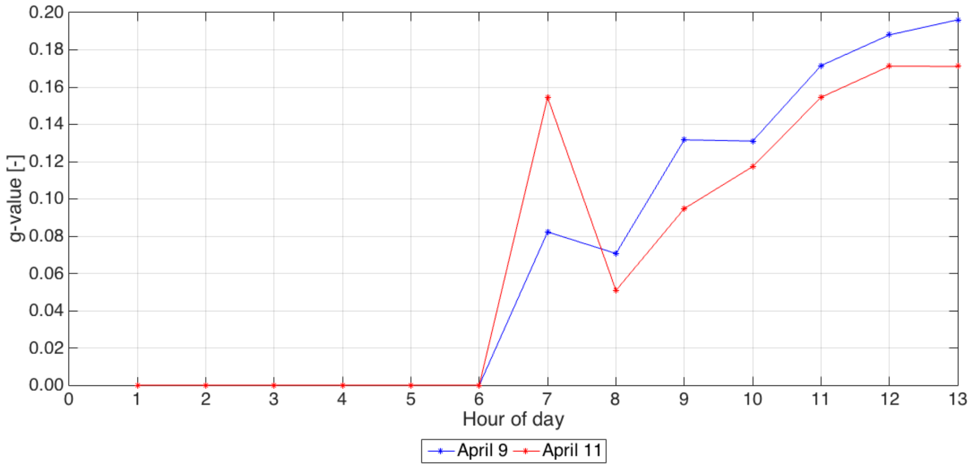

Figure 8.9: The total g-value for the double glazed window combined with the White Pearl solar shading on April 9 and April 11 respectively.

By comparing the g-value for the two different days it becomes clear that the radically increased g-value at hour 7 is a recurring tendency each day. Therefore this point is disregarded when describing the correlation between the g-value and the angle of incidence. It is considered fair to disregard this point when comparing the g-value to the angle of incidence, since it is caused by diffuse solar radiation.

To see the correspondence between the angle of incidence and the total g-value, these are plotted on the same graph in figure 8.10.

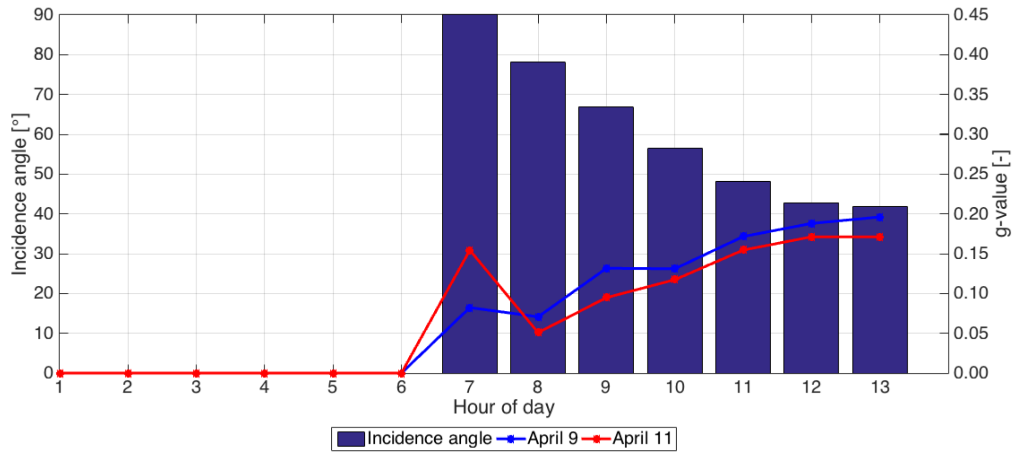

Figure 8.10: The incidence angle in the same graph as the total g-value for the double glazed window combined with the White Pearl solar shading during periods from hour 1 am till 13 pm.

Offhand there seems to be a relatively good correlation the between the two. Though to get a clear graphical picture of the correlation between the g-value and the incidence angle these are plotted against each other in figure 8.11 on the next page. This correlation is plotted for data as of point 8 up to and including point 13. That is from 7 am till 13 pm.

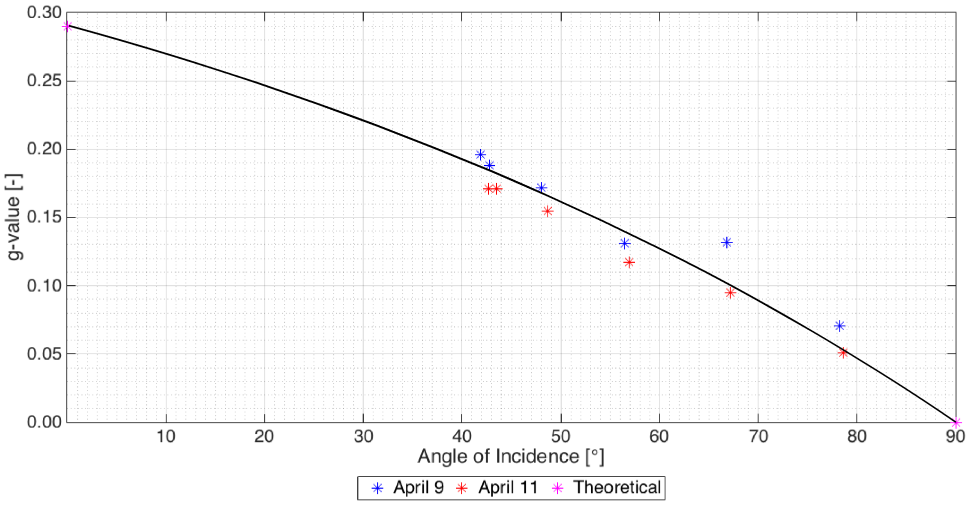

Figure 8.11: The correlation between the incidence angle and the total g-value for the double glazed window combined with the White Pearl solar shading during periods from hour 8 am till 13 pm.

In figure 8.11 two theoretical values are added to the graph. The one at incidence angle 0° is the theoretical total g-value of the double glazed window combined with the White Pearl shading calculated according to DS/EN 13363-1. This calculation is presented in chapter 6 on page 31, *Glazing and Shading Systems*, and is 0.29. The g-value from DS/EN 13363-1 is for a calculation at incidence angle 0°, which is why point [0°,0.29] is added to the graph. The other theoretical value is located in [90°,0]. This is made from the assumption that the g-value is zero when the sun does not inflict the window with direct solar radiation.
Because the measurements have been conducted in April the g-value is only measured for incidence angles down to around 42°, which is visible in figure 8.10 on the preceding page. The lower incidence angles occur in the winter months, so these have not been measured.
In figure 8.11 a trendline is added. This line is manually added by the project group to give a view of how the curve of the g-value is considered compared to the angle of incidence. In section 8.5 on page 58, this curve will be held up against the corrosponding curve for the remaining three combinations.

8.2 Combination 2: Double glazing/Charcoal Grey

In this section the combination of the double glazed window and the Charcoal Grey solar shading will be in focus. Measurements has been conducted for this combination during the period from April 4 till April 6.

In figure 8.12 on the next page the solar radiation outside the window is presented for this period alongside with the solar heat gain inside the room. On the right figure 8.13 on the facing page shows the total g-value for the morning period of all three days.

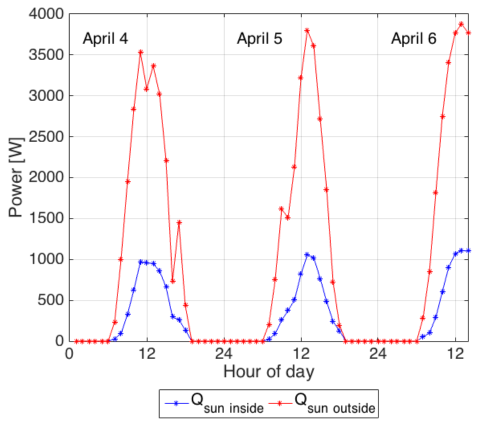

Figure 8.12: The solar radiation outside the window and the solar heat gain inside the room.

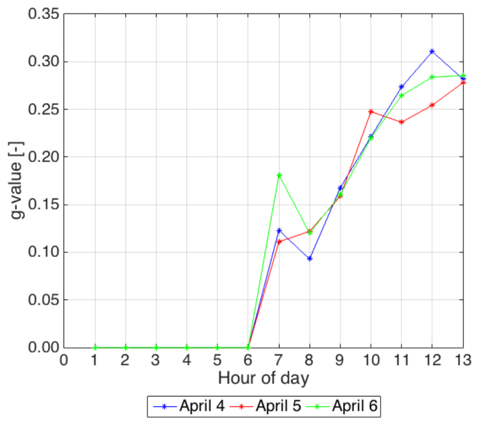

Figure 8.13: The total g-value for morning periods of all three days.

As for the first combination the afternoon periods for this combination give fluctuating results, which leads to suspicion of measuring error. Therefore it is also decided to disregard the afternoon periods when looking at the g-value for this combination.

Figure 8.12 shows that all three days has relatively sunny mornings, where the solar radiation rises in a reasonably steady curve. Therefore it has been decided to include all three days on the g-value plot in figure 8.13. To get a better idea of how sunny each of the three morning periods were, the amount of diffuse and direct solar radiation is plotted for April 4, 5 and 6 in figure 8.14, 8.15 and 8.16 on the next page respectively.

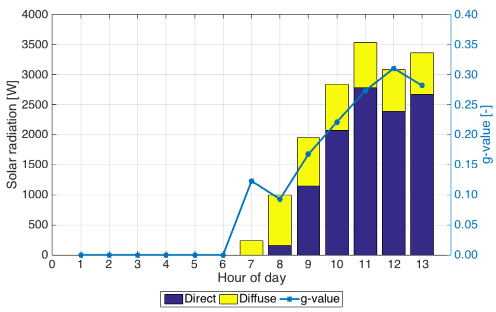

Figure 8.14: Direct and diffuse solar radiation for the 4th of April.

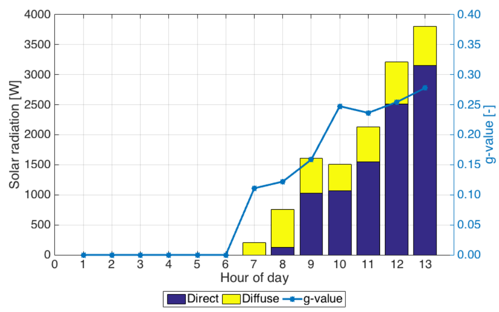

Figure 8.15: Direct and diffuse solar radiation for the 5th of April.

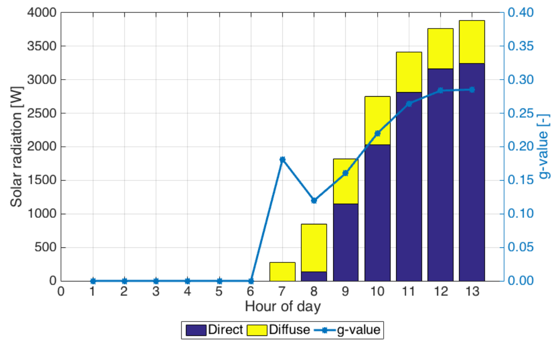

Figure 8.16: Direct and diffuse solar radiation for the 6th of April.

From the three figures it is visible that in hour 7 the same tendency as for the first combination is happening. So the present solar radiation is only diffuse, which leads to an enlarged g-value in this early morning hour.
In figure 8.14 on the preceding page the g-value at hour 12 is quite high compared to the other two days and it does not follow the tendency of the remaining curve. This can be explained with the drastic drop in solar radiation at hour 12 in figure 8.12 on the previous page.
By looking at the curves for diffuse and direct solar radiation it is clear that the 6th of April has the highest amount of direct solar radiation. Therefore the g-value curve for this day is smooth and in good correspondence with theory. Though the other two days also have fine periods with presentable data.

In figure 8.18 on the facing page the angle of incidence during the morning period is plotted along in the same graph as the g-value for the morning periods of all three days. The graph is plotted from hour 3, since data for the first two hour of April 4 is not available. Though the g-value and the incidence angle for this period would both be zero.

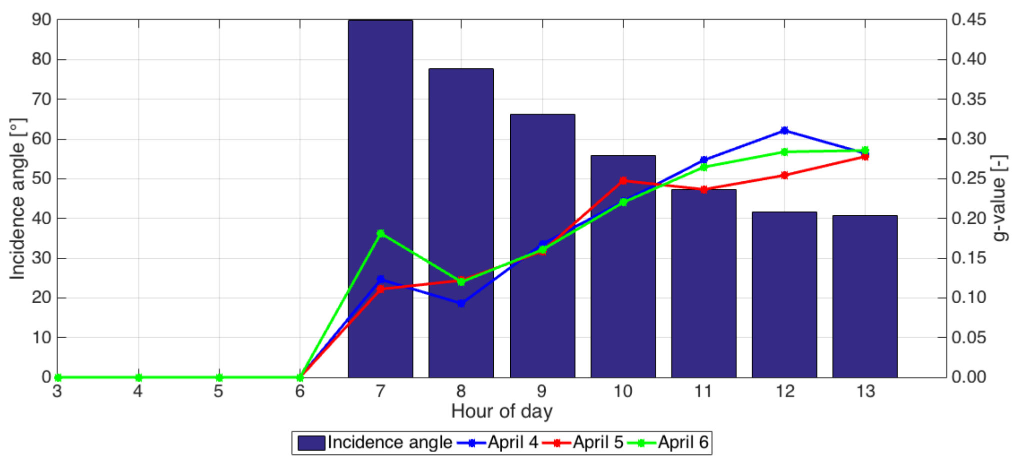

Figure 8.17: The incidence angle in the same graph as the total g-value for the double glazed window combined with the Charcoal Grey solar shading during periods from hour 3 am till 13 pm.

To get at clear picture of the correlation between the total g-value and the incidence angle, these are plotted against each other in figure 8.18 for all three days. Data from hour 8 till 13 have been used for all three days.

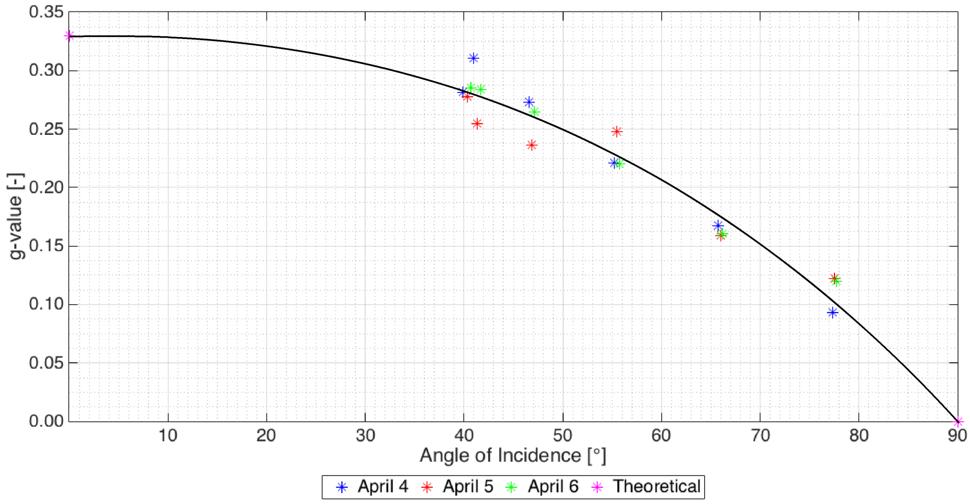

Figure 8.18: The correlation between the incidence angle and the total g-value for the double glazed window combined with the Charcoal Grey solar shading during periods from hour 8 am till 13 pm.

The theoretical point at the incidence angle of zero was obtained in chapter 6 on page 31. This give the theoretical point of [0°,0.33]. The graph in figure 8.18 will be compared to the corresponding graphs for the other three combinations in section 8.5 on page 58.

8.3 Combination 3: Triple glazing/White Pearl

In this section the combination of the triple glazed window and the White Pearl solar shading will be in focus. The measurements for this combination has been conducted in the period from April 29 to May 4.

The total solar radiation just outside the window is plotted in figure 8.19 on the next page along with the solar heat gain inside the room. To the right in figure 8.20 on the following page the total g-value for the morning period of May 2 and May 3 is plotted.

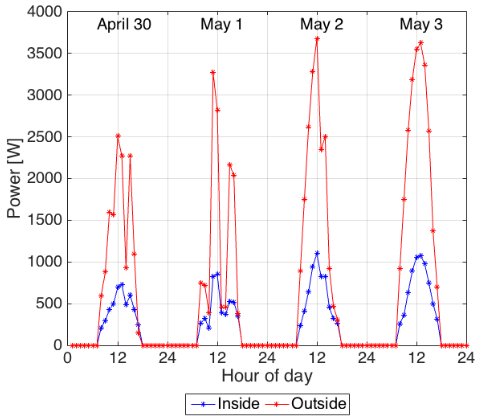

Figure 8.19: The solar radiation outside the window and the solar heat gain inside the room.

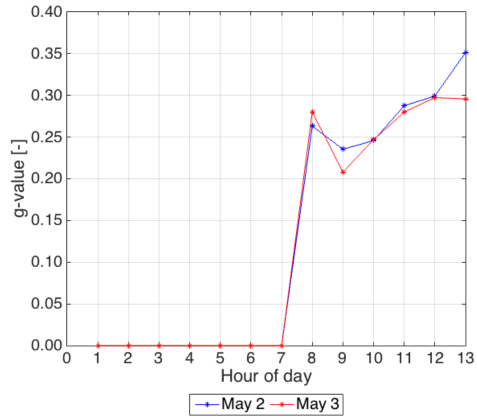

Figure 8.20: The total g-value for morning periods of all three days.

Figure 8.19 shows that April 30 and May 1 has a relatively low amount of solar radiation during the day. Whereas the 2nd and 3rd of May looks clear and sunny. Therefore the g-value for the morning periods of these two days is presented in figure 8.20. This figure shows that the g-value is zero until the 8th hour of the day. For the two previous combination the g-value had a value different from zero in the 7th hour. This is caused by the incidence angle, which above 90° before the 8th hour. This will be clear in figure 8.23 on the next page, where the g-value is plotted with the incidence angle.

To see an exact distribution of the direct and diffuse solar radiation during these two days, this is plotted along with the g-value for the 2nd and 3rd of May in figure 8.21 and 8.21 respectively.

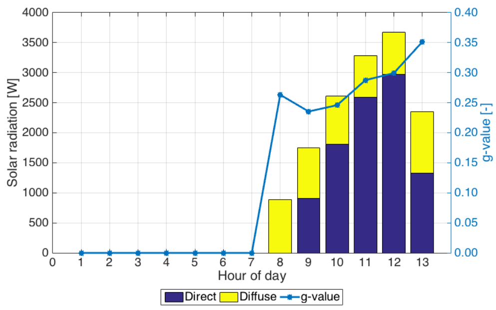

Figure 8.21: Direct and diffuse solar radiation for the 2nd of May.

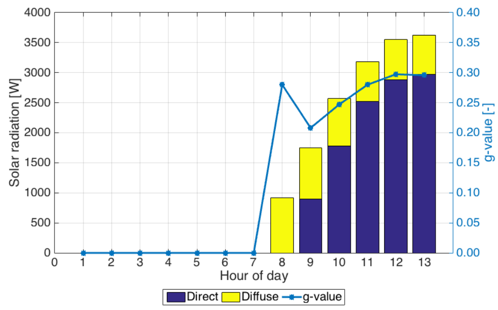

Figure 8.22: Direct and diffuse solar radiation for the 3rd of May.

Now the hour with diffuse but no direct solar radiation is shifted to the 8th as well. Therefore the g-value of this hour is disregarded as for the other combinations.
When looking at figure 8.21 it is seen that the direct solar radiation at hour 13 is drastically decreased, which results in a falsely increased g-value. Otherwise both curves look relatively smooth and according to theory.

The g-value and the incidence angle are plotted on the same graph in figure 8.23 on the facing page.

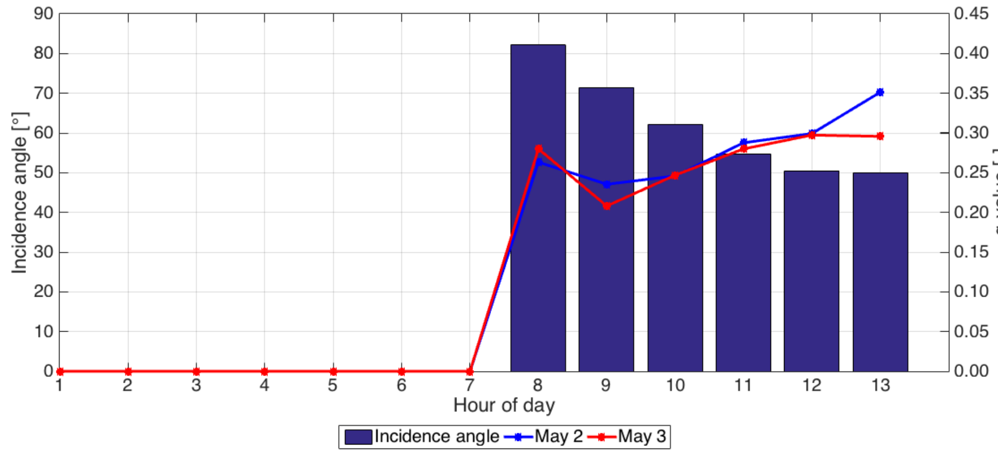

Figure 8.23: The correlation between the incidence angle and the total g-value for the triple glazed window combined with the White Pearl solar shading during periods from hour 1 am till 13 pm.

As mentioned this figure shows that the incidence angle is above 90° before the 8th hour.

In figure 8.24 the g-value and the incidence angle are plotted against each other to see the correlation between the two. Since the g-value at hour 8 is disregarded, the data used for the following graph is only from hour 9 to 13.

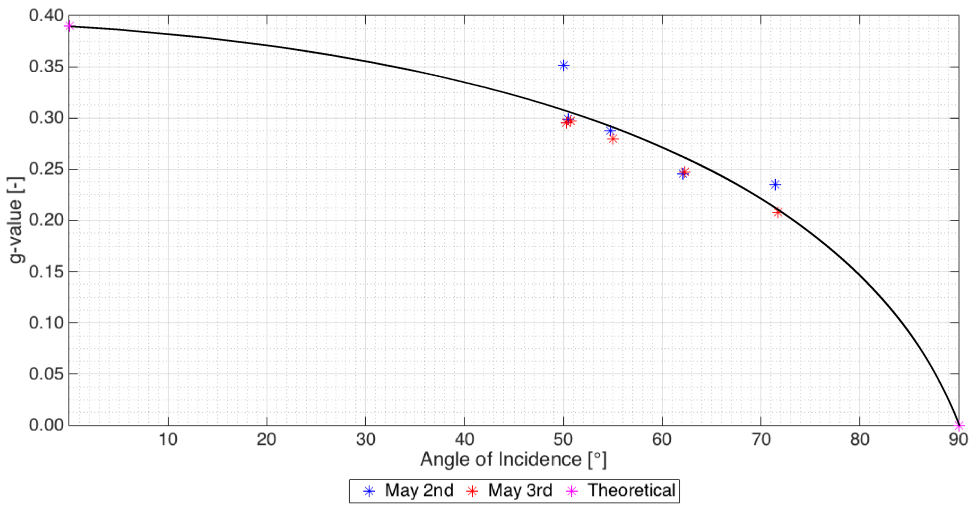

Figure 8.24: The correlation between the incidence angle and the total g-value for the triple glazed window combined with the White Pearl solar shading during periods from hour 9 am till 13 pm.

As the figure shows hour 9 to 13 corresponds to the incidence angles from approximately 50° to 71°, which is a relatively narrow spectrum. Therefore the exact fit of the curve is hard to determine.
The correlation graph in figure 8.24 will be compared to the corresponding graphs for the other combinations in section 8.5 on page 58.

8.4 Combination 4: Triple glazing/Charcoal Grey

In this section the combination of the the triple glazed window and the Charcoal Grey solar shading is in focus. In figure 8.25 the solar radiation outside the window and the heat gain inside the room is presented. To the right in figure 8.26 the total g-value for the morning periods of May 24 and May 26 is presented.

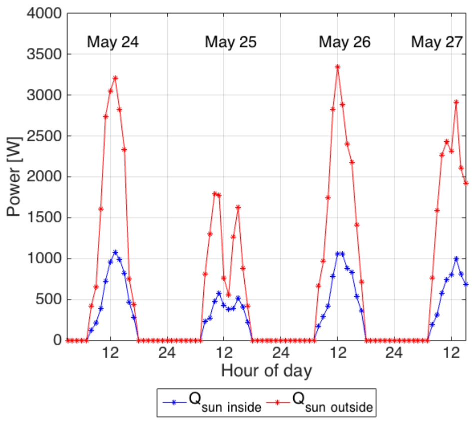

Figure 8.25: The solar radiation outside the window and the solar heat gain inside the room.

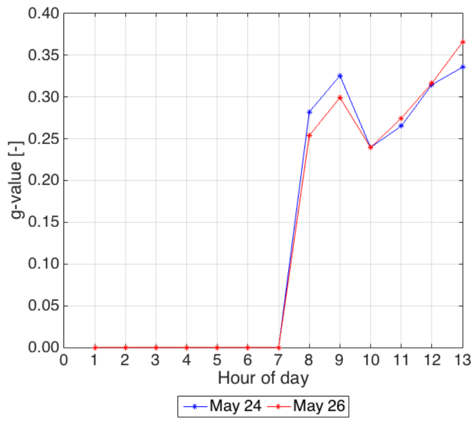

Figure 8.26: The total g-value for morning periods May 24 and May 26.

According to figure 8.25 May 25 and May 27 look to be relatively cloudy days. Whereas May 24 and May 26 look clear and sunny. Therefore these two days are picked out for the analysis of the g-value for this combination.

By taking a closer look at the direct and diffuse solar radiation for the two chosen days, the accuracy of the g-value for each hour can be evaluated. This is presented in figure 8.27 and 8.28 for May 24 and May 26 respectively.

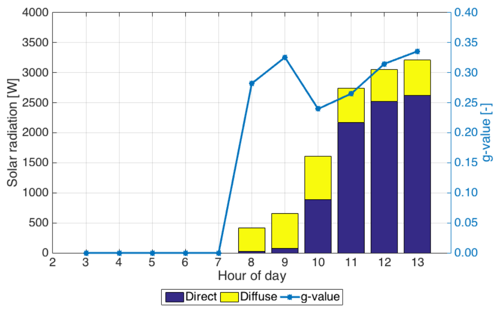

Figure 8.27: Direct and diffuse solar radiation for the 24th of May.

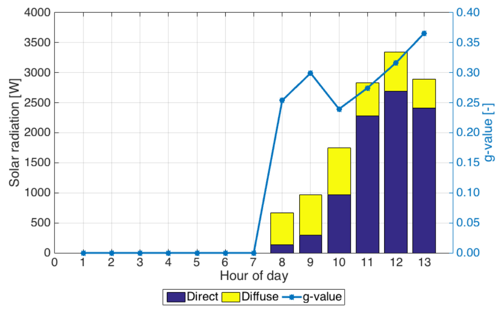

Figure 8.28: Direct and diffuse solar radiation for the 26th of May.

Unfortunately both days have a relatively limited amount of direct solar radiation during the first two hours of the days. Therefore the g-value does not follow the expected tendency for this period.

In figure 8.29 the g-value of both days is plotted along with the angle of incidence.

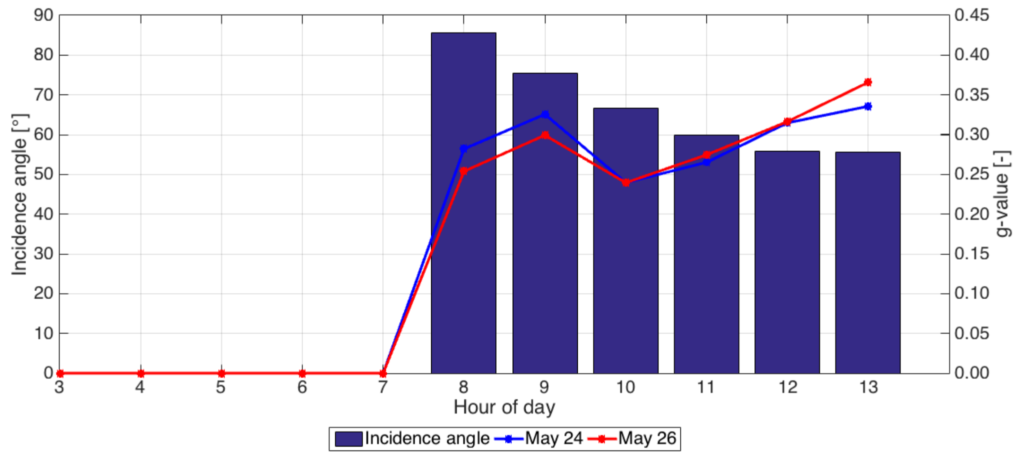

Figure 8.29: The correlation between the incidence angle and the total g-value for the triple glazed window combined with the Charcoal Grey solar shading during periods from hour 1 am till 13 pm.

Because there was not enough direct solar radiation during the first two hour of sunshine the g-value for hour 8 and 9 are disregarded in to correlation graph. The correlation between the g-value and the angle of incidence is presented in figure 8.30.

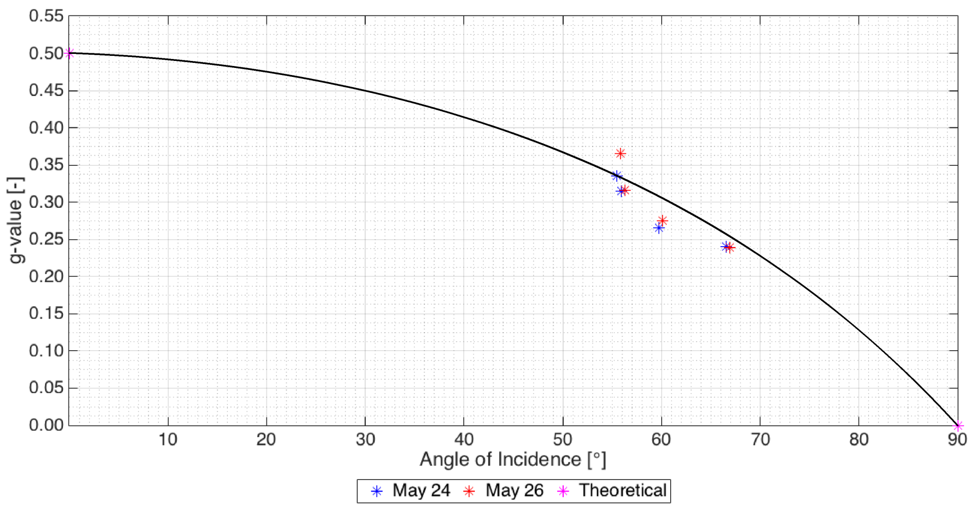

Figure 8.30: The correlation between the incidence angle and the total g-value for the triple glazed window combined with the Charcoal Grey solar shading during periods from 10 am till 13 pm.

Because the first two hours were disregarded it has only been possible to use data for incidence angles from approximately 55° to approximately 66°. This is a narrow spectrum, but these were the only data available during this period.
The correlation graph in figure 8.30 will be compared to the ones for the other combinations in section 8.5 on the next page.

8.5 Comparison

Now the total g-values correspondence to the angle of incidence has been derived for all four combinations. To get an idea of how the different curves look in correspondence to each other, the trendlines of all four combinations are plotted in the same graph in figure 8.31.

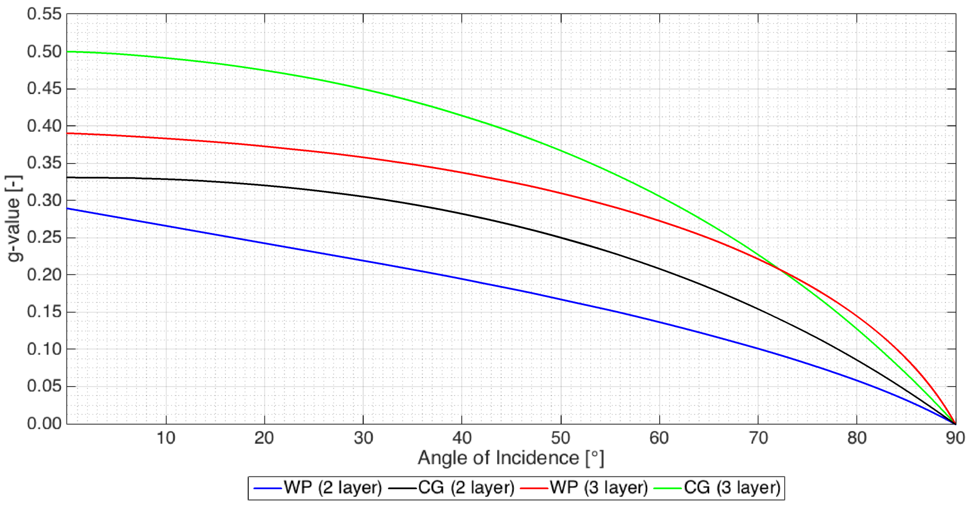

Figure 8.31: A comparison of the total g-values correspondence to the incidence angle for the four combinations of windows and shadings. CP is short for Charcoal Grey, WP is short for White Pearl.

When looking at the four curves it is noted that the combinations with the White Pearl shading generally leads to lower total g-value compared to the ones with Charcoal Grey. This was expected, since the White Pearl has a higher reflectance than the Charcoal Grey.

The curves also show that the combinations with the double glazed window has a lower total g-value compared to the ones with the triple glazed window. This was also expected, since the double glazed window has a significantly lower g-value than the triple glazed window.

When comparing the trend of the four curves the picture is more ambiguous. There is not a clear correlation between the trend for the window types or the shading types.
A reason for this could be that for some of the combinations the data used were located in a narrow spectrum, which only included g-values for a range of 20° incidence angles or less. Therefore the trends are not necessarily accurate.
Generally the graphs have a relatively smooth curvature except for the blue curve, which represents the combination of the double glazed window and the White Pearl solar shading. This curve is close to linear, which is not in line with the theory of the correlation between g-values and incidence angles presented in chapter 3 on page 17, *Solar Geometry*.

All the MatLab files used to make the graphs and calculations presented in this chapter are attached on the appendix CD as number 3.

9 Overestimation in BSim

In this chapter the extend to which BSim overestimates the total g-value of a combined window and shading system will be evaluated.

9.1 BSim Interpretation of g_w and SC

In this section an explanation is given on how the shading coefficient of a solar shading device and the g-value of a window is interpreted in BSim. This is done to give an idea of why the simulation tool overestimates the total g-value.

When defining a window in BSim there are two ways of giving the g-value of the window.

- One way is to give a single number for the g-value. In this case BSim generates a correlation between the g-value and the incidence angle on the current window. The entered g-value will be the one at an incidence angle of 0°. That is perpendicular to the window.

- The other option is to make a user defined curve for the windows g-value in correlation to the incidence angle.

From looking at the two ways of describing the g-value of a window in BSim it is clear that the source to overestimation of the total g-value is not in the interpretation of the window, since this is incidence angle dependent.

Shading in BSim is not given by a g-value but by a shading coefficient. The shading coefficient of a solar shading device is described in chapter 2 on page 5.
This is entered as a single value in BSim and the simulation tool considers it constant at all times. This means BSim does not take into account that the shading coefficient is dependent of the incidence angle even though it is in reality. This is the reason why BSim overestimates the g-value in BSim at certain incidence angles.

9.2 Design of BSim Model

The objective of creating this BSim model is to investigate in which extent BSim is overestimating the shading coefficent and thereby also the total g-value of a window with solar shading. In this section it is explained how the BSim model is built up, thus it can achieve the objective.

In BSim it is necessary to create a building before a window and a shading system can be created. However it should be noticed that in order to examine the objective of this model, it is only interesting to look at how much solar radiation is entering the room through the window and shading system in relation to the solar radiation on the external surface of the window. Therefore the design of the building and the systems in the building are not considered important. A simple building with an internal volume of 1 m^3 and a south facing 1 m^2 window is built up. A screenshot of the model can be seen at figure 9.1.

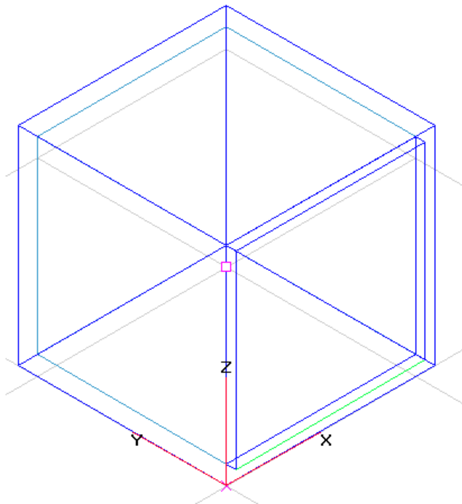

Figure 9.1: Screenshot of the BSim model.

During the examination of the total g-value in chapter 8 on page 43, an experimental total g-value curve was generated for each of the four combinations. To be able to evaluate these in BSim they have been put into the program as a user defined g-value curve of the window. Since the experimentally conducted g-values are all total g-values, that is the g-value of a combined window *and* shading system, imposing them as window g-values in BSim corresponds to having a constantly shaded window at all the times. Though this is not a problem, since the goal is to examine the difference between the total g-value of the experimental results and to the total g-value using the BSim shading method.

In the following the two different methods will be compared. For convenience a description of the two methods is given below along with a short notation which will be used henceforward in the chapter.

- The first method is the one where a regular BSim window and a regular BSim shading is used. In this case the window g-value is given to the program. The window g-values for the two different window types used in this project are the ones presented in table 6.3 on page 33.
  The shading in this method is added as a regular BSim shading by giving a constant shading coefficient corresponding to the given window and shading type. The shading coefficients for the four different combinations of window and shading types are also presented in table 6.3 on page 33.
  This method will have the notation "BSim" in the following graphs etc.

- The second method is the one where the total g-value from the experiments is imposed as a window g-value in BSim. Thereby no BSim shading device is added, and the

window can be considered always shaded with a changing total g-value dependent on the angle of incidence. The experimentally conducted total g-values have been read from the four curves in figure 8.31 on page 58.
This method will have the notation "EXP" in the following graphs etc.

9.3 Validation of BSim Model

In the previous section it was explained how the BSim model is built up. Before analysing the simulated results from the model, it is important to validate that the BSim model is realistic. As mentioned before, only results for the windows will be analysed, which means this validation is more of a validation of the window in the model rather than a validation of the model itself.

During the measurements in the Cube, the outdoor temperature and the solar radiation on the roof were measured among lots of other things. These two weather parameters are used to create a new weather file for the simulation model. By using the new weather file and simulating for the same period as the period, where the measurements were conducted, it would be expected that the simulated and measured solar heat gain in the room are more or less similar.

In figure 9.2 the experimentally measured solar radiation on the external surface of the window is shown together with the solar radiation entering the room, which is calculated from the energy balance. The corresponding simulated values from the BSim model are also shown on the graph. The experimental curves are made from measurements of a double glazed window with the white pearl solar shading, while the BSim curves are made from a simulation where the same window and shading is built up like the EXP method.

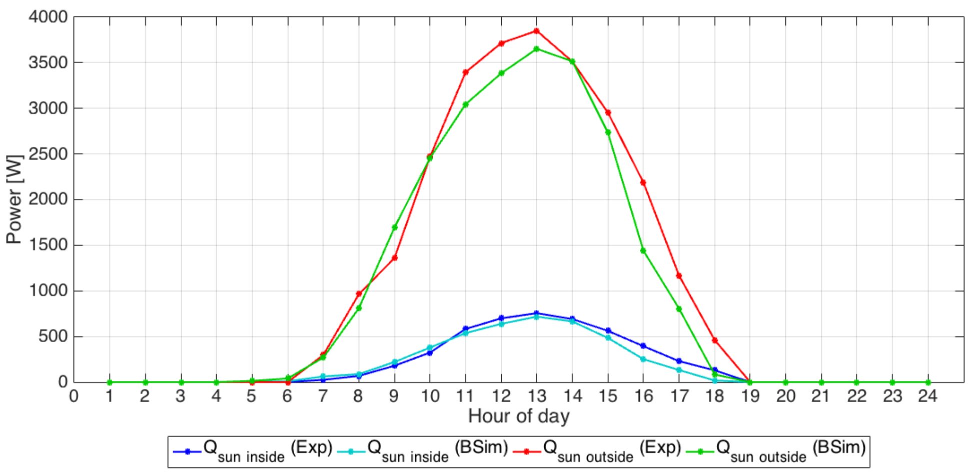

Figure 9.2: The measured and simulated solar radiation on the external side of the window and inside the room.

From figure 9.2 it is noticed that the measured and simulated solar radiation on the external surface of the window are not completely similar. Ideally these two curves should be identical, since used weather file consists of the measured solar radiation on a horinzontal surface in the. This is not the case because the solar radiation measured on the roof is global radiation. The distribution of diffuse and direct solar radiation is not known, why an estimation generating diffuse and direct radiation from global radiation is used before the solar radiation is implemented in the weather file. [Lund, 1985] Apparently this estimation does not fit perfectly with the solar radiation measured on the southern facade of the cube. As the two curves for solar radiation on the external surface of the window are not similar, it makes good sense that the curves for the internal heat gain are not similar either. When the curve for the simulated solar radiation on the external surface of the window is higher than the measured, the curve for the simulated internal solar heat gain is also higher than the measured, and opposite. This is a possitive correlation and it indicates that the total g-value of the window and solar shading built up in BSim is more or less the same as the one for the window and shading system used in the measurements. The validation is considered acceptable and simulations are made to determine the size of the overestimation of total g-value.

Some relevant specifications of the BSim model are listed in section A.3 on page 95, *Specifications of BSim Model*, in appendix. The BSim model is attached on the appendix CD as number 4.

9.4 Size of g_{tot} Overestimation

For the analysis in this section self-made weather data has been used. These consists of only direct solar radiation, which means no diffuse.

In figure 9.3 and 9.4 on the facing page the total g-value for both methods is presented using the double glazed window combined with the Charcoal Grey and the White Pearl shading respectively.

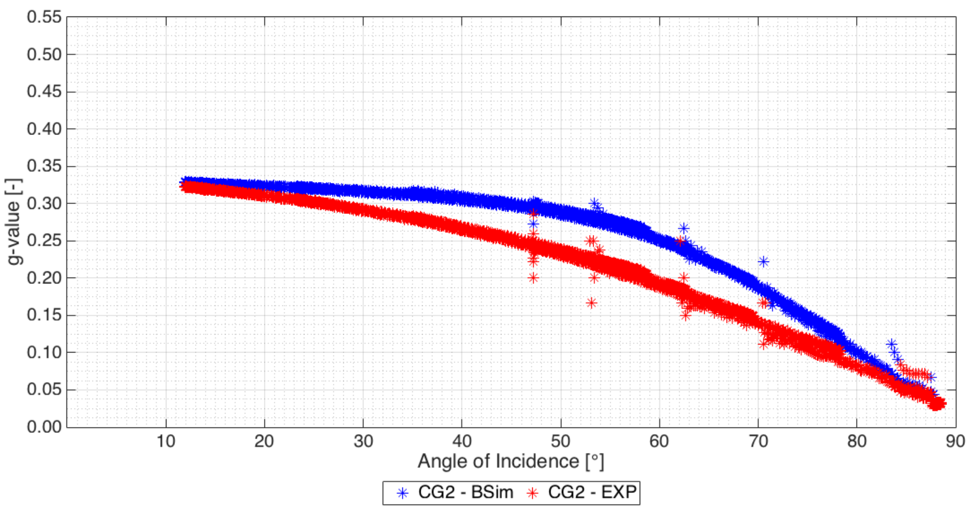

Figure 9.3: The BSim and the EXP method when using the Charcoal Grey solar shading combined with the double glazed window.

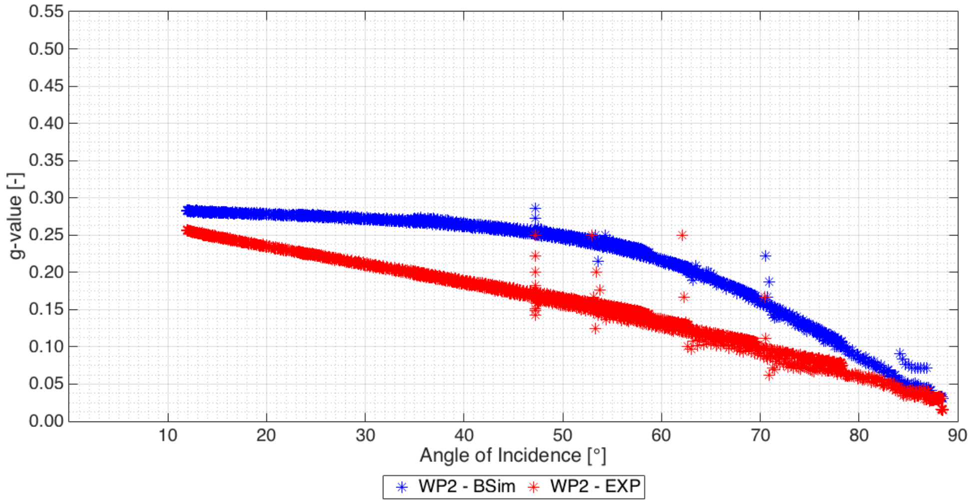

Figure 9.4: The BSim and the EXP method when using the White Pearl solar shading combined with double glazed window.

As expected both figures show that the BSim method overestimates the total g-value quite significantly. Though the almost linear tendency of the experimental curve in figure 9.4 lead to a relatively large difference even at lower incidence angles.
Before further conclusions are made the graphs for the remaining two combinations are presented. In figure 9.5 and 9.6 on the following page the total g-values using both methods are presented using the triple glazed window combined with the Charcoal Grey and the White Pearl shading respectively.

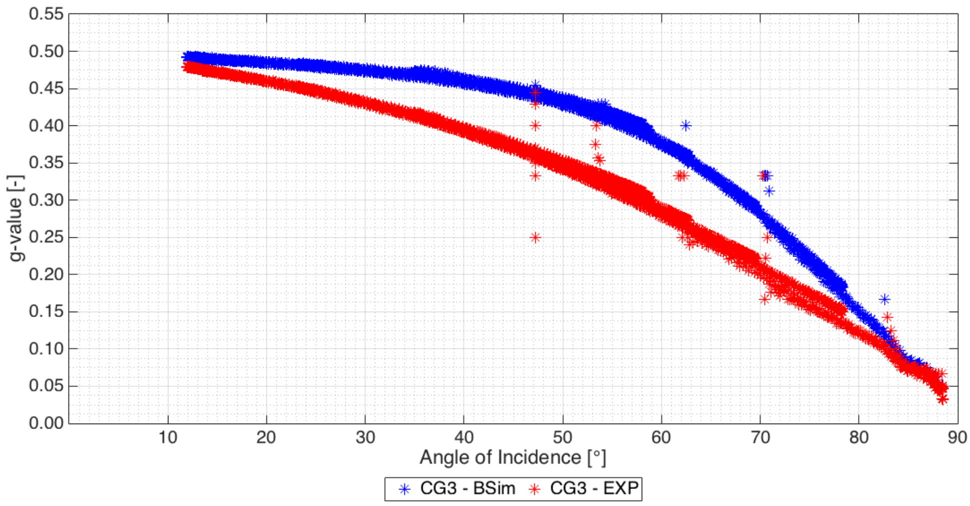

Figure 9.5: The BSim and the EXP method when using the Charcoal Grey solar shading combined with the triple glazed window.

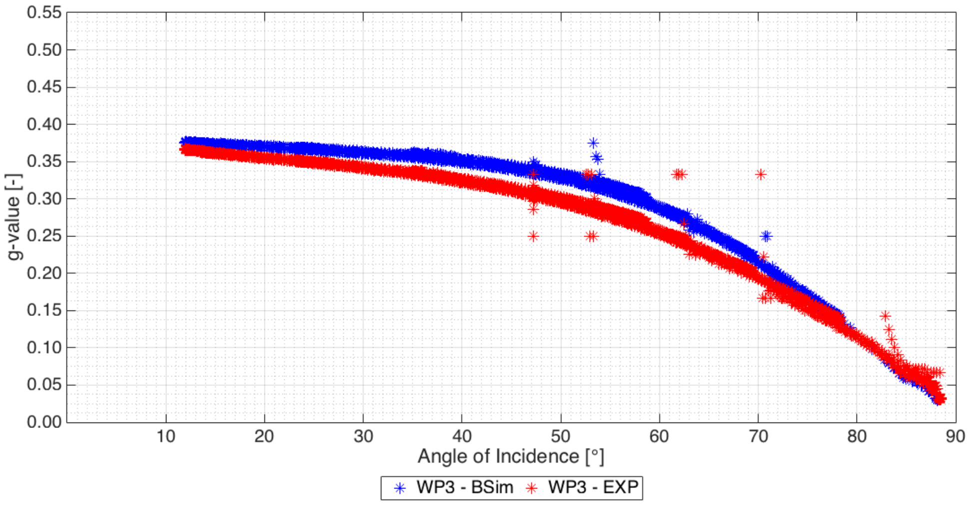

Figure 9.6: The BSim and the EXP method when using the White Pearl solar shading combined with triple glazed window.

The tendecy in these two figure is more or less the same, though for the situation where the combination of the triple glazed window and the white pearl is used, in figure 9.6, the difference between the two grahs is relatively small.

Generally it seems that the difference in total g-value for the two methods is largest between the incidence angles of 30° and 70°. It make good sense that the total g-value curves are getting close at low values of incidence angles, since the shading coefficient is calculated for a situation, where the incidence angles is 0°. Hence the g-value curves should get closer as the incidence angles approximates zero. The reason why the g-value curves are also getting closer at high values of incidence angles can be explained from the expression of the shading coefficient presented in equation 2.1 on page 5. When solving this equation for the total g-value it becomes clear that the BSim overestimation in total g-value will decrease as the incidence angle reaches high values. The total g-value is isolated from equation 2.1 in equation 9.1.

$$\begin{aligned} SC &= \frac{g_t}{g_w} \\ \Rightarrow g_t &= g_w \cdot SC \end{aligned} \tag{9.1}$$

Where:

SC	The shading coefficient of a solar shading device [-]
g_w	The g-value of the window [-]
g_t	The total g-value of a combined window and solar shading system [-]

The equations states that the total g-value can be calculated from the product of the window g-value and the shading coefficient. Consequently a lower window g-value would result in a smaller error between the total g-value of the BSim method and the total g-value of the real life EXP method.

To get a closer look at the absolute size of the overestimation in BSim, the error for each of the four combinations is calculated in equation 9.2.

$$Error = g_{tot(BSim)} - g_{tot(EXP)} \tag{9.2}$$

Where:

$Error$	The absolute error between the BSim method and the experimental method [-]
$g_{tot(BSim)}$	The total g-value calculated with a BSim window and shading [-]
$g_{tot(EXP)}$	The total g-value conducted from experiments [-]

The absolute error is calculated at every angle of incidence. The error is plotted in figure 9.7.

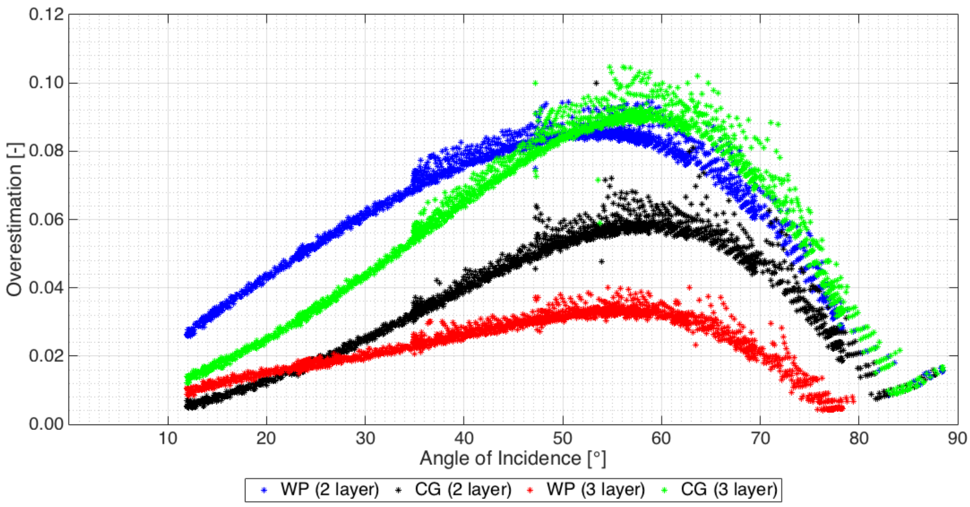

Figure 9.7: The absolute error between the total g-value of the BSim and the EXP method. WP is short for White Pearl and CG is short for Charcoal Grey.

From the plot it is visible that the peak of overestimation in BSim occurs around 50° or 60° for all four combinations. There is a relatively large difference in the error of the two triple glazed window combinations (the red and green curve). Whereas for the two double glazed window combinations (the black and blue curve) the error is more similar when combining this window with the highly reflecting and absorbing shading respectively.

Even though there is a relatively large difference in the size of the overestimation error for the four combinations, the tendency of the graphs is more or less alike. The error curves generally levels off when it as it approaches zero, whereas it has a steeper drop as it goes towards the higher incidence angles.
Moreover error curves in figure 9.7 support the statement the the error is largest within an interval of incidence angles between 30° and 70°. Therefore the next chapter will focus on

how many hours a year the incidence angle on a window is located within this interval. The incidence angle interval between 30° and 70° will be denoted *the critical interval* henceforward in the project.

The excel sheets used to examine the size of the overestimation are attached on the appendix CD as number 5.

10 Importance of Overestimation

The analysis in the previous chapter showed a tendency of largest error in total g-value within the critical interval of incidence angles between 30° and 70°. Therefore this chapter will be focused on an investigated of how long time during a year the incidence angles for a given window is located within this interval. This should lead to a better understanding of how critical the simulated overestimation in BSim is compared to the real life situation.

The orientation of a window plays a relatively big part when having to determine the incidence angle on a window. Therefore this chapter will be looking at four different orientations of a window.

The buildings in focus in this chapter are office buildings. These often have large window areas, which needs to be properly shaded. For office buildings it is typical to divide the day into working hours and non working hours. In this chapter working hours are considered the hours between 8 am and 4 pm. Whereas non working hours are the remaining hours of the day.

The working hours in an office are considered critical hours during a day. Within these hours the temperature has to be kept within the criteria of comfort, since the building is occupied.
Within working hours the internal heat load will be at its maximum. Therefore it is highly important to see if BSim overestimates the total g-value, and thereby the heat load from the sun, during these hours. Hence the focus in this chapter will be on working hours.

10.1 South

To begin with a south oriented window will be in focus. Figure 10.1 on the following page shows the cumulative frequency of the incidence angles on a southern faced window.

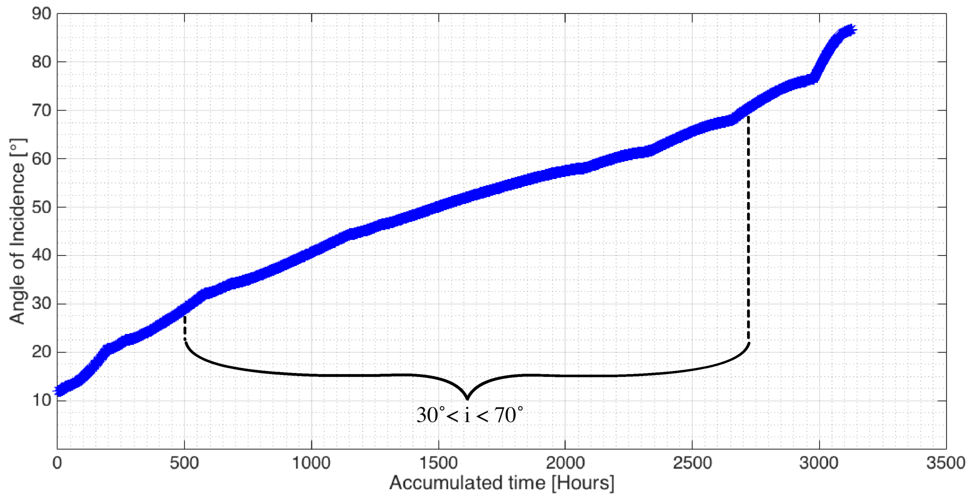

Figure 10.1: The cumulative frequency of the incidence angle on a south oriented window within working hours.

The figure shows that during a year solar radiation reaches the south oriented window for approximately 3100 hours.
In the figure an illustration of the amount of hours located within the incidence angle interval between 30° and 70° is given. This shows that for approximately 2200 hours of the year, the incidence angle on the south oriented window is within the critical interval of overestimation. This corresponds to around 71 % of the total amount of hours on the graph.
This analysis shows that the overestimation in BSim could lead to a relatively large error in the estimation of solar heat gain inside office buildings with southern faced windows.

To see if these critical hours are spread out evenly on the 12 months of the year or if they are more concentrated in specific months, a more detailed analysis of the data has been conducted. In this analysis the working hours within the critical incidence angle interval are summed up for each month an plotted in figure 10.2.

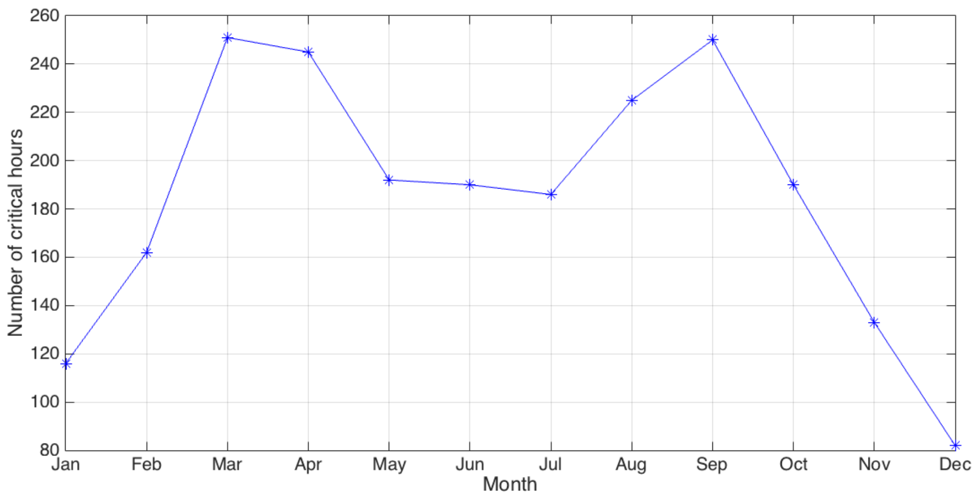

Figure 10.2: The monthly sum of working hours within the critical interval of incidence angles on a south oriented window.

This figure shows an interesting tendency. The number of working hours within the critical interval peaks in spring and autumn and has a slight drop in the summer period. Since the incidence angle in the winter period is relatively low, there are fewer hours within the critical interval during the winter period.
This means that for south oriented windows the total g-value using BSim is overestimated the most during spring and autumn and a bit less in summer.

To see if this is the case for other orientations of windows, the analysis is continued.

10.2 West

When putting a west oriented window in focus figure 10.3 shows the cumulative frequency of the incidence angle on a western faced window.

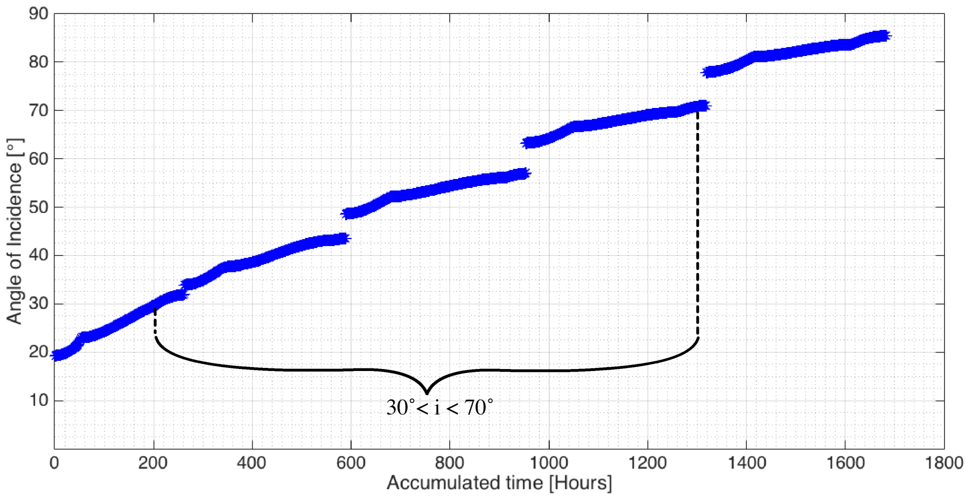

Figure 10.3: The cumulative frequency of the incidence angle on a west oriented window within working hours.

For a west oriented window the solar radiation reaches the window approximately 1700 hours during a year. The hours within the critical interval sums up to around 1100 hours, which corresponds to approximately 65 % of the total amount of hours.
So the overestimation in BSim is also of relatively hight importance when designing west oriented windows in office buildings.

As for the south oriented window, the hours within the critical interval has been summed up for each month. These results are plotted in figure 10.4 on the next page.

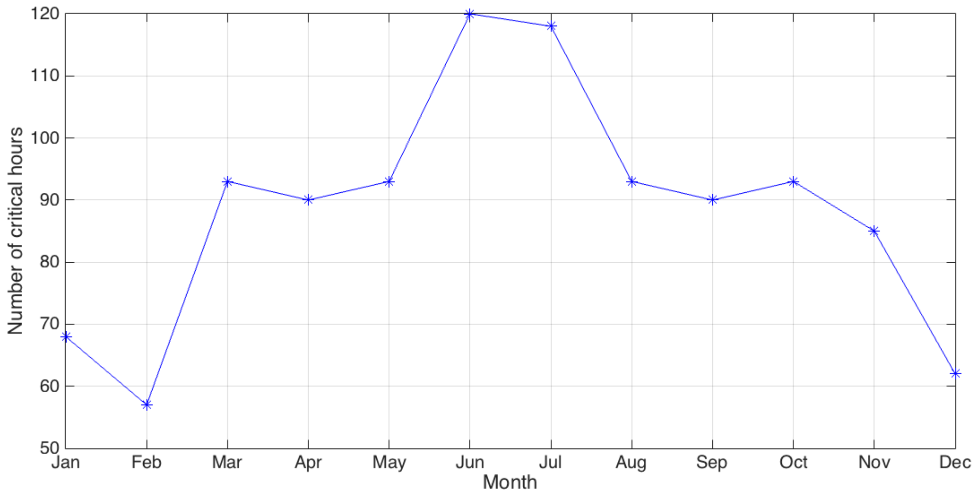

Figure 10.4: The monthly sum of working hours within the critical interval of incidence angles on a west oriented window.

This figure shows another tendency then the one for the south oriented window. For the west oriented window the number of hours within the critical interval peaks in the summer in June and July. Spring and autumn has a bit fewer hours within the critical interval and even fewer in the three winter months.
This means the total g-value in BSim is overestimated the most in June and July and less in the other months for a west oriented window.

The total number of hours within the critical interval for the west oriented window will be compared to the other orientated window in the end of this chapter.

10.3 East

Now an east oriented window is brought into focus. Figure 10.5 shows the cumulative frequency of the incidence angles on an eastern faced window.

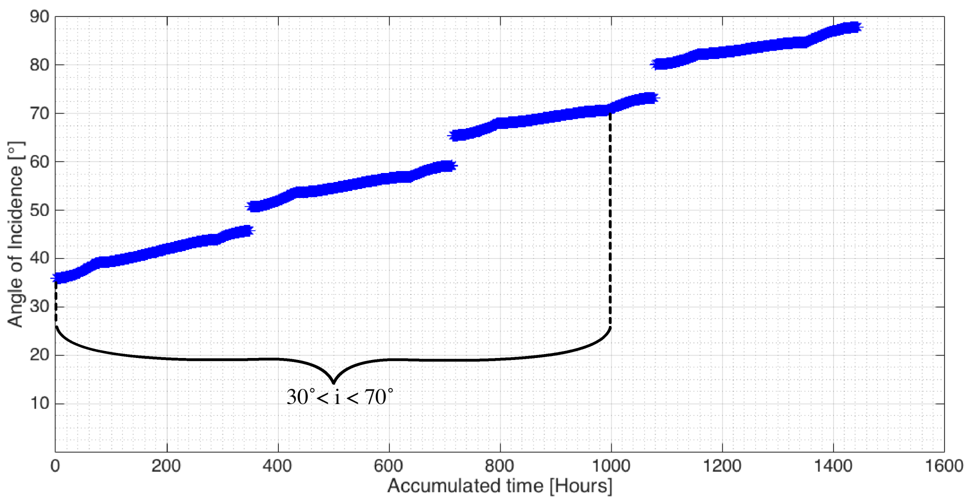

Figure 10.5: The cumulative frequency of the incidence angle on a east oriented window within working hours.

During a year there are around 1450 hours where the solar radiation reaches eastern oriented windows. Out of these hours the incidence angle is located within the critical interval of BSim overestimation for approximately 1000 hours. This corresponds to around 69 % of the total amount of hours on the graph.
So when designing an office building with east oriented windows the BSim overestimation of the total g-value does also become relatively important.

The hours within the critical interval for the east oriented window has been summed up and are plotted in figure 10.6.

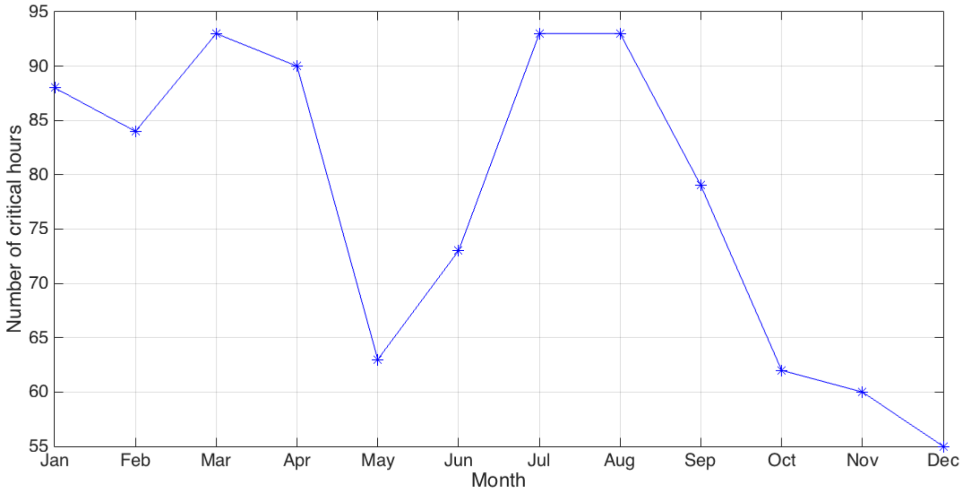

Figure 10.6: The monthly sum of working hours within the critical interval of incidence angles on an east oriented window.

This graph show a slightly different tendency then for the two other orientations. The amount of critical hours peaks in early spring as well as in July and August.

10.4 North

For north oriented window the solar radiation does not reach the window during the working hours of a whole year. Therefore the overestimation of the total g-value in BSim would be of little or no importance if designing north oriented windows in an office building.

10.5 Comparison

In this section the amount of hours within the critical interval will be compared for windows orientated towards south, west and east respectively. This should cast light on which window orientation is inflicted the most by the overestimation of the total g-value in BSim.

In figure 10.7 on the following page the amount of hours within the critical interval is presented for windows oriented towards south, west and east respectively.

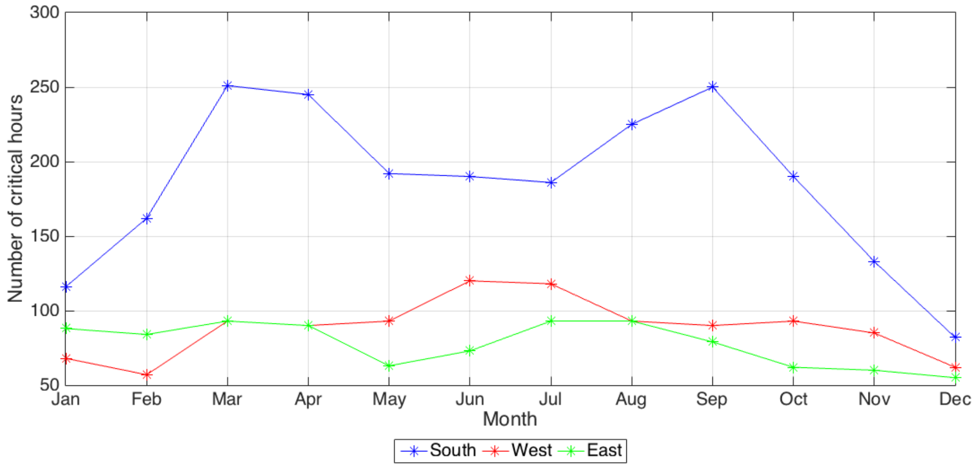

Figure 10.7: The monthly sum of working hours within the critical interval of incidence angles on a south, west and east oriented window respectively.

This plot gives a clear picture of the amount of critical hours for the three orientations compared. It is visible that the amount of critical hours for the south oriented window is significantly larger then the amount for both east and west in all 12 months. The amount of critical hours for east and west look relatively similar with a few exceptions.
From this correlations it would be fair to assume that the overestimation of the total g-value in BSim would have a larger influence on the simulated heat gain through a southern faced window compared to a west and east oriented window.

To see if this is the case, further analyses will be conducted throughout the following chapter.

The MatLab files used to examine the importance of the overestimation are brought on the appendix CD as number 6. Further an analysis of the hours outside working hours is presented in section A.4 on page 96, *Overestimation - Outside Working Hours*, in appendix.

11 Correction of Overestimation

In this chapter the impact of the total g-value overestimation on the yearly cooling demand in a building will be investigated. In addition, the impact on the cooling peak power in a building will be estimated.

For this chapter regular DRY weather data has been used.

When the effect on the cooling demand and peak power has been determined, a corrected shading coefficient will be estimated for all four window and shading combinations. This will be done for windows oriented towards south, east and west respectively.
The idea behind the corrected shading coefficient is to give consulting engineers a tool to correct the overestimation of the total g-value in BSim.

The first intermediate goal is to be able to estimate the difference in yearly cooling demand and peak power when using the BSim method and the real life situation from the EXP method. This is done in the following way:

- In the BSim method a regular BSim shading device in installed on the window. This is controlled so that it is always fully shading.
- In the EXP method the user defined window, simulating a window *and* shading in real life, is installed. This means that this method can also be considered as a window with shading, which is always fully shading.
- Both methods are simulated in BSim using DRY weather data.

The output of these simulations will be the solar heat gain inside the building in each of the two models. Since almost all modern office buildings in Denmark has a cooling system installed, it is assumed that whenever solar radiation reaches a window, the cooling system is activated. In this way the extra amount of solar radiation in the BSim method compared to the EXP method can be considered an additional cooling demand. So to estimate the difference in yearly cooling demand and peak power the solar heat gain of each method is compared over a year.

It is interesting to know the additional cooling demand since this will give an idea of how much BSim overestimates the energy consumption in a building.
The increase in cooling peak power could leads to an overestimation of the cooling compressor, which would be costly.

The combination with a double glazed window and the Charcoal Grey solar shading will be used as a thorough example on how to estimate the additional yearly cooling demand and peak power in the BSim method. This will be done for a south oriented window. The principal is the same for the other combinations. Therefore the remaining combinations will only be presented with explicit results.

11.1 South

The difference in cooling power over a year for the two methods is presented for the double glazed window and the Charcoal Grey combination in figure 11.1.

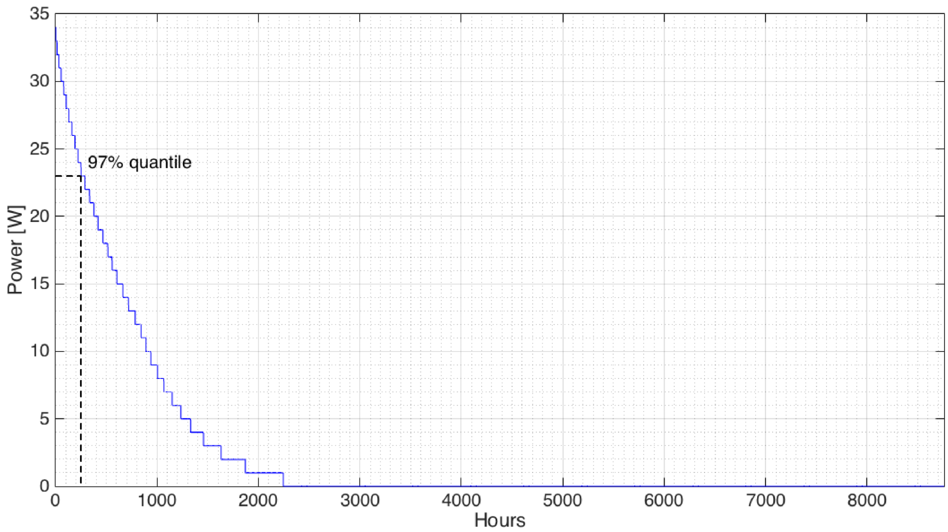

Figure 11.1: The overestimation in cooling power when using the BSim method compared to the real life EXP method. The cooling power is sorted from high to low during the 8760 hours of a year.

The figure shows the difference in cooling power during a whole year with sorted data from high to low. Be aware that this difference in cooling power is considered exactly the same as the difference in solar heat gain through the window.
From the figure both the difference in cooling demand over the year and the difference in peak power can be calculated. The difference in cooling demand is the area under the curve in figure 11.1. Therefore the curve is integrated to calculate the difference in cooling. For this combination of window and shading facing south, the difference in cooling demand is 22.5 kW.
The 97 % quantile of the curve is considered the addition in peak power. This is visually presented in figure 11.1. For this combination of window and shading facing south, the addition in peak power is 23 W.

Since the constant shading coefficient for the solar shading in BSim is the source to overestimation of both the cooling demand and peak power, this will be decreased until the addition in cooling demand over the year compared to the real life situation from the EXP method is zero. SC is changed by trial and error. The original SC is 0.93 for the combination with the double glazed window and the Charcoal Grey solar shading. This is decreased to an optimized value of 0.84, which leads to zero overestimation of the yearly cooling demand.
After the optimized SC is implemented in the BSim method, the difference in cooling power during the year is decreased to what is seen in figure 11.2 on the next page

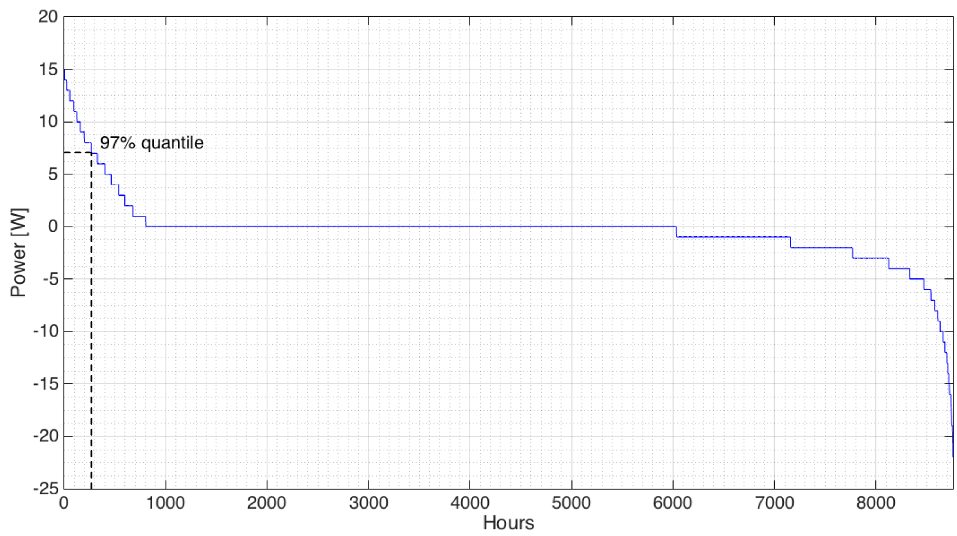

Figure 11.2: The overestimation/underestimation in cooling power when using the BSim method, with the optimized shading coefficient, compared to the real life EXP method. The cooling power is sorted from high to low during the 8760 hours of a year.

The figure shows that the cooling power is still overestimated in certain periods. However, this is compensated for by an underestimation in other periods of the year. When the curve is integrated over the whole year the total difference in cooling demand is zero.
The 97 % quantile is lowered to approximately 7 W, which is a 70 % decrease.

This analysis is made for the remaining three window and shading combinations facing south.
The differences in cooling demand and peak power for the original BSim method compared to the real life EXP solution are presented in table 11.1 for all four window and shading combinations.

		Double glazed	**Triple glazed**
Charcoal Grey	$\Delta Q_{\mathrm{Cooling}}$ [kW]	22.5	36.7
	Overestimated PP [W]	23	37
White Pearl	$\Delta Q_{\mathrm{Cooling}}$ [kW]	37.6	12.0
	Overestimated PP [W]	37	14

Table 11.1: $\Delta Q_{Cooling}$ is difference between the solar heat gain from the EXP method and the BSim method. *Overestimated PP* is the overestimated peak power calculated by the 97 % quantile.

The table shows that the combinations of triple glazed window and Charcoal Grey along with double glazed window and White Pearl overestimated both the yearly cooling demand and the peak power quite drastically before the correction factor was added. The two other combinations did also overestimate, though not as significantly.

After making the optimization for all four combinations, the results in table 11.2 on the next page are obtained .

		Double glazed	Triple glazed
Charcoal Grey	$SC_{Original}$ [-]	0.93	0.93
	$SC_{Optimized}$ [-]	0.840	0.835
	Difference [%]	9.7 %	10.2 %
	CF [-]	0.913	0.898
White Pearl	$SC_{Original}$ [-]	0.80	0.71
	$SC_{Optimized}$ [-]	0.660	0.680
	Difference [%]	17.5 %	4.3 %
	CF [-]	0.825	0.957

Table 11.2: *SC* is the shading coefficient. *Difference* is the difference between the original SC and the optimized. *CF* is the correction factor, which converts the original SC into the optimized.

From the table it becomes clear that when using the highly absorbing shading, Charcoal Grey, the correction factor is almost unaffected by the type of window.
On the other hand when using the highly reflecting shading, White Pearl, the type of window has a much larger effect on the correction factor. It is seen that the triple glazed window only needs a 4.3 % reduction in shading coefficient, which is the smallest of the four. Whereas the double glazed window need a 17.5 % reduction, which is by far the largest of the four combinations.

Table 11.2 also shows the correction factor for each combination. This factor decreases the original SC to the optimized one. This could be a handy tool for consulting engineers when estimating the yearly cooling demand and peak power of a cooling system for a window systems with shading facing south in BSim.

11.2 West

The analysis conducted for the south oriented window has also been performed for a west oriented window. As mentioned in the beginning of this chapter, only the results will be presented for this orientation, since the approach is the same.

For the four different combinations of windows and shadings the difference in cooling demand and peak power from the BSim method to the real life EXP method is presented in table 11.3.

		Double glazed	Triple glazed
Charcoal Grey	$\Delta Q_{Cooling}$ [kW]	10.4	17.5
	Overestimated PP [W]	15	24
White Pearl	$\Delta Q_{Cooling}$ [kW]	19.0	5.3
	Overestimated PP [W]	26	9

Table 11.3: $\Delta Q_{Cooling}$ is difference between the solar heat gain from the EXP method and the BSim method. *Overestimated PP* is the overestimated peak power calculated by the 97 % quantile.

Once again the combinations of triple glazed window and Charcoal Grey along with double glazed window and White Pearl overestimates both the yearly cooling demand and the peak power more than the other two.

The original and optimized shading coefficient is presented in table 11.4.

		Double glazed	Triple glazed
Charcoal Grey	$SC_{Original}$ [-]	0.93	0.93
	$SC_{Optimized}$ [-]	0.875	0.865
	Difference [%]	5.9 %	7.0 %
	CF [-]	0.941	0.930
White Pearl	$SC_{Original}$ [-]	0.80	0.71
	$SC_{Optimized}$ [-]	0.695	0.690
	Difference [%]	14.4 %	2.9 %
	CF [-]	0.856	0.971

Table 11.4: *SC* is the shading coefficient. *Difference* is the difference between the original SC and the optimized. *CF* is the correction factor, which converts the original SC into the optimized.

As for the south oriented window, the four combinations of the west oriented window shows the same tendency. The difference in SC from original to optimized is almost the same for the two combinations of the Charcoal Grey. Whereas for the White Pearl shading the double glazed window gives a significantly larger differences in the original and optimized SC compared to the triple glazed window.

11.3 East

Finally the analysis is made for the east oriented window as well. The overestimation in cooling demand and peak power for the BSim method compared to the real lift EXP method is presented in table 11.5.

		Double glazed	Triple glazed
Charcoal Grey	$\Delta Q_{Cooling}$ [kW]	10.4	17.5
	Overestimated PP [W]	14	23
White Pearl	$\Delta Q_{Cooling}$ [kW]	19.1	5.3
	Overestimated PP [W]	27	9

Table 11.5: $\Delta Q_{Cooling}$ is difference between the solar heat gain from the EXP method and the BSim method. *Overestimated PP* is the overestimated peak power calculated by the 97 % quantile.

The tendency follows the ones of the two previous orientations of the window. Again the combinations of triple glazed window and Charcoal Grey along with double glazed window and White Pearl overestimates both the yearly cooling demand and the peak power more than the other two.

The original and optimized SC is presented in table 11.6 for the four combinations of the east oriented window.

		Double glazed	Triple glazed
Charcoal Grey	$SC_{Original}$ [-]	0.93	0.93
	$SC_{Optimized}$ [-]	0.875	0.865
	Difference [%]	5.9 %	7.0 %
	CF [-]	0.941	0.930
White Pearl	$SC_{Original}$ [-]	0.80	0.71
	$SC_{Optimized}$ [-]	0.695	0.690
	Difference [%]	14.4 %	2.9 %
	CF [-]	0.856	0.971

Table 11.6: SC is the shading coefficient. $Difference$ is the difference between the original SC and the optimized. CF is the correction factor, which converts the original SC into the optimized.

The numbers almost match the ones of the west oriented window. Hence the tendency is alike.

11.4 Comparison

To be able to compare the four combinations for all three orientations of the window, table 11.7 shows the gathered results of the different combinations.

		South		West		East	
		Double	**Triple**	**Double**	**Triple**	**Double**	**Triple**
CG	$\Delta Q_{Cooling}$ [kW]	22.5	36.7	10.4	17.5	10.4	17.5
	SC difference [%]	9.7 %	10.2 %	5.9 %	7.0 %	5.9 %	7.0 %
WP	$\Delta Q_{Cooling}$ [kW]	37.6	12.0	19.0	5.3	19.1	5.3
	SC difference [%]	17.5 %	4.3 %	14.4 %	2.9 %	14.4 %	2.9 %

Table 11.7: $\Delta Q_{Cooling}$ is difference between the solar heat gain from the EXP method and the BSim method. $SC\ difference$ is the difference between the original SC and the optimized.

This table makes it clear that the tendencies for all three orientations of a window is more or less the same. It shows that the type of window impacts the difference in SC a lot when the highly reflecting solar shading, White Pearl, is used. On the other hand the type of window does not play a significant part for the difference in SC when the highly absorbing shading, Charcoal Grey, is used.

In chapter 10 on page 67 it was concluded that there was around twice as many hours within the critical incidence angle interval of 30° to 70° for a southern faced window compared to the west and east oriented window. This means that twice as many hours with solar

radiation on the south oriented window was located in an interval where the overestimation in BSim was largest. This indicated that the error during a year would be larger for the south oriented window.
Table 11.7 on the preceding page clearly shows that the error is indeed larger for the south oriented window, since the difference in SC is larger for all four combinations of the south orientation.

The excel sheets used to determine the correction of the overestimation is attached on the appendix CD as number 7.

12 | Conclusion

The initial statement in this project was that the solar shading coefficient is generally interpreted in a too simple way. Several simulation tools, including BSim, consider this coefficient a constant independent value. Though through the results of several experiments, conducted for this project, it was clarified that this value is indeed dependent on the incident angle of the solar radiation on the shading device.
The analysis of the experiments has shown that the shading coefficient is overestimated for a large range of incident angles. The overestimation is largest in the interval between 30° and 70°. To evaluate whether this can be considered logic or not, the interpretation of the shading coefficient in BSim has to be fully understood.
In BSim the shading coefficient is treated as if solar radiation is reaching the glazing and shading system at an incidence angle of 0° at all times. This means that BSim only is estimating the shading coefficient correctly when the solar radiation is perpendicular to the window. Although this is never the case in Denmark, since the incidence angle never gets below 10°. Hence the shading coefficient in Bsim is always overestimated to some extent compared to a real life situation. Logically the overestimation increases as the angle of incidence gets larger. Though when the incidence angle reaches a certain level, the BSim overestimation of the total g-value starts decreasing again. Since the total g-value is a product of the shading coefficient and the window g-value, a drastically decreased window g-value will result in the decreasing overestimation of the total g-value.

From looking at the solar radiations incidence angles on different oriented windows during a year, it has been estimated which orientation would be affected the most by the overestimation.
This analysis shows that a south facing window has around 2200 hours with solar radiation reaching the window with an incident angle within the before mentioned critical interval of 30° and 70°. On the other hand a west and east oriented window only has around 1000 hours with solar radiation reaching the window with an incident angle within the critical interval. Therefore it would be fair to assume that a south oriented window is affected the most by the overestimation in total g-value in BSim.

This is backed up by an analysis of cooling demand and peak power of a room with different oriented windows. A BSim model is used for comparison. In the BSim model, the combinations of window and shading system are built up both like the BSim method and EXP method. For the BSim method, the window g-value is dependent of the incident angle on the window, but the shading coefficient is considered constant at all times. For this method the shading is set to be always on. In the EXP method the total g-value of a combined window and shading system in a real life situation is used. This value is obtained from the experiment of the project and is dependent of the incident angle.
When simulating the two methods over a whole year with DRY weather data it becomes clear that the BSim method overestimates the amount of solar heat gain for south, east and west oriented windows. It seems fair to consider the overestimation of solar heat gain as the same as an overestimation in cooling demand. When comparing the overestimation of

cooling demand in a building with different orientated window, it proves that the cooling demand is overestimated the most for a south oriented window compared to a east and west oriented window.

A correction factor is made for the shading coefficient in order to eliminate the overestimation in cooling demand in the BSim method. This is done for all three orientations of windows, south, east and west, as well as for the four different combinations of window and shading systems.

This analysis shows a couple of interesting tendencies.
The first one being that for the south oriented windows that correction factor should be larger than the corresponding factors for the east and west oriented ones. This correlates with the two previous observations.
The other and maybe most striking tendency is that if a highly absorbing solar shading device is used, the effect of using a double or a triple glazed window is very insignificant to the correction factor. Whereas if a highly reflecting shading is used, using a double or a triple glazed window is of large significance to the correction factor of the shading coefficient. In the case of a highly reflecting shading a double glazed window, whith a low g-value, needs a high correction factor to decrease the overestimation. Whereas a triple glazed window combined with the highly reflecting shading needs a much lower correction factor.

13 Future Work

In the project, correction factors for the overestimation of internal solar heat gain on a yearly basis in BSim are determined. These factors are obtained on the basis of two different internal solar shadings and two different windows. Though, in order to validate the correction factors, further investigations would required. Measurements with several different types of solar shadings would result in more reliable and applicable correction factors. The correction factors are considered valid for the four different combinations of window and shading system. However it is more uncertain if they would be valid for different window and shading system. In order to determine whether this is the case or not, further measurements would be necessary.

As mentioned before the correction factors of the overestimation are determined on a yearly basis. Meaning that the correction factors are only applicable when simulating for a whole year. In many cases it is interesting to look at the internal solar heat gain in different periods of the year because it will affect the energy consumption of a building differently according to whether there is a heating demand or cooling demand. Therefore it would be relevant to make correction factors on monthly or even weekly basis.

Further it would be interesting to apply the correction factors on a case study building in BSim. The case study building should be considered representable for modern buildings. In this way it would be possible to analyse how the overestimaton of internal solar heat gain affects other relevant parameters like hours with excessive temperatures, total energy consumption etc. This would make it possible to conduct a much more complex analysis of the influence of the overestimation.

Bibliography

Charlotte B. Henriksen, Mathias Villumsen, 2012. Empirical and theoretical modelling of solar shading factor - Annex 1. Master's thesis, Aalborg University.

Dansk Standard, 2007. DS/EN 13363-1:2003+A1:2007 (E), Solar protection device combined with glazing - Calculation of solar and light transmittance - Part 1: Simplified method. 2nd edition.

Dreau, J. L., 2014. Energy flow and thermal comfort in buildings. Ph.D. thesis, Aalborg University.

Dreau, J. L., Heiselberg, P. K., Jensen, R. L., 2014. Experimental data from a full-scale facility investigating radiant and convective terminals. Tech. rep.

Energistyrelsen, June 2015. Bygningsreglementet.
URL `http://www.bygningsreglementet.dk`

Eniro Danmark A/S, June 2015. Krak.
URL `http://www.krak.dk`

European Commission, 2006. Communication from the Commission. Action Plan for Energy Efficiency. Tech. rep.

Furler, R., 1991. Angular dependence of optical properties of homogeneous glasses. ASHRAE Transactions.

H.E. Hansen, P. Kjerulf-Jensen, O. B. S., 2006. Varme- og Klimateknik, Grundbog. 3rd edition. Danvak ApS.

J. Karlsson, A. R., 2000. Modelling the angular behaviour of the total solar energy transmittance of windows. ASHRAE Transactions.

Karsten Duer, Jacob Brick Laustsen and Svend Svendsen, 2009. Ruder og vinduers energimæssige egenskaber.

Lund, H., 1985. Short Reference Years and Test Reference Years for EEC countries, appendix 3. Tech. rep.

Per Kvols Heiselberg, 2008. Microclimate of Buildings. Tech. rep.

Thermon, June 2015. Heat Transfer Compounds.
URL `http://www.thermon.com/us/heattransfer.aspx`

Thomasz M. Mróz, 2003. Overview of Retrofitting Measures. Tech. rep.

A Appendix

A.1 Measuring Devices and Uncertainties

The following will describe all used measuring devices in the Cube and give an overview of what they are measuring, where they are located, and what the accuaracy of each measuring device is.

Temperature
Air, operative and surface temperatures are measured at various points in the test zone. These different kind of temperatures are measured with different kinds of thermocouples. The thermocouples used to measure air and operative temperatures are shown in figure A.1.

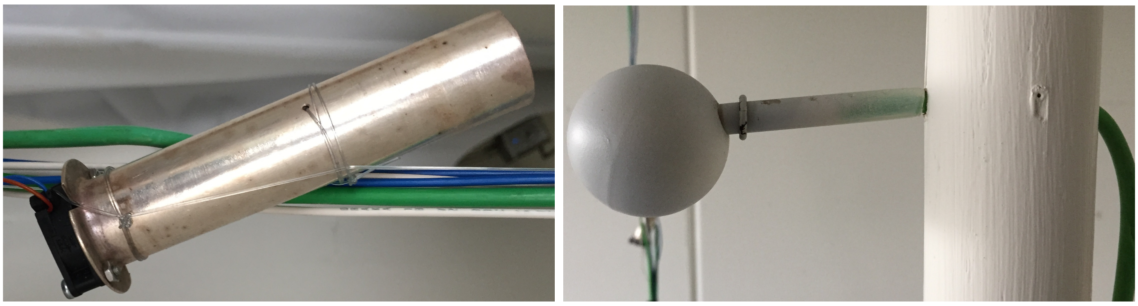

Figure A.1: The picture on the left shows a thermocouple used to measure air temperatures. The thermocouple is inserted in to a silver shield, which is mechanically ventilated. On the right picture, a thermocouple used to measure the operative temperatures is shown. This thermocouple is covered with a grey plastic envelope.

As it can be seen at the left picture in figure A.1, the thermocouples measuring air temperatures are protected by a silver shield, which reflects most of the radiation. A little fan is placed in the bottom of the silver shield to mechanically ventilate it and thereby secure that no heat is accumulated in the shield because of radiation. The picture on the right in figure A.1 shows a thermocouple used to measure operative temperature. The thermocouple is covered with a grey plastic envelope, which. Air and operative temperatures are measured at 0.1, 0.6, 1.1, 1.7 and 2.65 m above the floor. Air temperatures are also measured in the guarding zone, at the outdoor, in the inlets and outlets of the ventilation systems and between the window and the internal solar shading.

The surface temperatures are measured with thermocouples as shown in figure A.2 on the following page.

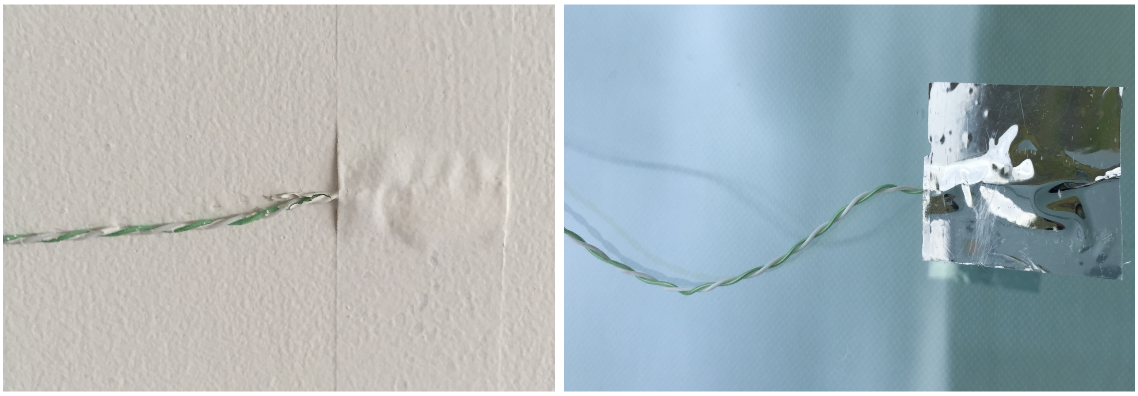

Figure A.2: The left picture shows a thermocouple used to measure surface temperatures on a wall. The thermocouple is placed together with heat transfer compound and is covered up with some tape. On the right picture, a thermocouple used to measure the surface temperature of the window is shown. In this case reflecting tape is used to avoid impact from radiation.

The thermocouples shown in figure A.2 are placed with heat transfer compound and covered up with a piece of tape. The heat transfer compound provides an efficient thermal connection between the thermocouple and the surface by avoiding the small air gaps. [Thermon, 2015] Reflecting tape is used when the surface is exposed for direct solar radiation. The thermocouples measuring surface temperatures are distributed on the walls, floor, ceiling and window of the test zone.

All the temperatures are measured with Type K thermocouples. The thermocouples measuring surface and air temperatures have an accuracy of $\pm$ 0.15 K, while the thermocouples measuring operative temperature have an accuracy of $\pm$ 0.30 K. [Dreau, J. L., Heiselberg, P. K., Jensen, R. L., 2014] Because of the big number of thermocouples, all these are connected to three compensation boxes. From here the thermocouples are connected to Helios data loggers that log all the temperatures. The Helios data loggers are also connected to an ice point reference.

Irradiance

The outdoor irradiance is measured by two pyranometers. One is placed vertically beside the window at the southern façade of the Cube. This can be seen at figure A.3.

Figure A.3: Vertical pyranometer placed at the southern façade measuring irradiance.

The other pyranometer is located horizontally at the top of the roof of the Cube. The one on the roof is a CM22-pyranometer, while the one on the southern façade is a CM21-pyranometer. The CM22-pyranometer are measuring irradiance with an accuracy of ± 2 % and the CM21-pyranometer is measuring with ± 3 % [Dreau, J. L., Heiselberg, P. K., Jensen, R. L., 2014]. The data logged from the pyranometers are logged through a Helios data logger.

Water flow rate and water temperature

The size of the cooling power released from the chill beam and the radiant wall is calculated from the measured water flows and water temperatures. The flow is measured on the inlet, while the temperature is measured both at the inlet and return to know how much energy is released. The temperature sensors and flow meter can be seen at the left picture in figure A.4.

Figure A.4: The picture on the left shows temperature sensors and flow meter installed on inlet and return pipes. On the right picture, a Brunata energy meter is shown.

The temperature sensors and flow meters from the left picture in figure A.4 are connected to Brunata energy meters, which are shown on the right picture in the same figure. The measured values for the chill beam are logged through a Helios data logger, while the measured values for the radiant wall through a BTR. The accuracy of the temperature sensors is ± 0.057 % and the accuracy of the flow meters is ± 0.9 l/h [Dreau, J. L., Heiselberg, P. K., Jensen, R. L., 2014].

Power

As earlier mentioned electrical radiators heat up the test zone. In order to measure the effect that these are performing, the radiators are connected to a power meter. The power meter can be seen in figure A.5 on the next page.

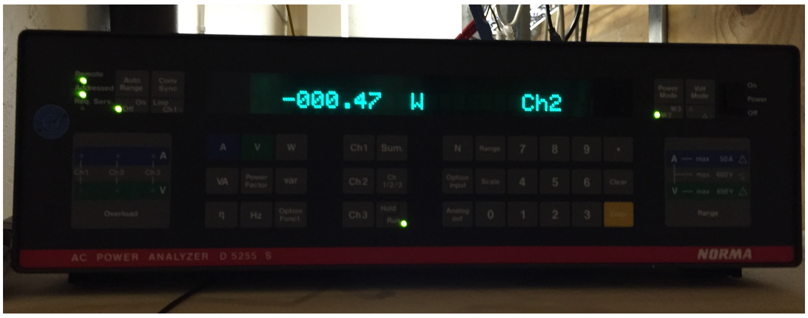

Figure A.5: Power meter measuring the effect of the radiators.

The power meter has an accuracy of ± 0.2 %, and the measured effects of the power meter are logged by a Helios data logger.

Pressure difference

Furness pressure transducers are used to measure pressure differences. The pressure difference between the test zone and the guarding zone is measured. This pressure difference between the zones is kept close to 0 during all measurements in order to minimize the infiltration between the zones. The transducers are also measuring the pressure difference over an orifice plate located before the inlet of the ventilation system to the test zone. This pressure difference is used to calculate the air flow rate. A Furness pressure transducer is shown in figure A.6.

Figure A.6: The Furness pressure transducer used to measure the pressure differencs.

The measured pressure differences are logged through a Helios data logger. The Furness pressure transducer has an accuracy of ± 7.5 % [Dreau, J. L., Heiselberg, P. K., Jensen, R. L., 2014].

A.2 Data Sheets of Glazing and Shading Systems

In this section three data sheets for the different windows and solar shadings are presented. The data sheets are presented in the following order:

- Data sheet for the double glazed window

- Data sheet for the triple glazed window

- Data sheet for both the Hhite Pearl and Charcoal Grey solar shading

PILKINGTON

Light 65%

16%

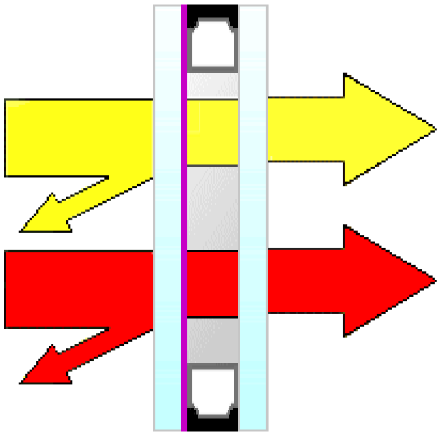

Energy 36%

35%

Description

Position	Product	Process	Thickness (nominal) mm	Weight kg/m^2
Glass 1	Pilkington Suncool 66/33	Annealed	6	15
Cavity 1	Argon (90%)		12	
Glass 2	Pilkington Optifloat Clear	Annealed	6	15
Product Code	6C(66)-12Ar-6		24	30

Performance

Light		
Transmittance	LT	65%
	UV %	11%
Reflectance Out	LR out	16%
Reflectance In	LR in	18%

Energy		
Direct Transmittance	ET	32%
Reflectance	ER	35%
Absorptance	EA	33%
Total Transmittance	g	36%
Shading Coefficient Total		0.41
Shading Coefficient Shortwave		0.37

Sound Reduction	R_w dB ($C;C_{tr}$)	31 (-1; -4)
Thermal Transmittance	W/m^2K	1.2

Ra	93

Performance Code	
U-value/Light/Energy	1.2 / 65 / 36

The values of some of characteristics are displayed as NPD. This stands for No Performance Determined.

Pilkington Spectrum allows you to combine a wide range of products available from Pilkington and determine their key properties such as light transmittance, g value and U value. The program includes restrictions that prevent some combinations being selected that may be considered unwise or impractical. Even with these restrictions, it is still possible to create product combinations that may not be available from your supplier. Please check with your supplier that your chosen product combination is possible, available in the sizes required and in a timescale appropriate to your project. Furthermore, it is essential that you check that your product combination is appropriate for satisfying local, regional, national and other project-specific requirements.

Calculations are made according to EN standards 410 and 673/12898

Pilkington Spectrum Version 4.0.0 12/06/2013

Expert results

Glazing design

Internal use only

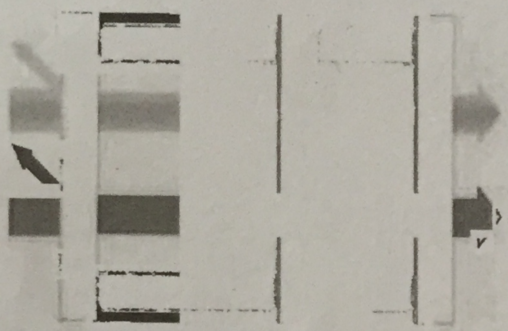

Aalborg Uni
Build Up TGi for test

	First glazing	Sec…	
Gas		Argon 90% 29.00mm	Argon 90… 16.00mm
Coating		PLANITHERM XN	PLANITHE… ULTRA N II
First glass	PLANICLEAR 6.00mm	PLANICLEAR 6.00mm	PLANICLE… 6.00mm
Coating			
Layer			
Coating			
Second glass			
Coating			

Luminous factors (EN410-2011) : (D65 2°)

Transmittance		Outdoor reflectance		Indoor reflectance	
TL :	71.5 %	RLe :	15.4 %	RLi	15.7 %
L*	87.7		46.2		46.6
a*	-4.7		0.5		-0.4
b*	3.3		-5.7		-6.5
	95.9		95.5		

UV factors (EN410-2011)

TUV :	24.4 %	RUV	25.3 %

Energy factors (EN410-2011)

TE :	43.9 %	REe :	31.1 %	REi :	30.6 %
AE1	10.2 %				
AE2	8.8 %				
AE3	6.0 %				

Solar factors (EN410-2011) :

g 0.540 Shading coef. 0.620

U-value (EN673-2011) - 0° related to vertical position

Ug 0.56 W/m².K

Calumen II

CALUMEN® II is a simulation software to calculate key performance of glass such as light transmission, solar factor or thermal insulation coefficient. Computed values are indicative and subject to change. They can not be used to guarantee performance of the products.

These values are calculated according to EN410-2011 and EN673-2011 standards. Tolerances are defined according to EN 1096-4 or ISO9050 -2003 standards. Nevertheless, user must check the feasibility of the associated products, in particular in terms of thickness and colour. Furthermore, it is his responsibility to check that the resulting combination of glazing meets regulatory requirements at national, local or regional level.

• Calculation software verified
• EN 410 and EN 673

Calculation rules and functional output of Calumen II have been validated by TÜV Rheinland Quality Report 11923R-11-33705

→Optical factors (cont'd)

Rv **Visible light reflectance:** proportion of light reflected by the fabric.

Tdif **Diffuse transmission factor:** correlation of the two factors above: Tdif = Tv – OF.
It is indicated as **Tvndif** for the aspects of glare and shape recognition (outward visibility / night privacy). A low figure shows a better visual comfort.

However, for natural light control, it is indicated as **Tvdifh**. It is used to ascertain a fabric's light diffusion capacity. A high figure means more natural light.

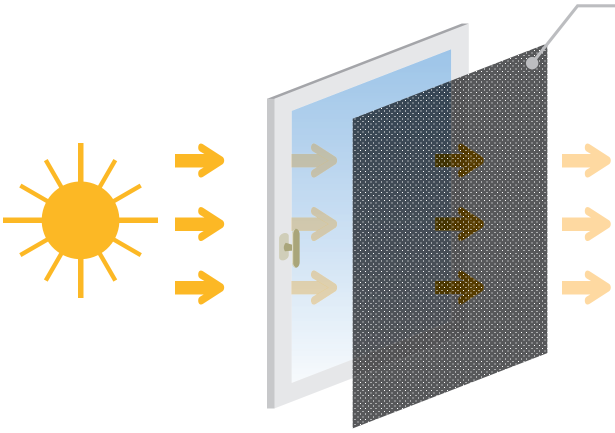

→ Internal Protection

Dark colour **Charcoal** 3030	Light colour **White** 0202
Visual transmission (Tv or TL)	
Tv = 6%	**Tv = 21%**
Thermal transmission Total solar factor (gtot or fs)	
gtot = 0,54	**gtot = 0,35**

Thermal and optical factors in the European standard EN 14501

E-Screen 7505

Openness Factor **OF 5%** Colours	Thermal factors					Optical factors			
	Fabric			Fabric + glazing					
	Ts	Rs	As	gv=0,59	gv=0,32	Tv	Rv	Tvndif	Tvdifh
				gtot internal blind					
0202 White	22	67	11	0,35	0,25	21	75	14	17
0220 White Linen	18	62	20	0,37	0,25	16	68	10	13
0207 White Pearl	17	52	31	0,40	0,26	14	56	8	12
2020 Linen	23	51	26	0,40	0,26	19	56	14	16
2022 Linen Stone	20	54	26	0,39	0,26	17	58	11	14
0720 Pearl Linen	17	45	38	0,42	0,27	15	48	8	12
0707 Pearl	18	38	44	0,44	0,27	15	41	9	12
3001 Charcoal Grey	9	11	80	0,52	0,29	8	10	1	6
3006 Charcoal Bronze	8	6	86	0,54	0,30	8	6	1	6
3030 Charcoal	6	6	88	0,54	0,30	6	5	0	5

gv = 0,59: solar factor of standard glazing (C), low-emission 4/16/4 double glazing filled with Argon (U value thermal transmittance = 1,2 W/m²K).
gv = 0,32: solar factor of standard glazing (D), reflecting low-emission 4/16/4 double glazing filled with Argon (U value thermal transmittance = 1,1 W/m²K).

Samples tested according to EN 14500 standard defining the measurements and calculation methods as specified in the standard EN 13363-1 "Solar protection devices combined with glazing calculation of solar and light transmittance – Part 1: simplified method" and EN 410 "Glass in building – Determination of luminous and solar characteristics of glazing".

A.3 Specifications of BSim Model

In this section some of the specifications of the BSim model are listed. Note that far from all specifications of the BSim model are given. The BSim model is attached on the appendix CD.

- The g-values of the windows in the model are calculated from the two parameters *GrossSun* of the window and *GrossSun* of the thermal zone. GrossSun of the window is defined in the program as the solar radiation on the on the external side of the transparent area. GrossSun of the thermal zone is defined as the total solar radiation through all the windows in the thermal zone.

- The parameter *Lost* under thermal zone is set to 0. Lost is defined as the part of the entered solar radiation, which is lost due to reflection from curtains,house plants, filth on the glazing, reflective surfaces in the room etc.

- The parameter *Horizon* is set to 0. This parameter is the general altitude angle for the building, meaning the angle between the horizontal plane and the horizont.

- Three different weather files are used for the simulations. For the validation part a weather file is used, where the measured outdoor temperature and solar radiation from the Cube is implemented. For the simulations used to determine the size of the overestimation, a weather file with only direct solar radiation is used. In this weather file the direct solar radiation is set to $1000\,\mathrm{W/m^2}$, while the diffuse radiation is set to $0\,\mathrm{W/m^2}$. For the simulations used to determine the correction of the overestimation standard DRY weather data from 2013 is used.

- As earlier mentioned the built up of the building is not considered important for the objective of the model. Walls, floor and ceiling consist of $0.05\,\mathrm{m}$ concrete. The internal volume of the building is $1\,\mathrm{m^3}$, while the external volume is$1.331\,\mathrm{m^3}$. The internal floor area is $1\,\mathrm{m^2}$ and the external floor area is $1.21\,\mathrm{m^2}$. The window towards south has a glazing area of $1\,\mathrm{m^2}$.

- When creating the window and solar shading as a combination through the EXP method, a user defined curve for the g-value in relation to the incidence angle is implemented in a glazing material under the tab *UserDefined*. When editing the properties of a glazing material, there is also a tab called *Additional*. In this tab the transmittance, absorptance and reflectance of both sides of the glazing are given. They are assumed to be identical on both sides of the glazing. How the This size of the transmittance, absorptance and reflectance is calculated and listed in table A.1 on the next page.

Blind	Window	τ	ρ	α
White Pearl	Double glazed	12 %	41 %	47 %
Charcoal Grey	Double glazed	16 %	36 %	48 %
White Pearl	Triple glazed	16 %	43 %	41 %
Charcoal Grey	Triple glazed	22 %	33 %	45 %

Table A.1: Factors calculated for EXP created windows in BSim, where τ is the transmittance, ρ is the reflectance, and α is the absorbance.

A.4 Overestimation - Outside Working Hours

Even though the working hours in an office building are considered the critical hours, a brief analysis of the non working hours will be conducted as well.
In figure A.7 the cumulative frequency of the incidence angle on a south, west, east and north oriented window outside working hours is presented.

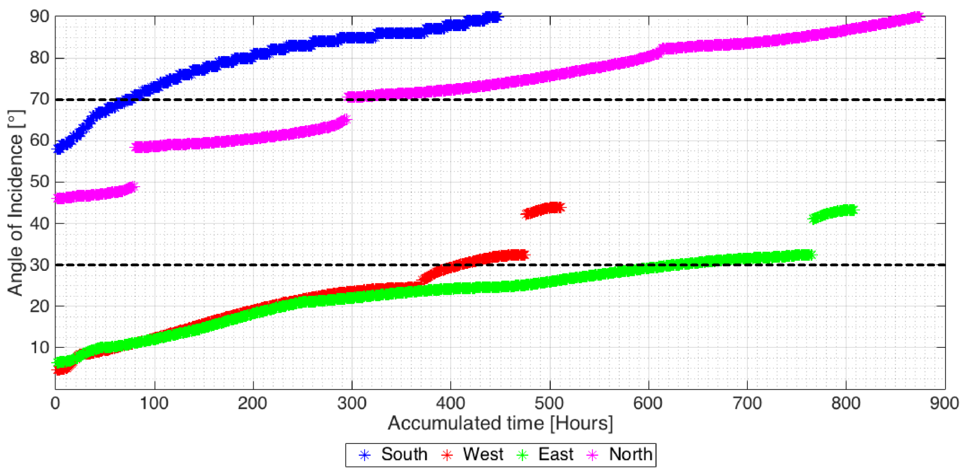

Figure A.7: The cumulative frequency of the incidence angle on a south, west, east and north oriented window outside working hours.

From the figure it becomes visible that the amount of hours within the BSim overestimation interval is limited to around 100 hours for both a south, west and east oriented window. A north oriented window, which was inflicted by direct solar radiation zero hours during a year, is reached by solar radiation around 300 hours during non working hours.

Since north oriented room are not inflicted by any direct solar radiation during the working day it is unlikely that the solar radiation outside working hours should have a significant effect to the energy consumption of the room.